INVESTIGATIONS OF PLASMID-HOST CELL INTERACTIONS IN RECOMBINANT *Escherichia coli* POPULATIONS

Thesis by

Jin-Ho Seo

In Partial Fulfillment of the Requirements

for the Degree of

Doctor of Philosophy

California Institute of Technology

Pasadena, California

1986

(Submitted July 1, 1985)

Acknowledgements

I would like to express my deepest appreciation to Dr. Jay Bailey for his valuable advice, financial support, and critical discussion throughout the writing of this work. I also thank Dr. Judy Campbell for donation of recombinant microorganisms. Special thanks are due to Dr. Friedrich Srienc for his assistance in flow cytometry analysis.

Finally, my sincerest appreciation and gratitude go to my wife, Sunghea, for her endless understanding and encouragement during my stay at Caltech.

ABSTRACT

Plasmid-host cell interactions have been characterized experimentally for recombinant *Escherichia coli* populations. The plasmids used contain pMB1 replication origins and propagate in *E. coli* at different copy number levels ranging from 12 to 408. Host *E. coli* HB101 strains transformed with those plasmids were used throughout this research.

The specific growth rate and amount of cloned-gene product (β-lactamase) were determined in batch cultivations as a function of plasmid copy number. Maximum specific growth rates in LB and M9 media were reduced monotonically for increasing plasmid content per cell. The maximum specific growth rate for a recombinant strain with copy number 408 was reduced by 25% relative to the plasmid-free strain. The ratio of β-lactamase specific activity to plasmid content, as a measure of the overall efficiency of plasmid-gene expression, declines by a factor of 7 as the copy number increases from 12 to 408. The relationship between copy number and cloned-gene product activity can be reasonably approximated by a parabolic equation, with approximately linear proportionality for copy numbers up to 60 but subsequently with reduction in the product/copy number ratio.

Investigations of environmental effects on plasmid content and β-lactamase activity have also been done in batch and continuous bioreactors. Plasmid copy number decreased when specific growth rate was increased by varying medium composition in a batch fermentor, or when dilution rate (inverse of residence time) was increased by increasing medium flow rate in a continuous fermentor. The response of plasmid-gene product formation to growth conditions in these two different reactor types is interesting. Batch experiments showed that the specific activity of β-lactamase is a gradual

decreasing function of specific growth rate, whereas product activity has a maximum with respect to dilution rate in chemostat growth. Comparative analysis of genetic and environmental effects implies that both plasmid content and growth conditions should be taken into account in determining the productivity of recombinant cell populations.

Further insight into the host-vector interactions was obtained by exploring plasmid amplification behavior and cell-cycle characteristics in the recombinant strains. Chloramphenicol-derived amplification kinetics were measured using flow cytometry, which allows direct determination of the total cellular DNA content after staining with mithramycin, a DNA-specific fluorescent dye. Both rates of plasmid amplification and final contents of amplified plasmids were found to be proportional to the average initial plasmid copy number obtained at steady-state growth.

The measurements of the cell-cycle parameters in *E. coli* cells were performed using experimentally determined single-cell DNA content frequency functions in connection with mathematical analysis of cell growth. Plasmid-containing cells exhibit C and D times that are approximately 14 and 24 percent, respectively, smaller than corresponding values in the plasmid-free host. Mean cell sizes and cell mass at the point of replication initiation decrease 38 and 18 percent, respectively, relative to plasmid-free cells. These results agree qualitatively with the previous findings with *E. coli* B/r carrying F plasmids of various sizes. Interestingly, the effects of plasmid presence on C, D, average cell size, and initiation mass were found to be approximately independent of plasmid copy number in these host-vector systems.

Finally, mathematical description of plasmid propagation in cells which reproduce by binary fission was presented using a segregated, population balance model. With the population balance equations, the probability of plasmid loss, distribution of cellular plasmid content, and specific rate of product synthesis were determined based on different single-cell models of plasmid replication, partition, and gene expression. Control modes of plasmid replication during cell growth markedly affect the distribution of plasmid content and accordingly the specific rate of gene product synthesis. The degree of selection required for stable maintenance of plasmid-harboring populations was derived by analyses that focused on the transient growth of plasmid-containing and plasmid-free cells in partially selective medium.

Table of Contents

INTRODUCTION

The advent of recombinant DNA technology has generated great impact on the development of strains which can produce useful proteins in large quantity. A schematic diagram of a recombinant cell is shown in Figure 1. Recombinant cells have two different DNAs: the host cell chromosome and recombinant plasmids. Microorganisms widely used as host cells include *Escherichia coli*, *Bacillus subtilis*, and *Saccharomyces cerevisiae*. The essential components of cloned plasmid DNA are product and selection genes and an origin of replication. The product gene contains the genetic instructions for the protein of interest. The selection gene provides the host cell with antibiotic resistance or complementation of host cell mutations. The selection markers provide convenient means for stable maintenance of plasmid-containing cells. In order to make a desired product, the plasmid must utilize the host cell's protein synthesis machinery, which is also used to synthesize many kinds of the cell's proteins. It is reasonably expected that there is competition between the cellular activities directed by the plasmid and the chromosome for the cell's limited pools of catalytic assemblies, precursors, and metabolic energy. The understanding of this interaction will be very important for determination of the productivity of recombinant DNA systems.

Among the parameters considered in maximizing the productivity are the number of plasmid molecules, the stability of the vector, the efficiency of gene expression, and bioreactor operating strategy. Understanding the effects of each of these factors on productivity is the central motivation of

the present work. Before the present research is outlined, a brief background on each parameter effect will be presented.

Previous experiments have shown that the amount of the gene product accumulated in recombinant cells is proportional to the number of plasmid copies in the cell [1]. However, the presence of plasmid exerts a negative effect on host cell growth. As discussed earlier, the plasmid reduces host-cell biosynthetic activities by redirecting the synthetic potential into making plasmids and their products. The magnitude of plasmid-mediated perturbation on host-cell growth and biosynthetic activities should be enhanced as the plasmid copy number increases. Consequently, the above arguments suggest that there exists an optimum copy number for maximum productivity.

Plasmid stability implies the stable retention of plasmids in a growing cell population. Once plasmid-free cells are generated from plasmid-containing cells, the former will exceed the latter in number due to growth advantage in nonselective medium. Many researchers have attempted to stabilize the recombinant plasmid during propagation in cell populations. Potential solutions to the plasmid stability problem include modification of genetic structure of plasmid and host cell (for instance, insertion of the *par* locus), application of selective pressure in favor of the plasmid-containing population in growth medium, and integration of the cloned gene into the chromosomal DNA [2].

Another approach to improvement of the product yield is to use efficient gene expression systems. In procaryotes such as *E. coli* and *B. subtilis*, gene expression efficiency can be increased by altering the promoter, the

ribosome binding site, and their positions relative to the structural gene. Post-translational modifications must be taken into account in eucaryotic cells such as *S. cerevisiae* and animal and plant cell lines. In this introduction, promoter strength effects will be discussed. The interested reader should consult with the books [3,4]. A promoter is a DNA site at which RNA polymerase binds and initiates transcription reactions to make mRNA. Promoters vary considerably in their strength, which is defined operationally as the efficiency of initiation of transcription. Promoter strength determines the rate of the transcription of the gene and ultimately the level of the cloned-gene protein. Promoters frequently used in expression vectors for *E. coli* are *lac*, *trp*, λp_L , and *ompF* promoters [5]. In production of human insulin using recombinant *E. coli* [6], the product yield was improved by switching to the stronger promoter (*trp*) from the *lac* promoter. Regulated promoters have an advantage over nonregulated promoters in that cloned-gene expression may be controlled through manipulation of growth conditions [7]. This approach is very useful because we can avoid competitive interactions between the plasmid and chromosomal DNA by keeping gene expression low in the early stages of fermentation.

The productivity of a recombinant DNA system can be further increased by optimizing growth environment. The optimization of growth conditions has been successfully applied to many existing fermentation processes such as antibiotics production. In growth of recombinant cells, special attention would be paid to media composition and temperature control because the variation of these parameters may activate proteolytic degradation of proteins foreign to the host cell [8]. In addition, gene expression efficiency of a recombinant vector containing a regulated promoter depends on growth

conditions as described previously. In the case of a temperature-inducible promoter, an increase in the temperature of culture medium can increase promoter activity and thus the amount of the gene product [7,9]. However, induction of the promoter decreases the viability of the plasmid-carrying cells and plasmid stability such that the fraction of the plasmid-harboring cells declines at a faster rate [9]. Accordingly, culture temperature should be balanced between the rate of gene expression and the number of the production cells.

The objective of this thesis is experimental and theoretical characterization of interactions between plasmid and host-cell functions in recombinant *E. coli*. The bacterium *E. coli* is the best understood microorganism to date and has been most widely used in genetic engineering. The plasmids used in this study provide good model systems to assess the extent of plasmid-mediated interference on host cell functions and the dependency of any such interference on plasmid copy number. The thesis consists of five chapters. Each chapter contains a separate introduction summarizing related work and presenting the motivation for that part of the work.

In Chapter 1, experiments are described which study the relationships among plasmid copy number, host-cell growth, and product formation. Effects of plasmid content on growth properties of the host-cell and cloned-gene product formation (β-lactamase) were explored using a series of copy number mutants. This effect is called a *gene-dosage effect*. Effects of growth media (or growth rate) on plasmid content and β-lactamase activity, termed here the *environmental effect*, was investigated in a batch reactor. In order to evaluate environmental effects under well-defined experimental conditions, a continuous culture system was employed. Chapter 2 deals with

dilution rate effects on plasmid content, β-lactamase activity, and overall productivity in a recombinant DNA system. Also, comparison of experimental results obtained in batch and continuous reactors is provided.

The next two chapters are devoted to application of flow cytometry to study of the complex interactions between plasmids and host-cells. Flow cytometry allows experimental access to the distribution of cell states in the population. Flow cytometry data in conjunction with segregated population equations provide convenient tools for quantitative determinations of single-cell parameters or intrinsic kinetic forms which are difficult or impossible to estimate from nonsegregated simulations and experiments. Chapter 3 summarizes studies of chloramphenicol-induced plasmid amplification in *E. coli*. In Chapter 4, the basic cell-cycle parameters of plasmid-carrying *E. coli* populations were estimated using both single-cell DNA content distribution functions determined with flow cytometry and mathematical analyses of cell growth. Measurements of cell-cycle parameters as a function of plasmid copy number allows evaluation of the effect of competition between plasmid and chromosomal DNA on nuclear and cell division cycle control.

Chapter 5 describes theoretical analysis of plasmid propagation and product synthesis in unstable recombinant organisms using a segregated population balance model. The segregated models enable theoretical derivations of the degree of plasmid loss and of a condition for stable maintenance of the plasmid-carrying population.

REFERENCES

1. Uhlin, B., and K. Nordstrom, *Plasmid*, **1**, 1 (1979)

2. Bertani, L.E., and G. Bertani, p. 917 in *Plasmids in Bacteria*, Ed. D. Helinski, S.N. Cohen, D. Clewell, D. Jackson, and A. Hallaender, Plenum Pub. Co. (1984)

3. Old, R.W., and S.B. Primrose, *Principles of Gene Manipulation*, Univ. Cal. Press (1981)

4. Glass, R.E., *Gene Function*, Univ. Cal. Press (1982)

5. Burnett, J.P., p259 in *Experimental Manipulation of Gene Expression*, Ed. M. Inouye, Academic Press (1983)

6. Windass, J.D., C.R. Newton, J.D. Maeyer-Guiynard, U.E. Moore, A.F. Markham, and M.D. Edge, *Nucleic Acids Res.*, **10** , 6639 (1982)

7. Weinstock,G.M., p31 in *Genetic Engineering Vol. 6*, Ed. J.K. Setlow and A. Hallaender, Plenum Pub. Co. (1984)

8. Goldberg, A.L., and A.C. St. John, *Ann. Rev. Biochem.*, **45**, 747 (1976)

9. Siegel,R., and D.Y. Ryu, *Biotech. Bioeng.*, **27**, 28 (1985)

FIGURE CAPTIONS

Figure 1 Schematic representation of a recombinant cell.

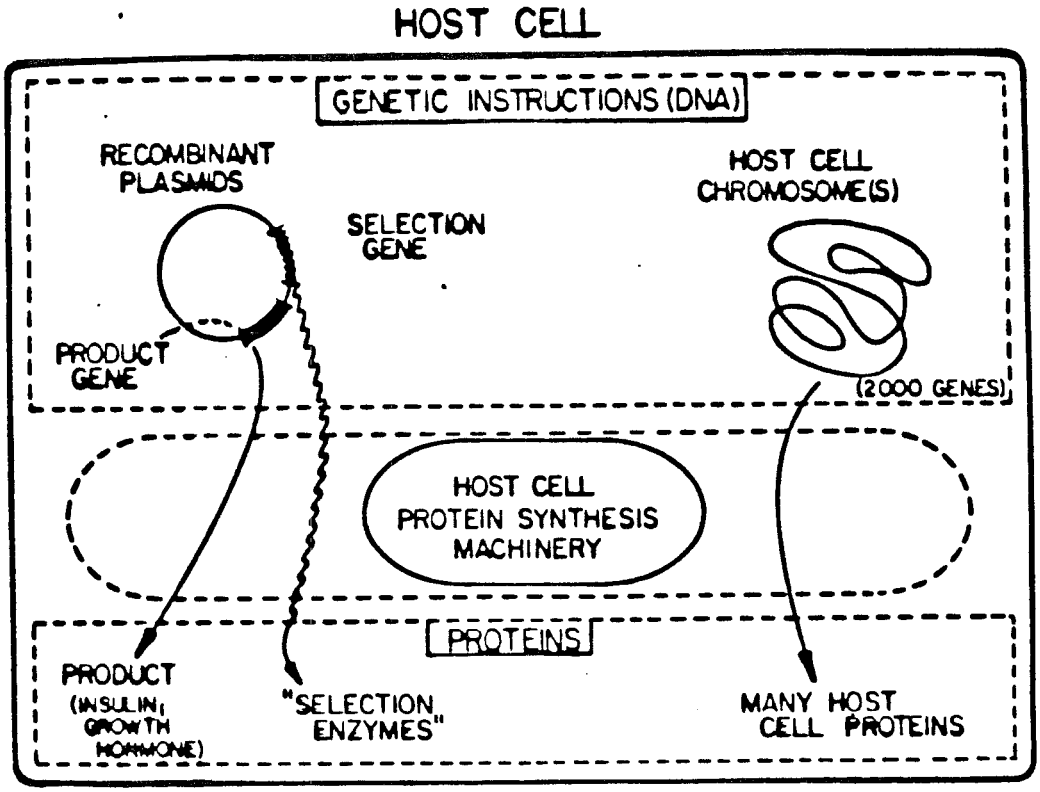
HOST CELL
GENETIC INSTRUCTIONS (DNA)
RECOMBINANT PLASMIDS
SELECTION GENE
HOST CELL CHROMOSOME(S)
PRODUCT GENE
(2000 GENES)
HOST CELL PROTEIN SYNTHESIS MACHINERY
PROTEINS
PRODUCT (INSULIN, GROWTH HORMONE)
"SELECTION ENZYMES"
MANY HOST CELL PROTEINS

Figure 1.

CHAPTER 1: EFFECTS OF RECOMBINANT PLASMID CONTENT ON GROWTH PROPERTIES AND CLONED GENE PRODUCT FORMATION IN *Escherichia coli*

(The text of Chapter 1 consists of an article which will appear in *Biotechnol. Bioeng.*, in press (1985).)

SUMMARY

Plasmid-host cell interactions have been investigated experimentally using *Escherichia coli* HB101, plasmid RSF1050 which contains the origin of replication of pMB1, and four other closely related copy number mutant plasmids. Growth characteristics of these recombinant strains and β-lactamase activity expressed from a plasmid gene were investigated in Luria broth (LB) and in minimal medium (M9) containing in some cases casamino acids or different concentrations of α-methylglucoside, a competitive inhibitor of glucose transport. Maximum specific growth rates in LB and minimal media were reduced for increasing plasmid content per cell. Plasmid copy number increased when specific growth rate was reduced by changing medium composition. Growth rates of high copy number strains were less sensitive to α-methylglucoside than lower copy number strains and the plasmid-free host. The overall efficiency of plasmid gene expression, measured as the ratio of β-lactamase specific activity to plasmid content, decreased significantly with increasing plasmid content in LB medium.

INTRODUCTION

Valuable proteins native to both procaryotic and eucaryotic cells can be synthesized in bioreactors using genetically engineered microorganisms. The usual strategy for formulating a production organism is introduction into a suitable host, often the bacterium *Escherichia coli*, of a recombinant plasmid carrying the gene for the product of interest and suitable associated control sequences for efficient expression. Among the important considerations in design of the host-vector expression system and also in design and operating strategy for the bioreactor process is the cellular content of plasmids and thus of product gene copies. Previous experiments have shown in some cases that the amount of cloned-gene protein product accumulated in recombinant cells is directly proportional to the plasmid copy number (plasmid molecules per chromosome molecule).[1] On the other hand, it has also been shown that cells with plasmids grow more slowly than cells without plasmids and that, in the case of cultures containing highly amplified plasmids, cells become nonviable.[2] These effects of increasing plasmid content presumably occur because of competition between plasmid DNA and plasmid-derived messenger RNA on the one hand and chromosomal DNA and chromosomal-mRNA on the other for the cell's limited pools of initiation factors, enzymes, ribosomes, metabolic energy, and biosynthesis precursors. Accordingly, there is a tradeoff between high plasmid content, which is detrimental to host cell growth and protein synthesis, and low plasmid content, which reduces the intracellular concentration of the product gene.

The objective of this study is experimental characterization of the influence of plasmid content on host-cell growth and cloned-gene product synthesis. In order to maintain as much similarity as possible in all genetic

and metabolic factors except plasmid copy number, the same host strain has been employed in all of these experiments. A set of closely related copy number mutant plasmids, all enabling constitutive expression of the enzyme β-lactamase, was employed in this work. Experiments were designed to characterize growth properties of different recombinant strains carrying these different plasmids. Also, the specific activity of β-lactamase was measured as a function of plasmid content and growth rate. Influence of growth medium on plasmid content was also determined.

MATERIALS AND METHODS

Bacterial Strains and Plasmids

Escherichia coli HB101 ($Pro^-Leu^-Thi^-RecA^-$) was used as a host strain throughout this study. The diagram in Fig. 1 illustrates the distinct copy number control features of the five different plasmids used in this study. The plasmid RSF1050 is a derivative of pMB1 which includes the origin of replication of that plasmid and also a gene labeled Ap^r which provides expression of β-lactamase enzyme in *E. coli*.[3] Also indicated in the map of this plasmid is the gene for a small RNA called RNA I which has been established as the primary inhibitor of plasmid DNA replication in pMB1 and also ColE1, NTP1, p15A, and C1oDF13. Plasmid pFH118, a high copy number derivative of RSF1050, contains a 16-base pair insert in the RNA I coding region.[4] Plasmids pDM246, pDM247, and pDM248 were obtained by inserting into pFH118 one copy of the wild-type RNA I gene, two copies of the RNA I wild-type gene, and one copy of the mutant RNA I gene, respectively.[5] The copy numbers of each of these plasmids in *E. coli* HB101 in LB medium, indicated in parentheses below each plasmid name, are reasonable relative to each other in view of the inhibitory role of RNA I.

Media and Cultivation

Growth media are Luria broth (LB) supplemented with phosphate buffer[6], M9 minimal medium enriched with 50 mg leucine, 200 mg proline and 0.2 mg thiamine HCl per liter (M9), and M9 medium plus 0.4% Casamino Acids and 0.2 mg/L thiamine HCl (M9C).[7] All media contain 0.2% glucose as a carbon source. Cells were preincubated at 37° C in a growth medium containing 70% of the corresponding minimum inhibitory content (MIC) of ampicillin (Na-salt, Sigma Chemical, St. Louis, MO) for the plasmid of interest. The MIC value of each strain was determined in LB medium by Dennis *et al.*[6] When grown to the exponential phase 0.5 ml cells were inoculated into 50 ml of amplicillin-free medium prewarmed at 37° C in a shaker (New Brunswick Sci., Edison, NJ). Cell growth in the shaker at 37° C was followed by measuring optical density with a Klett-Summerson spectrometer with a green filter. From three to seven replicate experiments were conducted for each strain and each medium, and the standard deviation in each case was approximately 5%. Initial medium pH was 7.0 in all cases, and no change in pH occurred before harvesting.

Determination of β-Lactamase Activity

Cells (20 ml) were harvested during exponential phase and chilled on ice for 10 min. Sample preparation followed the method proposed by Yamamoto *et al.*[8] The harvested cells were washed twice with 50 mM phosphate buffer (pH 7.0) containing 0.14 M NaCl and 10 mM $MgSO_4$ and then suspended in 0.1 M phosphate buffer (pH 7.0). Cell lysis was done by sonication (Model W-375, Ultrasonics, Inc.) for 2 minutes. Cell lysates were centrifuged at 15,000 rpm for thirty minutes at 4° C using a Beckman centrifuge (Model J-21B). The supernatant was taken for determinations of β-lactamase activity and total

protein.

The activity of β-lactamase was assayed by the iodometric method.[9,10] Test tubes containing 0.5 ml of 20 mM benzyl penicillin (K-salt, Sigma) dissolved in 0.1 M phosphate buffer (pH 7.0) were preincubated at 30° C in a water bath. An appropriate volume of sample taken from the cell lysate supernatant was added and the final volume adjusted to 3 ml by adding 0.1 M phosphate buffer. (The appropriate sample volume was chosen to maintain linearity of the calibration for each strain and medium examined.) The hydrolysis reaction was stopped at different times by adding 5 ml iodine reagent, and, after ten minutes at room temperature, the absorbance at 490 nm was determined with a Spectronic 21 spectrophotometer (Bausch and Lomb, Rochester, NY). After determining total cell protein using Sigma Protein Kit No. 690 (Sigma), the specific activity of β-lactamase was computed based on the formula derived by Sawai *et al.*[10] One unit of β-lactamase specific activity is defined as the quantity that hydrolyzes 1 μmole of benzyl penicillin per minute and per mg. of cellular protein at 30° C.

Copy Number Determination

Copy numbers for all plasmids in cells grown in LB medium have been determined by the method of Moser and Campbell.[5,6] The procedure of Clewell and Helinski[11] was applied to determine relative plasmid content in different media. Supercoiled plasmid DNAs were purified by several extractions with phenol and a mixture of chloroform and isoamyl alcohol (99:1) and purified further by ethanol precipitation. The plasmid DNAs were analyzed by 0.9% agarose gel electrophoresis for 500V-hr. The plasmids were stained with ethidium bromide (1 μg/ml in E buffer) for 30 minutes, and measurements of each band density in negatives of gel photographs were done with a

scanning densitometer (Hoefer Scientific Instruments, San Francisco, CA) coupled to a digital integrator (Model C-R3A, Shimazu Corp., Kyoto, Japan). Other investigators have suggested that EtBr staining is more efficient when linearized rather than when supercoiled DNA is analyzed.[12] Accordingly, *EcoR* I digests were also analyzed on 0.9% agarose gel. Relative plasmid contents determined by this measurement agreed with those obtained using the undigested supercoiled DNA. Plasmid copy number (number of plasmid copies per chromosome equivalent) was converted to the number of plasmid copies per cell assuming that chromosomal content varies with growth rate according to the Cooper-Helmstetter model.[13] In these calculations, the C and D intervals were presumed to be the same for all strains grown in LB medium (C = 40 min., D = 20 min.[14]).

RESULTS

Growth Kinetics

Both segregational instability (birth of plasmid-free cells or cells unable to grow well under the imposed environmental conditions due to irregular plasmid partitioning at cell division) and structural instability (changes in the plasmid nucleotide sequence resulting in altered phenotype) need to be carefully considered in conducting growth rate experiments with recombinant cells and interpreting the results. Considering first segregational instability, several theoretical analyses have defined quantitatively the relationship between true growth rates of the plasmid-free and plasmid-containing cells, the frequency of plasmid loss at division, and the apparent overall growth rate of the population in selective and nonselective environments.[15-20] Such analyses clearly show that increasing instability implies reduced overall growth rates in selective media, and this property has

frequently been applied in qualitative experimental characterization of relative instability of different plasmids. Accordingly, in order to study the physiological effects of propagating plasmids and synthesizing their products, it is important to isolate, carefully, data pertaining to plasmid-containing cells relative to overall population data. The two are equivalent only for the case of stable plasmids. Fortunately, experimental tests of all of the plasmids used in this investigation show highly stable behavior. Cells taken from growth on nonselective media plated on selective and nonselective plates give identical counts, and growth rates of each strain in selective and nonselective media are identical.

These data also indicate that structural instability is not a problem so far as retention of ability to express β-lactamase activity is concerned (over the range of the number of generations involved in these experiments). Structural instability was noted in some experiments, however, with respect to maintenance of copy number. It was observed in early experiments that β-lactamase activities produced by cultures of strains carrying pFH118 and pDM248 were sometimes much lower than in other experiments. A probable cause for such behavior is sharp reduction in copy number associated with recombination between plasmids or deletion of some or all of the 16-base pair insert in the mutant RNA I gene. In order to minimize wasted effort on measurements characterizing revertants of the high copy number mutations, each strain was precultured in a medium containing sufficient ampicillin to prevent growth of low-copy number revertants. Cells from this preculture were transferred to nonselective, ampicillin-free medium and allowed to attain exponential phase growth again before rate measurements were conducted, and samples were taken for analysis.

Table I lists relative values of the experimentally determined copy numbers and specific growth rates for growth in LB medium of the recombinant strains investigated. Because of the differences in replication regulation among the plasmids considered, the trends in relative plasmid content from strain to strain are expected to be similar in other media. Consequently, to provide a basis for comments on relative copy number effects, the copy numbers listed in Table I will be called the "reference copy numbers" for each strain.

Specific growth rates of all strains with plasmids are lower than for the plasmid-free host as has been previously reported for other *E. coli* systems.[21,22] Specific growth rate decreases as copy number increases. Because all of the plasmids are stable, these differences in growth rate may be ascribed to reduction in host-cell biosynthetic activity for native components as a result of redirection by the plasmids of host-cell synthetic potential into plasmids and plasmid products. This effect, as expected intuitively, increases as cellular plasmid content increases. Similar trends were observed in analyses of cell cycles of *E. coli* B/r harboring F' plasmids of various sizes, where generation times and DNA replication time increased with increasing plasmid size .[23] Also, *E. coli* containing an R1 plasmid and a temperature-sensitive replication inhibitor was found to give decreasing growth rates at elevated temperatures which correspond to higher copy numbers.[2]

The effect of growth medium on the maximum specific growth rate of the plasmid-free host and all of the recombinant strains, is listed in Table II. The trend of growth rate variation with respect to type of plasmid is the same in all three media considered: maximum specific growth rate decreases

as the plasmid replication control system is changed to enable larger plasmid content per cell. Growth rate reductions tend to be greatest in M9 medium and smallest in M9C medium.

Plasmid Content at Different Growth Rates

To examine the influence of growth rate on copy number, strains HB101:pDM246 and HB101:pDM247 were grown in different media supporting different specific growth rates. The experimental results are plotted in Fig. 2. The overall trend is declining plasmid content as specific growth rate increases. Similar behavior has been reported for R1 plasmid,[24] for pVH5 plasmid,[12] and has been simulated by a detailed, genetically structured mathematical model of λdv plasmid replication.[25] An opposite trend, with increasing copy number as a function of specific growth rate, has been reported for plasmid pLP11 of *Bacillus stearothermopilus*.[26] Data at the two lowest specific growth rates indicated in Fig. 2 were obtained by adding different quantities of α-methylglucoside (α-MG), a competitive inhibitor of glucose transport, to M9 minimal medium. Interestingly, the data for both pDM246 and pDM277 suggest a maximum with respect to plasmid content near the lowest growth rates considered. Further studies are necessary to verify this possibility.

Specific growth rates of around 0.75 and 1.2 hr^{-1} were obtained using M9C and LB media, respectively. Although the primary effect of changing media is here assigned to changes in specific growth rate, it should be kept in mind that these two media are substantially different from the others, may evoke different pathways and regulatory responses from the cells, and so may cause changes in DNA and protein synthesis beyond those indicated only by the change in specific growth rate. While this potential factor should not be

overlooked, the measurements of plasmid content (and of corresponding β-lactamase activity, next section) follow a smooth trend in terms of specific growth rate alone.

Parameters for Monod Kinetics and for α-Methylglucoside Inhibition

The dependence of growth rates on limiting nutrient (glucose) concentration and upon α-MG was determined for all strains. α-MG is transported into the cells by the glucose transport system but is metabolically inert and is not used for growth.[27,28] All of these kinetic data could be reasonably fit by the following modified Monod equation which includes competitive inhibition by α-MG:

$$\mu = \frac{\mu_{max}[S]}{K_S + [S] + \frac{[I]}{K_I}} \qquad (1)$$

where [S] and [I] are glucose and α-MG concentrations (g/l), respectively. Maximum specific growth rate μ_{max} and Monod constant K_S values were estimated from experimental data with results as indicated in Table III. Again, the maximum specific growth rates decrease as plasmid content, indicated here by reference copy number, increases. Variations in the measured Monod costants are of similar order of magnitude as the experimental error in estimation of these constants and so cannot be considered significant. (Earlier investigators have also observed greater experimental error in experimental determination of the Monod constant.[29])

To determine the effect of competition for glucose transport into the cells, experiments were done at large substrate concentrations relative to K_S. Under these conditions, Eq. (1) may be simplified to the following form:

$$\mu = \frac{\mu_{max}}{1 + \frac{[I]}{[S]K_I}} \quad . \tag{2}$$

According to this equation, it is the ratio between the inhibitor and substrate concentration which determines specific growth rate. Experimental data are consistent with this functional dependence (Fig. 3). The different symbols in Fig. 3 correspond to different glucose concentrations, and the growth rate data still correlate closely with the inhibitor to glucose concentration ratio only. The solid line in Fig. 3 was drawn using Eq. (2) and the K_I value listed for strain HB101:pDM246 in Table III. Experimentally determined values of K_I, indicative of the sensitivity of growth rate to the presence of inhibitor for the different strains, are also listed in Table III. These results show that the strains with largest plasmid content are least affected by α–MG inhibition. A reasonable hypothesis consistent with this result is slowdown of intracellular reaction caused by plasmid presence which makes membrane transport less important in limiting overall growth rate.

An approximate overall yield factor $\bar{Y}_{X/S}$ has been measured for each strain (Table III). This value, which gives a qualitative indication of growth yields, is defined as the increase in cell mass density from inoculation to sampling divided by the total decrease in glucose concentration between the same two times. These figures indicate decreased cell yields from glucose as a result of carrying an increased plasmid burden. Decreased yield has been reported also for *E. coli* cells carrying an R1 plasmid.[22]

Cloned Gene Product Accumulation

The specific activity of β-lactamase, defined as the enzyme activity for penicillin G hydrolysis divided by the protein content of the culture, has been

measured for several recombinant strains in several different media. The specific cloned gene product activity for strains *E. coli* HB101:pDM247, HB101:pDM246, and HB101:RSF1050 were determined in media which support different growth rates of these strains. Again, highest growth rates were obtained in Luria Broth, intermediate growth rates in M9C medium, and lowest growth rates in M9 medium, with α-MG added to provide still lower growth rates. The experimental measurements are plotted in Fig. 4; the lines have been drawn to show the trends. In each case, there is a sharp decline in specific activity with increasing specific growth rate. This decline is consistent with the experimental data already shown in Fig. 2 which indicate that plasmid content per cell also declines sharply as growth rate increases.

Values of β-lactamase specific activities are listed in Table I for all strains grown in LB medium. Since the ratio of product activity to number of plasmid copies declines with increasing plasmid content in LB medium, it is clear that in this case gene product activity is not proportional to gene dosage. In particular, the relationship between copy number and cloned-gene product activity in LB medium can be reasonably approximated by a parabolic relationship similar to that used in previous mathematical modeling work[20] to calculate the rate of product formation r_p as a function of the number of plasmids per cell n_p:

$$r_p = k_p n_p (1 - c n_p) \tag{3}$$

where k_p and c are constants.

This type of relationship is consistent with the linear proportionality reported in other studies which is valid over relatively low copy number ($cn_p \ll 1$).[1] A similar concave relationship was obtained by Dennis *et al.*[6] in

(3)

experiments relating the minimum inhibitory concentration of ampicillin with plasmid copy number . Based on these data for LB medium, the parameter c in Eq. (3) is of the order of 10^{-3}, indicating nonviability of cells at approximately 1000 plasmid copies per cell. This agrees qualitatively with experiments with runaway plasmids which reach this order of magnitude in plasmid content and which render their host cells nonviable[2].

It is interesting to examine the relationship between plasmid content per cell and specific activity of β-lactamase, the cloned-gene product, with growth rate as a parameter. This relationship is illustrated in Fig. 5 for HB101:pDM246 and HB101:pDM247 by the triangles, the trend of which is indicated by curve A. It is interesting that, when plasmid content per cell is changed by varying the growth rate, the specific activity of β-lactamase increases as copy number increases, corresponding to reduced specific growth rate of the recombinant population. However, part of this effect may be due to reduction in protein content per cell as a function of growth rate, so that, at lower growth rates, a unit amount of cellular protein corresponds to a larger number of cells. On the other hand, when cellular plasmid content is changed by changing the plasmid replication control system (different strains in LB medium), specific activity of the cloned-gene product as a function of plasmid copy number Curve B, based on values in Table I is a concave function as just discussed. Recall also (see Fig. 1 and Table I) that, although strains with higher plasmid content grow slightly more slowly than strains with fewer plasmids, the growth rate variation along curve B is much less than that which accompanies different copy numbers along curve A.

DISCUSSION

This study was undertaken to investigate specifically the connection between plasmid content and host cell growth and product synthesis. In order to accomplish rational design of plasmids and host-vector systems with required and optimized properties in a process context, it is essential to understand and eventually to connect in predictive, quantitative fashion the influences of plasmid design at the molecular scale with functional properties of the recombinant organism at the bioreactor level. In this work, differences primarily in RNA I primary structure and content have been related to the corresponding growth and product formation kinetics of recombinant *E. coli*. Much more experimental and mathematical modeling research remains to progress from this and similarly focused studies to achieve the desired global objective.

The trends observed in these experiments can be used to guide choice of functional forms to represent the influence of plasmid content on host cell growth and cloned-gene expression in kinetic models of recombinant cultures. An important point which requires careful attention in any such modeling activity is the combined effect which plasmid copy number molecular controls and cell environment and growth rate exert in determining plasmid content per cell.

The data in Fig. 5 provide an interesting example of significantly different results from environmental and from genetic manipulation of cellular plasmid content. Either by reducing growth rate through medium composition change (Curve A) or by altering RNA I form and/or content (Curve B), a range of cellular plasmid contents up to around 110 plasmids per cell can be obtained. At the upper end of this range, the cloned-gene product specific

activity achieved by environmental manipulation is more than double that obtained by genetic manipulation. This result emphasizes the importance of optimizing both bioreactor conditions and host-vector genetic properties in order to maximize productivity of recombinant cell populations.

This research complements previous investigations by Siegel and Ryu[12] which have explored the influence of induction of a cloned strong promoter and subsequent high expression of the cloned-gene on growth properties of the recombinant strain. In practice, expression plasmids which combine such regulated promoters and plasmid copy number control systems, which can be manipulated by altering medium temperature or composition, will enable most complete optimization of productivity through manipulation of reactor-operating conditions. The effects of different operating strategies on batch and continuous bioreactor performance with unstable recombinant organisms, using models with functional representation of plasmid content inhibition based upon these experiments, have been simulated and will be reported in the near future.

Acknowledgement: This work was supported by the National Science Foundation.

REFERENCES

1. B. Uhlin and K. Nordström, *Plasmid* **1**, 1 (1979).

2. B. E. Uhlin, S. Molin, P. Gustafsson, and K. Nordström, *Gene* **6**, 91 (1979).

3. R. Heffron, P. Bedinger, J. J. Champous, and S. Falkow, *PNAS(US)* **74**, 702 (1977).

4. F. Heffron, M. So and B. J. McCarthy, *PNAS(US)* **75**, 6012 (1978).

5. D. Moser and J. L. Campbell, *J. Bacteriol.* **154**, 809 (1983).

6. K. Dennis, F. Srienc and J. E. Bailey, *Biotechnol. Bioeng.*, submitted 1984.

7. R. L. Rodriguez and R. C. Tait, *Recombinant DNA Techniques, An Introduction* (Addison-Wesley Publishing Co., 1983).

8. T. Yamamoto, S. Yamagata, K. Horii and S. Yamagishi, *J. Bacteriol.* **150**, 269 (1982).

9. M. G. Sargent, *J. Bacteriol.* **95**, 1493 (1968).

10. T. Sawai, I. Takahashi, and S. Yamagishi, *Antimicro. Agents & Chemoth.* **13**, 269 (1978).

11. D. B. Clewell and D. R. Helinski, *PNAS(US)* **62**, 1159 (1969).

12. R. Siegel and D. Y. Ryu, *Biotechnol Bioeng.*, **27**, 28 (1985).

13. S. Cooper and C. Helmstetter, *J. Mol. Biol.* **31**, 519 (1968).

14. C. Helmstetter and O. Pierucci, *J. Mol. Biol.* **102**, 477 (1976).

15. T. F. Anderson and E. Lustbader, *PNAS(US)* **72**, 4085 (1975).

16. F. M. Stewart and B. R. Levin, *Genetics* **87**, 209 (1977).

17. T. Imanaka and S. Aiba, *Ann. N.Y. Acad. Sci.* **369**, 1 (1981).

18. J. E. Bailey, M. Hjortso, S. B. Lee and F. Srienc, *Ann. N.Y. Acad. Sci.* **413**, 71 (1983).

19. S. H. Kim and D. Y. Ryu, *Biotechnol Bioeng.* **26**, 497 (1984).

20. J. H. Seo and J. E. Bailey, *Biotechnol. Bioeng.*, **27**, 156 (1985).

21. J. Inselburg, *J. Bacteriol.* **133**, 433 (1978).

22. R. Klemperer, N. Ismail and M. Brown, *J. Gen. Microbiol.* **115**, 325 (1978).

23. M. Weinberger and C. Helmstetter, *J. Bacteriol.* **137**, 1151 (1979).

24. B. Engberg and K. Nordström, *J. Bacteriol.* **123**, 179 (1975).

25. S. B. Lee and J. E. Bailey, *Biotechnol. Bioeng.* **26**, 66 (1984).

26. J. Koizumi, Y. Monden, and S. Aiba, *Biotechnol. Bioeng.* **27**, 721 (1985).

27. D. P. Kessler and H. V. Rickenburg, *Biochim. Biophy. Res. Comm.* **10**, 482 (1963).

28. M. T. Hansen, M. L. Pato, S. Molin, N. P. Fill, and K. von Meyenburg, *J. Bacteriol.* **122**, 585 (1975).

29. T. E. Shehata and A. G. Marr, *J. Bacteriol.* **107**, 210 (1971).

TABLE I

Plasmid content, specific growth rates and cloned gene product (β-lactamase) specific activity for recombinant *E. coli* grown in LB medium at 37° C

Strain	Reference copy number	Relative copy number	Relative specific growth rate	Relative cloned gene product specific activity
HB101 host only	0	0	1	0
pDM247	12	1	0.92	1
pDM246	24	2	0.91	2.1
RSF1050	60	5	0.87	4.2
pDM248	122	10.2	0.82	5.4
pFH118	408	34	0.77	7.0

Host: *E. coli* HB101
*For pDM247, copy number = 12, specific growth rate = 1.27 $hr.^{-1}$, β-lactamase specific activity = 1.4 units/mg protein.

TABLE II

Plasmid content effects on recombinant *E. coli* maximum specific growth rates. Values shown are the ratio of measured specific growth rate to specific growth rate of the plasmid-free host in the same medium. *E. coli* HB101 specific growth rates: LB medium: 1.38 $hr.^{-1}$; M9C medium: 0.79 $hr.^{-1}$; M9 medium: 0.41 $hr.^{-1}$.

Strain	Reference copy number	Relative specific growth rates		
		M9	LB	M9C
pDM247	12	0.93	0.92	0.97
pDM246	24	0.88	0.91	0.94
RSF1050	60	0.88	0.87	0.88
pDM248	120	0.78	0.82	0.84
pFH118	408	0.68	0.77	0.82

TABLE III

Maximum specific growth rate μ_{max}, Monod constant K_S, average yield factor $\bar{Y}$, and inhibition constant K_I for α-methylglucoside in M9 medium

Strain	Plasmid molecular weight (MD)	μ_{max} (1/hr.)	K_S (MG/L)	K_I (MG/L)	$\bar{Y}\left(\frac{\text{g cell}}{\text{g glucose}}\right)$
HB101	-	0.42±0.01	14.0±3.8	5.53±0.44	0.35±0.02
pDM247	5.85	0.38±0.01	11.9±1.7	9.11±1.15	0.32±0.02
pDM246	5.68	0.36±0.01	15.5±2.6	7.74±1.49	0.31±0.02
RSF1050	5.50	0.36±0.02	17.7±5.9	5.91±0.8	0.30±0.02
pDM248	5.69	0.32±0.01	16.1±4.9	9.83±1.05	0.28±0.02
pFH118	5.51	0.27±0.02	13.9±1.5	11.3±11.3	0.25±0.02

Figure Captions

Figure 1: Genealogy of the plasmids used in this study and the RNA I genes included in each.

Figure 2: Experimentally determined cellular plasmid content as a function of specific growth rate of *E. coli* HB101 with plasmids pDM246 (▲) and pDM247 (●). Lines drawn to illustrate trends.

Figure 3: Inverse of specific growth rate of *E. coli* HB101:pDM246 versus the ratio of competitive inhibitor (α–methylglucoside) to glucose concentration. Line corresponds to Eq. (2) with K_I and μ_{max} from Table III. (▲= 1 g glucose/L; ●= 2 g glucose/L).

Figure 4: Dependence of specific activity of the cloned-gene product (β-lactamase) on specific growth rate for *E. coli* HB101 containing plasmids pDM247 (▲), pDM246 (●), and RSF1050 (■). Reference copy numbers are given in parentheses. Lines show trends.

Figure 5: Variation of β-lactamase specific activity with number of plasmids per cell. Data near curve A illustrate this relationship for pDM247 (Δ) and pDM246 (▲) in different media which support different growth rates. Data (O) following the trend indicated by curve B are for different recombinant strains all grown in LB medium.

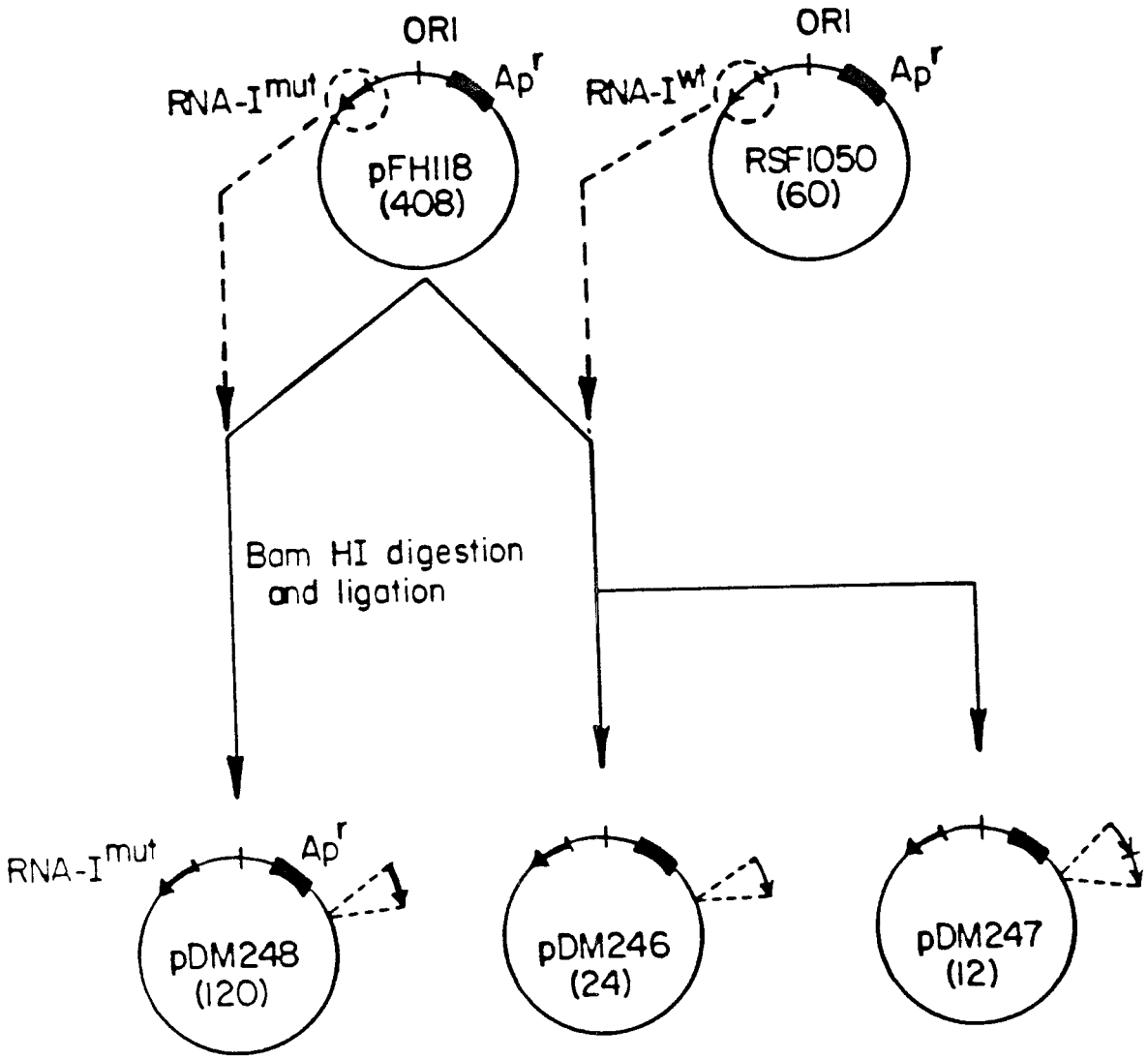
ORI
RNA-I mut
Ap r
pFH118
(408)
ORI
RNA-I wt
Ap r
RSF1050
(60)
Bam HI digestion
and ligation
RNA-I mut
Ap r
pDM248
(120)
pDM246
(24)
pDM247
(12)

FIGURE 1

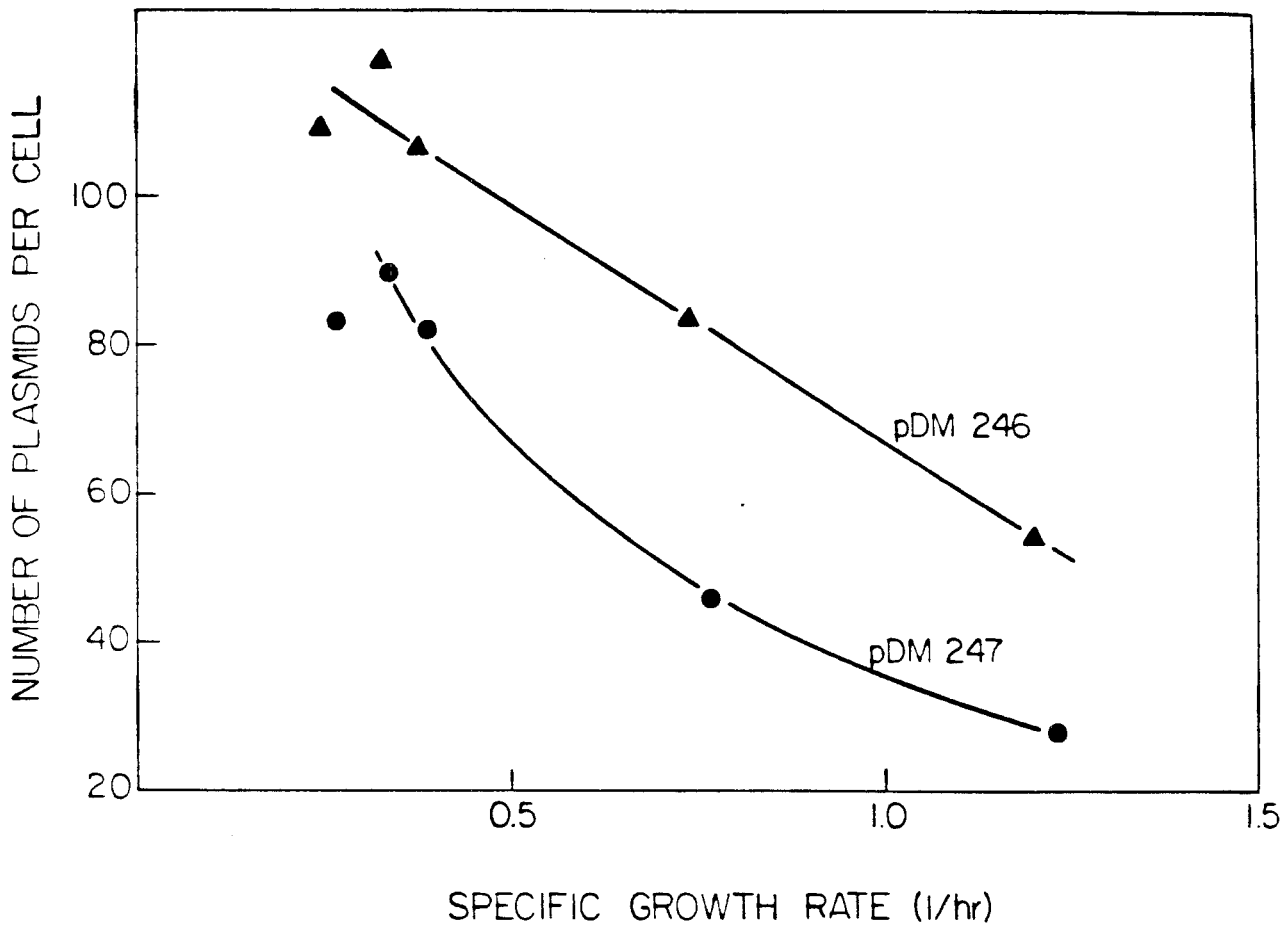
NUMBER OF PLASMIDS PER CELL
100
80
60
40
20
0.5
1.0
1.5
SPECIFIC GROWTH RATE (1/hr)
pDM 246
pDM 247

FIGURE 2

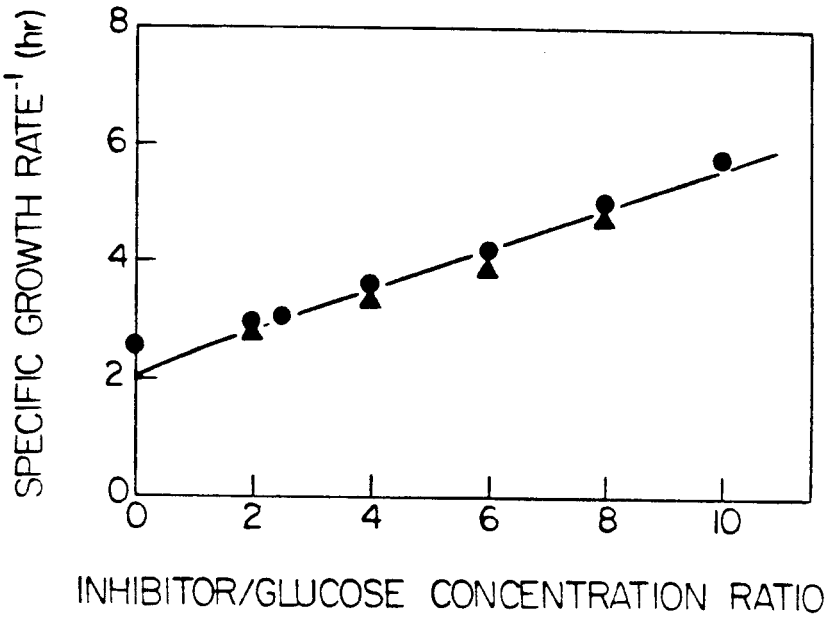
SPECIFIC GROWTH RATE^{-1} (hr)
0
2
4
6
8
0
2
4
6
8
10
INHIBITOR/GLUCOSE CONCENTRATION RATIO

FIGURE 3

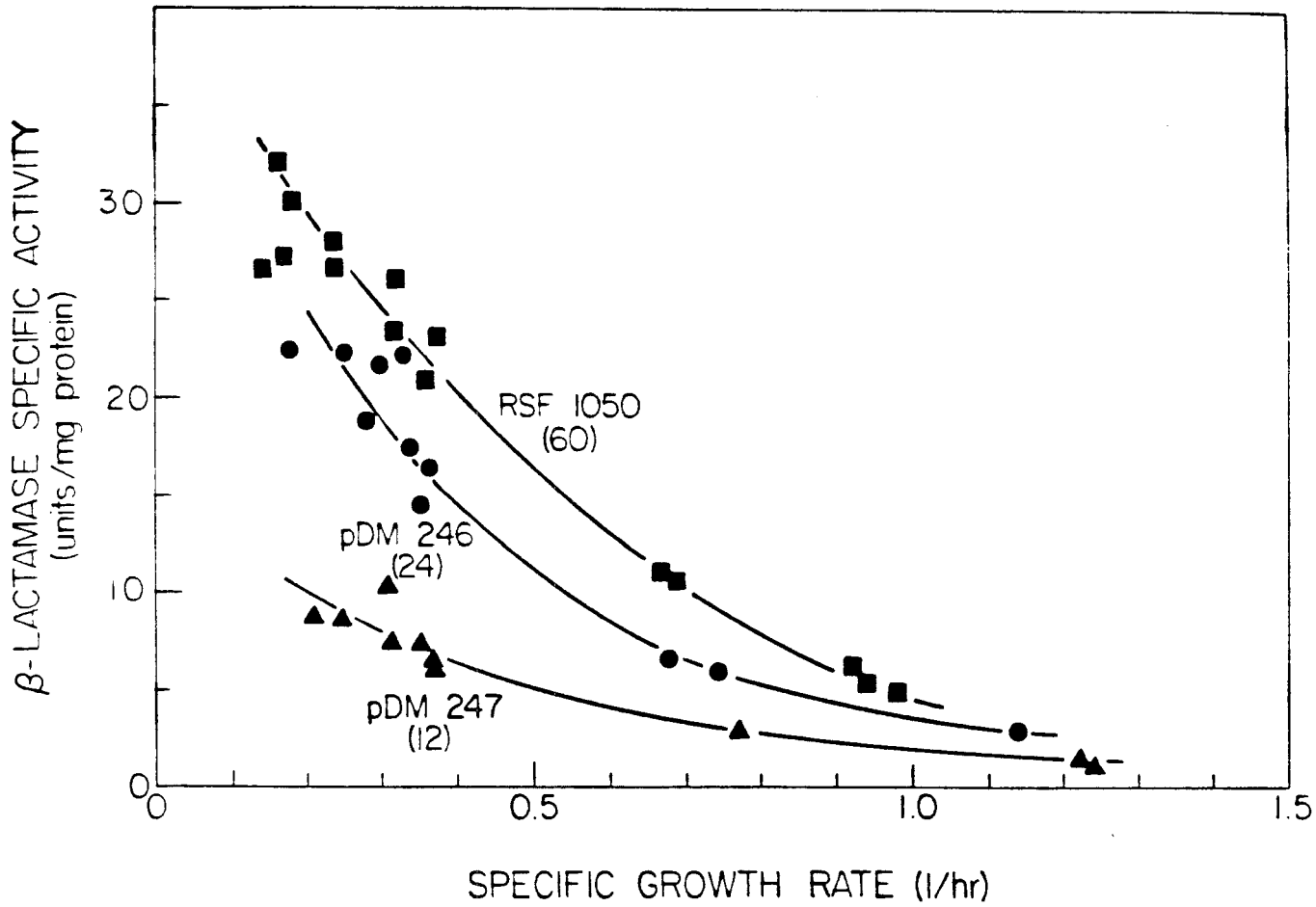
β-LACTAMASE SPECIFIC ACTIVITY
(units/mg protein)
30
20
10
0
0
0.5
1.0
1.5
SPECIFIC GROWTH RATE (1/hr)
RSF 1050
(60)
pDM 246
(24)
pDM 247
(12)

FIGURE 4

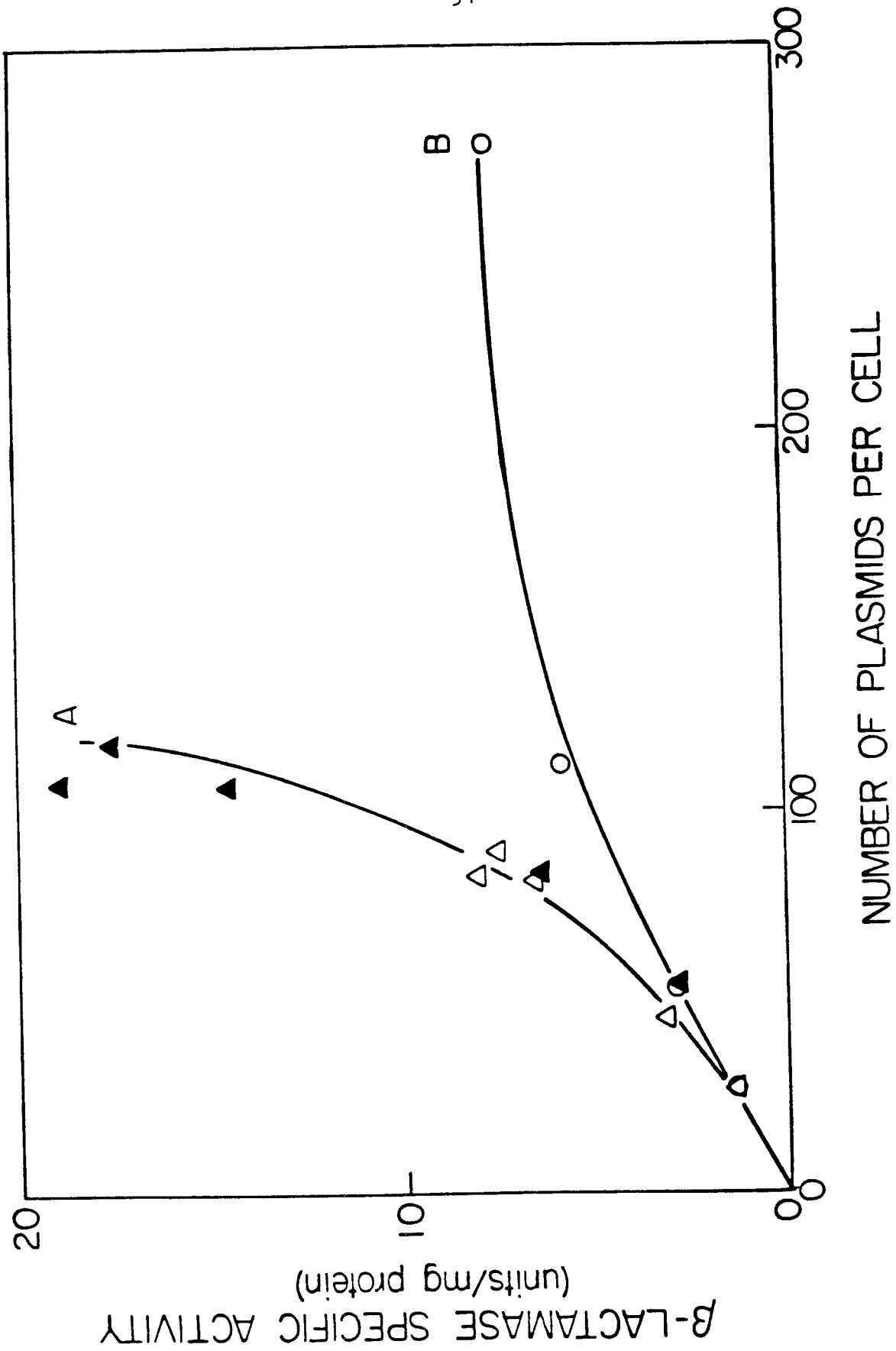
β-LACTAMASE SPECIFIC ACTIVITY
(units/mg protein)
20
10
0
0
100
200
300
NUMBER OF PLASMIDS PER CELL
A
B

Figure 5

CHAPTER 2: CONTINUOUS CULTIVATION OF RECOMBINANT *Escherichia coli*: EXISTENCE OF AN OPTIMUM DILUTION RATE FOR MAXIMUM GENE PRODUCT CONCENTRATION

INTRODUCTION

Investigations of environmental effects on host-plasmid interactions in batch cultivation have already been done for recombinant *Escherichia coli* strains containing a series of plasmid copy number mutants [1]. In particular, quantitative relationships between plasmid content, host-cell growth rate, and cloned-gene product accumulation were obtained. The experimental information implies that both the number of plasmid copies per cell and growth conditions are important in determining the amount of the cloned gene product accumulation in the cell. In other words, specific growth rate along with plasmid content should be considered as a determinant of productivity of recombinant DNA systems.

The objective of this study is experimental characterization of the effect of environmental conditions on physiological properties, plasmid content, and cloned-gene product in recombinant *E. coli* cells using a continuous fermentor. A typical approach is to use different medium composition to obtain different growth rates [1]. However, changes in growth medium may evoke alterations in control of expression of various genes and also in DNA and protein biosynthesis. In order to evaluate environmental effects under well-defined experimental conditions, a continuous culture system was used and dilution rate was altered in order to obtain different specific growth rates. The population parameters determined as a function of dilution rate include yield factor, plasmid content, activity of β-lactamase (cloned-gene product), and overall productivity of recombnant cells. The results obtained from chemostat experiments have been compared with measurements from batch experiments using the same recombinant strain.

MATERIALS AND METHODS

Bacterial Strains and Growth Conditions

Host *E. coli* strain HB101 ($Pro^-Leu^-Thi^-RecA^-$) transformed with the plasmid pDM246 was used throughout this study [1,2]. The plasmid pDM246 is a derivative of plasmid pMB1 and contains a gene for the β-lactamase enzyme. M9 medium supplemented with 2 g/L glucose, 4 g/L Casamino Acids (Difco, Detriot, MI), and 0.2 g/L thiamine HCl, termed M9C, was used for batch inoculum growth and continuous culture [3]. Ampicillin-containing plates were made by adding 50 mg/L ampicillin (Sigma, St.Louis, Mo) to Luria broth solidified with 15 g/L agar [1]. Cells were preincubated overnight in a medium containing 1 mg/ml Amp. The preincubated cells were inoculated into a prewarmed fermentor. A Bioflo model C30 fermentor (New Brunswick, Edison, NJ) with a working volume of 330 ml was employed for continuous experiments. The temperature of the vessel was maintained at 37°C with a temperature controller included in the system. The pH was controlled at 7.0 by buffering the medium with phosphate buffer. Steady-state was assumed when the culture optical density (590 nm) was constant which occurred after three mean residence times had passed. The flow rate was determined by measuring effluent from the vessel with a graduated cylinder.

Assays

Yield Coefficient

Dry weight of recombinant cells was measured by the filtration method. 20 ml of sample were filtered on a preweighed 25 mm diameter 0.22 μm Milli-

pore membrane filter and then washed with an equal volume of distilled water. Following the wash, samples were dried for several hours at 90°C in an oven. Glucose concentration in supernatant after centrifugation of broth was determined using Sigma Glucose Kit comprised of glucose oxidase and peroxdase. Yield coefficient, $Y_{x/s}$, is defined as g dry cell mass per g glucose consumed.

β-Lactamase Activity

Preparation of samples and determination of activity have been described in the previous paper [1]. Sample preparation involved a modification of the method used by Yamamoto *et al* [4]. The activity of β-lactamase was assayed by the iodometric method [5,6]. The method used in this study determines total content of β-lactamase present in the cells. One unit of β-lactamase activity is defined as the quantity that hydrolyzes 1 μmole of benzyl penicillin per min at 30°C . After measuring total cellular protein using Sigma Protein Kit No. 690, the specific activity of β-lactamase (activity per mg of cellular protein) was calulated.

Plasmid Content

Plasmid content in the samples taken at different dilution rates was determined by the modified method of Moser and Campbell [2]. Culture samples were diluted with fresh medium to give the same optical density readings at 590 nm. The plasmid content was determined by comparing fluorescence intensity of the samples with that of anHin III digest of λ plasmid used as a standard. 100 ng of λ plasmid were loaded on the gel. Band densities in negatives of gel photographs were determined using a scanning densitometer

(Hoefer Sci. Instru., San Francisco, CA) connected with a digital integrator (Model C-R 3A, Shimazu Corp., Kyoto, Japan).

RESULTS

Growth Properties

Instability of plasmids produces plasmid-free segregants such that the fraction of the plasmid- containing cells decreases from unity initially to smaller values as fermentation proceeds. Therefore, it is necessary to examine plasmid stability in carrying out experiments with recombinant cells and interpreting the results. Cell numbers were counted by spreading culture samples in Amp-containing (selective) and Amp-free (nonselective) plates after serial dilutions. Colonies on the selective plates represent the plasmid- containing cells, while colonies on the nonselective plates denote total viable cells. The numbers of colonies on the different plates are equivalent only for the case of stable plasmids.

As Table 1 lists, cell numbers determined on selective and nonselective plates yield essentially identical counts, implying that the plasmid pDM246 used has segregational stability in the *E. coli* HB101 host. In addition, gel electrophoresis of the plasmid DNA purified from culture at different dilution rates showed the same location relative to a λ plasmid used as a size standard, indicating overall structural stability (i.e., no major deletions; changes in nucleotide sequence are not precluded) of the plasmid pDM 246 (Figure 2). Thus, the plasmid pDM246 shows highly stable behavior during propagation of recombinant cells.

Figure 1 illustrates the yield factor of glucose as a function of dilution rate. Yield coefficient decreases as dilution rate increases over the range studied.

Plasmid Content at Different Dilution Rates

Quantitative determinations of plasmid content were made from electrophoretic analysis of plasmid DNA. The fluorescence pattern of a 0.9 % agarose gel after staining plasmid DNA with ethidium bromide is shown in Figure 2. All plasmid DNAs isolated from the different samples have the same size. The lower band in each sample lane corresponds to plasmid DNA.

Plasmid contents are plotted in Figure 3 as a function of dilution rate. The overall trend is that plasmid content exhibits a maximum near the lowest dilution rates investigated and then decreases as dilution rate increases beyond this point. Such a maximum in plasmid content with respect to specific growth rate was suggested from the earlier study in which different media were used to vary specific growth rate [1]. The previous experimental data for these batch experiments with the HB101:pDM246 strain are included in Figure 3 for comparison. Interestingly, although the experimental strategies employed are different, the resulting responses of plasmid content with respect to environmental variations agree qualitatively well with each other. Decreasing plasmid content for increasing specific growth rate has been observed in batch experiments with *E. coli* harboring R1 plasmid [7] and continuous culture of *E. coli* with ColE1-like plasmid pPLc23 *trpA1* [8], and simulated by a mechanistic computer model for plasmid λdv replication [9].

Cloned-Gene Product Formation

The amount of β-lactamase expressed from the plasmid DNA was measured for samples taken at different dilution rates. Figure 4 diagrams the effect of dilution rate on the activity of β- lactamase based on ml of culture broth. The gene product concentration has a maximum at a dilution rate of 0.4 hr^{-1} . This pattern is consistent with the relationship between plasmid content and dilution rate determined under the same conditions (Figure 3). Productivity, defined as the dilution rate times the amount of β-lactamase per ml of culture, also shows a maximum of 3.4 units per ml of culture per hr at a dilution rate of 0.5 hr^{-1}. This finding clearly demonstrates the existence of an optimum dilution rate to maximize product concentration and productivity. An optimum specific growth rate was suggested in studies of *E. coli* with plasmids containing the *lac* promoter-operator function using molecular mechanistic models [9].

The specific activity of β-lactamase based on total cellular protein is shown as a function of dilution rate in Figure 5. Figure 5 also depicts the specific activity of β-lactamase determined at different specific growth rates in a batch reactor. The solid lines were drawn to show the trends. In the batch experiments, specific growth rate was changed by altering growth medium. The results obtained through these two modes of growth rate manipulation exhibit qualitatively different trends. The chemostat data show a maximum in specific activity with respect to dilution rate, whereas the batch data illustrate a progressive decrease in specific activity with specific growth rate.

It is noteworthy that 0.6 $\frac{\text{unit}}{\text{ml}}$ of β-lactamase activity was found in fermentaton broth from the sample taken at dilution rate 0.34 hr^{-1}. This

corresponds to about 7 % of the β-lactamase activity accumulated in the cells. It is unclear whether the presence of the enzyme in the broth is due to cell lysis or leakage from the cells.

DISCUSSION

In this work, environmental effects on host-plasmid interactions in recombinant *E. coli* were explored using a continuous fermentation process. Cell growth yield factor based on glucose declines as dilution rate increases. Both plasmid content and cloned-gene product concentration exhibit maxima with respect to dilution rate. This study has experimentally demonstrated the existence of an optimum operating condition for maximum productivity.

The trend of dilution rate effects on yield coefficient observed in these experiments is interesting and unexpected. Here, the yield coefficient decreases for larger values of dilution rate. According to the classical model of Pirt based upon substrate utilization for maintenance [10], measured overall yield coefficient increases with increasing dilution rate. For recombinant cells, specific growth rate may indirectly alter yield by changing the plasmid copy number, thereby altering cell composition. Theoretical analysis of maximum yield factors for recombinant cells gives the intuitively reasonable conclusion that growth yields are reduced by larger plasmid content and more plasmid gene expression [11]. Previous experimental studies of overall yield coefficients for recombinant *E. coli* have shown decreasing yield factor for increasing plasmid content per cell for ColE1-like plasmids [1] and R1 plasmid [12]. Since the effect of increasing specific growth rate is

to decrease plasmid content over most of the growth rates considered, it is expected in this connection that growth yields would increase as dilution rate increases. The contrary experimentally observed trend suggests that true growth yield and/or maintenance requirements are changing with specific growth rate for these recombinant cells.

It is interesting to compare experimental data obtained in chemostat cultivation with those measured in a batch mode. The response of plasmid content to change in specific growth rate is qualitatively similar for these different operating regimes. However, the response of product accumulation to growth rate change differs depending on reactor operating mode. Differences in product formation between batch and continuous experiments may result from differences in the cell's physiological states and regulatory pathways in the two reactor configurations. This comparison illustrates the difficulties in interpretation and generalization of experimental data on growth rate effect on protein biosynthesis, and, in particular, cloned-gene product formation.

REFERENCES

1. Seo, J.H. and J.E. Bailey, *Biotech. Bioeng.*, in press (1985)

2. Moser, D.R., and J.L. Cambell, *J. Bacteriol.*, **154** , 809 (1983)

3. Rodriguez, R., and R.C. Tait, in *Recombinant DNA Techniques : An Introduction*, Addison-Wesley Pub. Co. (1983)

4. Yamamoto, T., S. Yamagata, K. Horii, and S. Yamagishi, *J. Bacteriol.*, **150** , 269 (1982)

5. Sargent, M.G., *J. Bacteriol.*, **95** , 1493 (1968)

6. Sawai, T., I. Takahashi, and S. Yamagishi, *Antimicro. Agents Chemothr.*, **13** , 269 (1978)

7. Engberg, B., and K. Nordstrom, *J. Bacteriol.*, **123** , 179 (1975)

8. Siegel,R., and D.Y. Ryu, *Biotech. Bioeng.*, **27** , 28 (1985)

9. Lee, S.B., and J.E. Bailey, *Biotech. Bioeng.*, **26** , 66 (1984)

10. Pirt, S.J., *Proc. Roy. Soc., B.*, **163** , 224 (1965)

11. Da Silva, N.A., and J.E. Bailey, *Biotech. Bioeng.*, in press (1985)

12. Klemperer, R., N. Ismail, and M. Brown, *J. Gen. Microbiol.*, **115** , 325 (1978)

Table I

Number of cells in amp-free and amp-containing plates, optical density at 590 nm, and dry cell weight determined at various dilution rates

Dilution rate (hr^{-1})	Cell number per unit		O.D. at 590 nm	Dry cell weight (g-cell/g·l-culture)
	Amp^-	Amp^+		
0.23	2.02×10^9	1.94×10^9	0.985	1.16
0.34	1.67	1.83	0.929	1.14
0.44	1.47	1.69	0.869	0.94
0.57	1.47	1.17	0.782	0.86
0.59	1.04	1.11	0.770	0.81
0.64	0.19	0.20	0.173	0.19

FIGURE CAPTIONS

Figure 1 Dependence of yield factor on dilution rate. The yield factor was measured as g dry cell mass per g glucose consumed.

Figure 2 Comparison of plasmid content. 100 ng of the Hin III digest of λ plasmid was used as a standard (lane 1). The plasmid shown in lane 2 was isolated from cells exponentially growing in M9C medium in batch culture at 37°C . The plasmids in lane 3 through 7 were separated from the samples at dilution rates as indicated in the figure. The lower band in each lane except lane 1 represents supercoiled plasmid DNA, and the upper band is chromosomal DNA.

Figure 3 Experimentally determined cellular plasmid content as a function of dilution rate (●) and specific growth rate (▲). The batch data are from Ref.(1).

Figure 4 Effect of dilution rate on β-lactamase activity per unit volume of culture (●) and on the productivity of chemostat (▲). The productivity is defined as dilution rate times β-lactamase activity per culture volume.

Figure 5 Comparison of the specific activity of β-lactamase - specific growth rate relationship between continuous (●) and batch (▲) experiments. The specific activity of β-lactamase is defined as overall activity divided by total cellular protein.

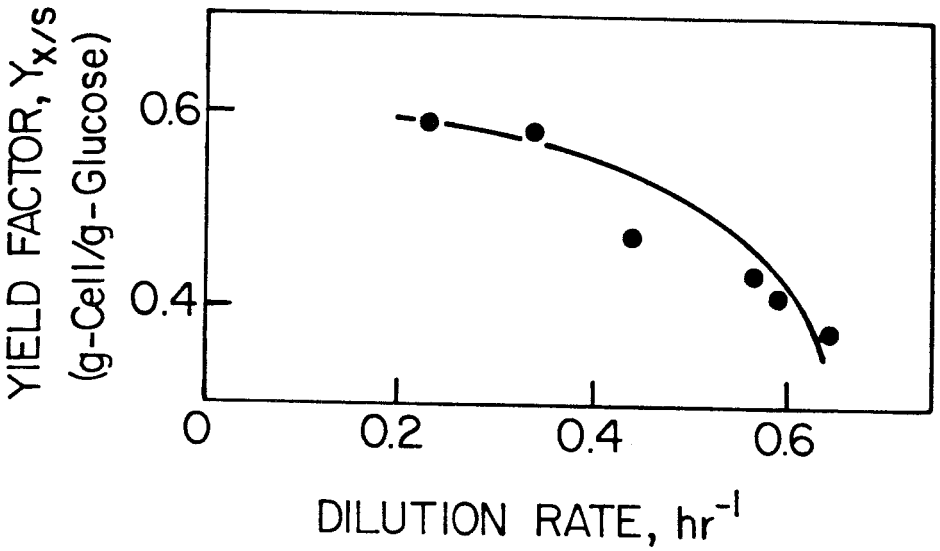
YIELD FACTOR, $Y_{x/s}$
(g-Cell/g-Glucose)
0.6
0.4
0
0.2
0.4
0.6
DILUTION RATE, hr^{-1}

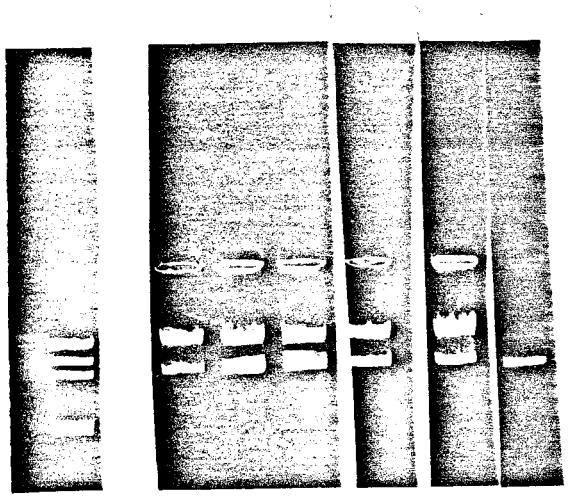

Lane	Plasmid DNA
1	Hind III Digest of λ Plasmid
2	pDM246 from Batch Culture
3	pDM246 at D = 0.23 hr^{-1}
4	pDM246 at D = 0.34 hr^{-1}
5	pDM246 at D = 0.44 hr^{-1}
6	pDM246 at D = 0.56 hr^{-1}
7	pDM246 at D = 0.59 hr^{-1}

Figure 2

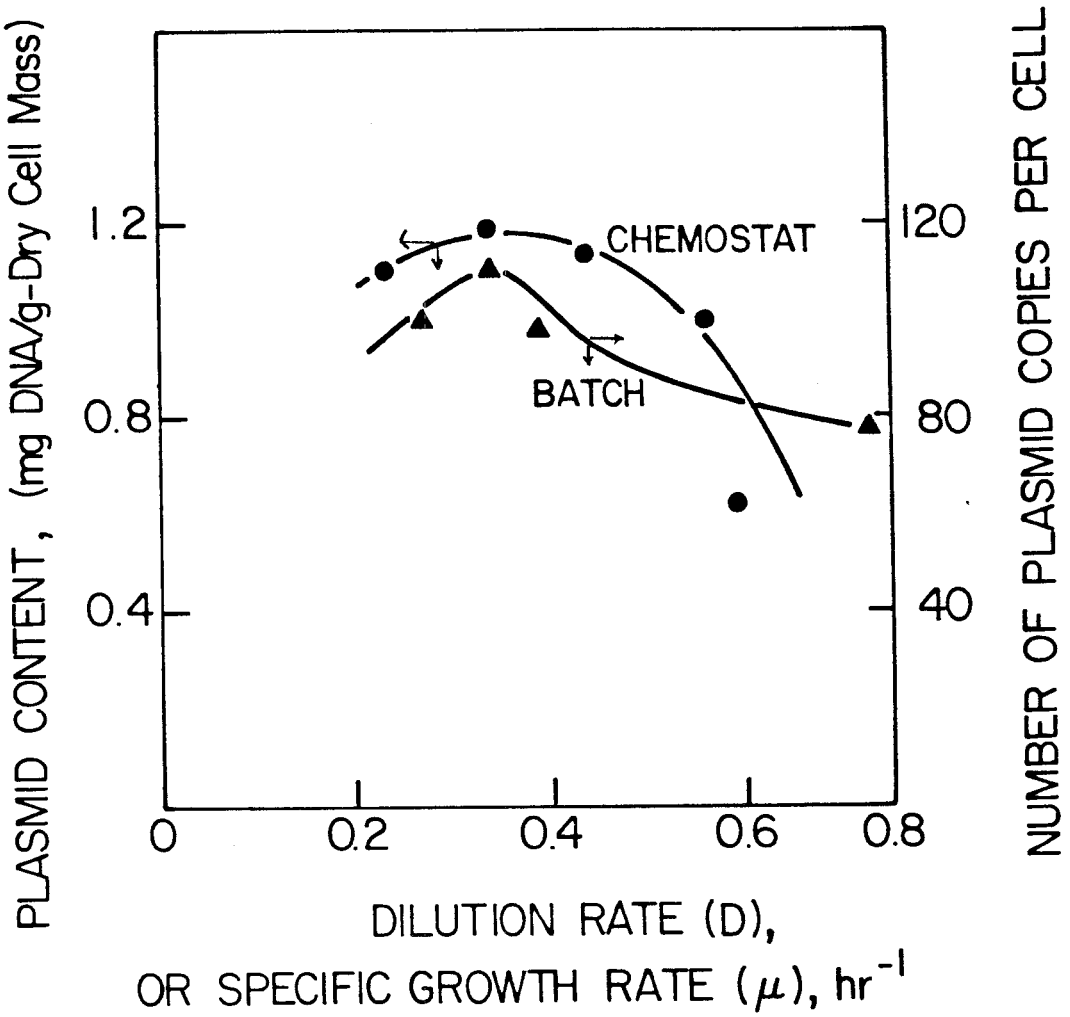
PLASMID CONTENT, (mg DNA/g-Dry Cell Mass)
1.2
0.8
0.4
120
80
40
CHEMOSTAT
BATCH
0
0.2
0.4
0.6
0.8
NUMBER OF PLASMID COPIES PER CELL
DILUTION RATE (D),
OR SPECIFIC GROWTH RATE (μ), hr⁻¹

Figure 3

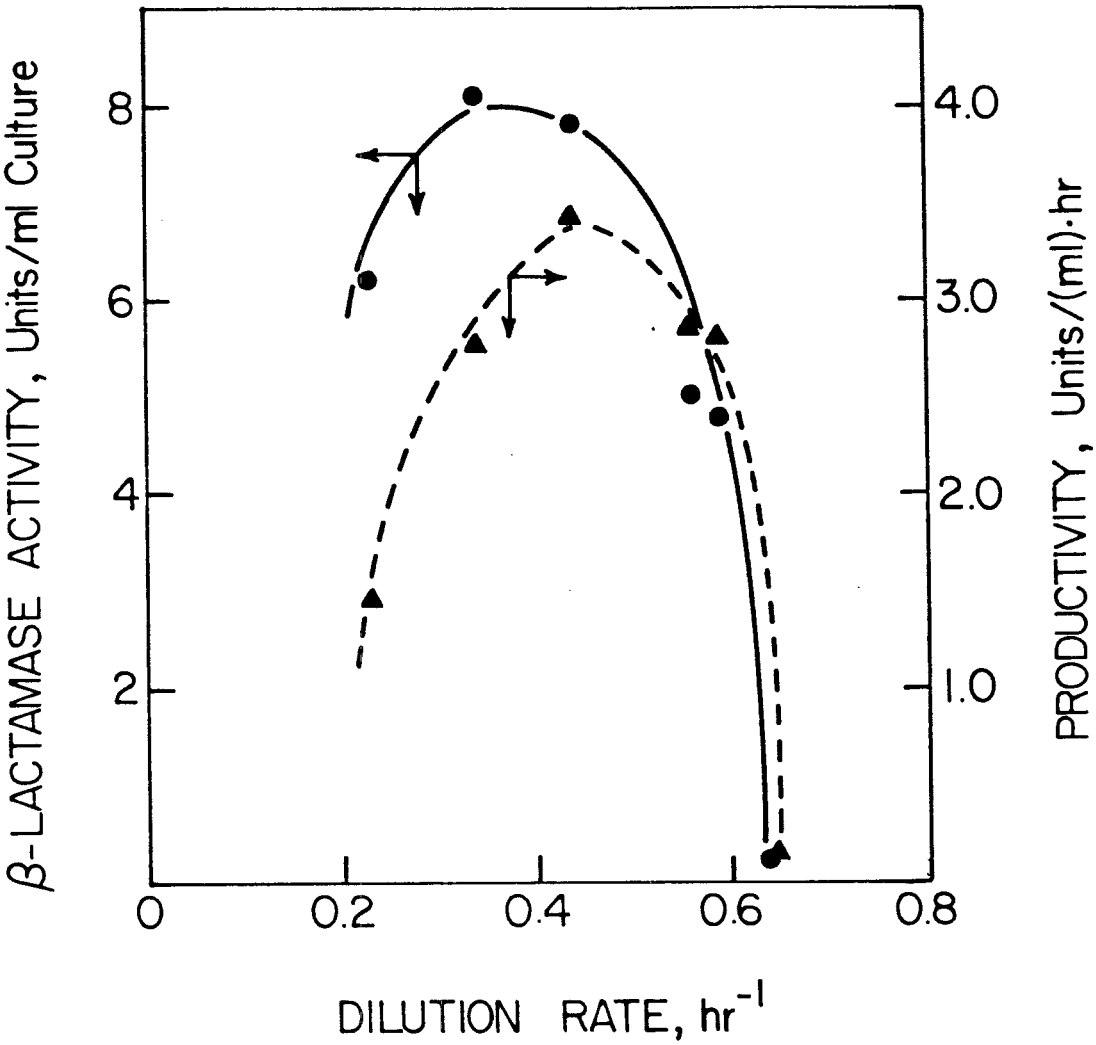
β-LACTAMASE ACTIVITY, Units/ml Culture
PRODUCTIVITY, Units/(ml)·hr
DILUTION RATE, hr⁻¹
0
0.2
0.4
0.6
0.8
2
4
6
8
1.0
2.0
3.0
4.0

Figure 4

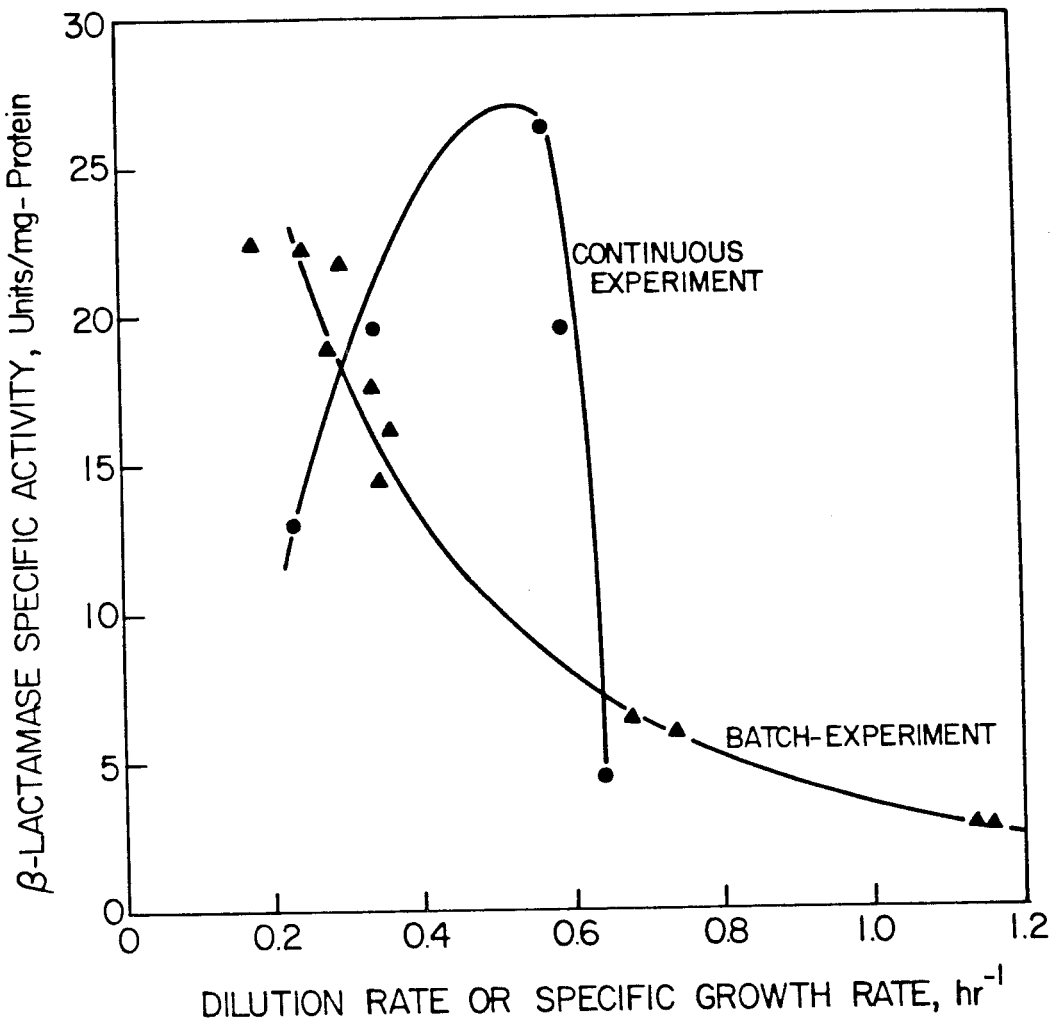
30
25
20
15
10
5
0
0
0.2
0.4
0.6
0.8
1.0
1.2
β-LACTAMASE SPECIFIC ACTIVITY, Units/mg-Protein
DILUTION RATE OR SPECIFIC GROWTH RATE, hr⁻¹
CONTINUOUS EXPERIMENT
BATCH-EXPERIMENT

Figure 5

CHAPTER 3: FLOW CYTOMETRY ANALYSIS OF PLASMID AMPLIFICATION IN *Escherichia coli*

(The text of Chapter 3 consists of an article which will appear in *Biotechnol. Prog.*, in press (1985).)

SUMMARY

Large quantities of cloned DNAs for use in characterization or in subsequent recombinant plasmid construction may be obtained by plasmid amplification, which is the increase of cellular plasmid DNA content relative to the amount of host cell chromosomal DNA. Plasmid amplification has been investigated with flow cytometry in chloramphenicol (Cm) treated cell populations of *Escherichia coli* HB101 carrying plasmids with pMB1 replication origins at different copy number levels ranging from 12 to 122. The flow cytometry method is based on the determination of the total cellular DNA content after staining with mithramycin, a DNA-specific fluorescent dye. This method permits direct measurements of the rate of plasmid amplification and classification of cell populations according to chromosomal replication forks at the time of Cm treatment. Both initial rates of plasmid amplification and final contents of amplified plasmids were found to be proportional to the average initial plasmid copy numbers. The maximum degree of amplification , defined as the ratio of plasmid content after 18 hours' incubation to the preamplificaton plasmid content at steady-state growth, was approximately equal for the strains studied. Larger cells with four active chromosomal replication forks at Cm addition exhibit faster plasmid replication rates than cells initially at earlier cell cycle states. A kinetic model was proposed which agrees well with the present and previous experimental observations. This work clearly demonstrates the advantage of flow cytometry for experimental analysis of plasmid propagation in recombinant organisms.

INTRODUCTION

Plasmid amplification is a common technique used for preparation of recombinant plasmids in large quantities and for overproduction of the plasmid-encoded gene product. The methods frequently used for amplification are amino acid starvation [1], chloramphenicol addition [2], and temperature shift [3]. Shifting to a nonpermissive temperature can cause runaway replication of plasmid containing a temperature-sensitive replication control [3,4,5]. When protein synthesis is inhibited by either amino acid starvation or chloramphenicol (Cm) addition, initiation of chromosomal DNA is prevented and on-going chromosomal replication is completed. However, plasmids containing ColE1 types of replication origins continue to replicate up to a level determined by growth conditions, yielding an increase in plasmid content relative to the chromosomal DNA [6,7,8]. This occurs because ColE1 and other relaxed replication plasmids do not require any plasmid-encoded proteins for replication *in vivo* [7,8,9]. These amplifiable plasmids have served as popular vectors for cloning of genes as well as convenient means for investigating biochemical mechanisms involved in plasmid replication [9,10].

Previous investigations of plasmid replication kinetics in the presence of Cm included purification of plasmid DNA through several density gradient centrifugations and measurement of radioactively labelled plasmid and chromosomal DNAs in the corresponding bands [6,7,8]. The degree of plasmid amplification was given as the $^{3}H/\ ^{14}C$ ratio of plasmid DNA after cells grown initially in a [^{14}C] thymine-harboring medium were resuspended in a growth medium containing [^{3}H] thymine and Cm [3,6]. These methods have the disadvantage of requiring isotopic labels, involve lengthy protocols, and they

cannot differentiate amplification characteristics of different cell subpopulations.

In this work, we describe a new experimental technique based on flow cytometry enabling convenient determination of plasmid amplification in *E. coli* . The entire DNA content of individual cells is determined after staining the DNA with mithramycin, a DNA-specific fluorescence dye [11]. Plasmid DNA normally represents only a minor fraction of the total DNA of a cell such that one cannot expect a significant difference between the single-cell DNA content distributions of exponentially growing plasmid-free and plasmid-containing cell populations. In addition, the interpretation of such histograms is difficult since the plasmid content affects the host-cell generation time, which influences the chromosome content.

However, the addition of Cm to a growing *E. coli* population causes cells to stop chromosome initiation and allows only completion of active replication cycles [2,6]. After chromosomal replication is terminated, any further increase in cellular DNA content can be attributed exclusively to plasmid DNA . Large plasmid contents achieved during amplification perturb the distribution of single-cell DNA content sufficiently to permit flow cytometric analysis of amplification based on total DNA measurements. In order to relate amplification rate to plasmid content, a series of pMB1-type plasmids propagated by *E. coli* at different copy numbers has been studied.

MATERIALS AND METHODS

Bacterial Strains and Plasmids

Throughout this study *Escherichia coli* HB101 ($Pro^{-}Leu^{-}Thi^{-}RecA^{-}$) was used as a host strain for the plasmids pDM247, pDM246, RSF1050, and pDM248 [12,13]. The copy numbers of plasmids (number of plasmid copies per chromosome equivalent) in *E. coli* HB101 in Luria broth medium are given in Table 1 [12]. All plasmids contain the β-lactamase gene. The plasmids are nearly identical except the type and number of gene copies for RNA I, the plasmid-specified inhibitor of replication [13].

Media and Cultivation

Growth media used are Luria broth buffered at pH 7.0 with phosphate buffer (LB) [14] and M9 minimal medium complemented with 0.4% Casamino Acids and 0.2 mg/L thiamine HCl (M9C) [12]. Glucose (2 g/L) was used as a carbon source in all media. Cells were preincubated at 37°C in a growth medium containing sufficient ampicillin (Na-salt, Sigma Chemical, St.Louis, Mo) to ensure maintenance of plasmid copy number in the cells. 0.5 ml of preincubated cells were inoculated into 50 ml of prewarmed medium at 37°C in 250 ml Erlenmeyer flask and aerated in a shaker [New Brunswick Sci., Edison, NJ]. Growth rate was monitored by measuring the optical density with a Klett-Summerson spectrometer with a green filter. When grown to the mid-exponential phase, 200 mg/L chloramphenicol (Sigma) was added to stop protein synthesis. The pH of the medium remained constant during incubation.

Fixation and DNA Staining

Samples taken at different intervals after Cm addition were immediately fixed with 10 volumes of ice-cold 70% ethanol and stored in a refrigerator overnight. DNA staining procedures followed the method described by Steen *et al.* [11]. The fixed cells were washed once in 0.1 M Tris buffer (pH 7.4), sedimented by centrifugation and resuspended in the DNA staining solution containing 100 mg/L mithramycin (Sigma) dissolved in 0.1 M Tris buffer (pH 7.4) with 25 mM $MgCl_2$ and 100 mM NaCl. The stained cells were immediately used for flow cytometry analysis.

Flow Cytometry Analysis

DNA-associated fluorescence and light-scattering intensities from individual cells were analyzed on a flow cytometer (Model 50 H, Ortho Instruments, Westwood, MA) with an argon-ion laser tuned at 456 nm and 0.1 W. Distributions were obtained by measuring fluorescent intensities and light-scattering characteristics generated by 10^5 cells of a flow rate of approximately 2000 cells/sec. Data acquisition and analyses were done on a Cytomic 12 computer (Kratel GbmH, Stuttgart, FRG) equipped with a plotter (Model CX-4800, Itoh Elect. Corp.) and a printer (Okidata).

RESULTS

Single-Cell DNA Distribution

Mithramycin was used for DNA staining in *E. coli* cells. This stain is known to bind to the cellular DNA specifically and quantitatively giving proportionality between fluorescent intensity and DNA content [11]. Figure 1 shows an experimentally determined dual parameter (mithramycin fluorescence - light scatttering) frequency function for *E. coli* HB101 cells exponentially grown in LB medium at 37°C . Also illustrated in the back panel is the single-parameter DNA fluorescence histogram, which was obtained by integration over the entire range of light-scattering coordinates. It has been demonstrated in a related flow cytometry instrument that the light-scattering signal, which is a measure of cell size, is linearly proportional to the total cellular protein content determined by staining with fluorescein isothiocyanate (FITC) [15].

In order to convert the single-cell DNA content from measurements in channel number to values in chromosome equivalents, it is necessary to compare the fluorescence signals with known cellular DNA contents. For this purpose Cm was added to an exponentially growing culture of (plasmid-free) *E. coli* HB101. As stated earlier, the Cm-treated cells ultimately reach an integer number of full chromosomes by completing the round of replication in progress at the point of Cm addition (although at slower rate than the normal chromosome replication rate [16]) . The dual parameter flow cytometry data and single-cell DNA distribution of HB101 cells grown in Cm for 4 hours are given in Figure 2 . Two peaks in Figure 2 correspond to those of 2 and 4 genome equivalents (G), respectively. Based on this type of meas-

urement, a calibration factor of channels/genome equivalent was determined for each experimental run.

Using this calibration, the mean DNA content per cell can be determined after calculating the average channel number from flow cytometry single-cell DNA fluorescence measurements. The average DNA content of each strain at balanced growth has been compared with that calculated theoretically using the Cooper-Helmstetter equation [17], the observed generation time of the corresponding strain, and values of C = 40 min and D = 20 min typical for many *E. coli* strains . Table 1 summarizes results for *E. coli* HB101 strains grown in LB and M9C media and plasmid-containing HB101 strains grown in LB medium. The experimental chromosomal DNA content results for plasmid-free HB101 cells grown in two different media agree nicely with the theoretical values. However, the average chromosome contents of plasmid-containing cells are lower than the corresponding theoretical values after taking into consideration the contributions of plasmid DNA in the total DNA content. The discrepancy between experimental and theoretical results is presumably due to difference in cell cycle parameters between the host cell and the host cell with plasmids. Smaller values of the average chromosome content per cell for a certain generation time correspond to reduced values of the C and/or D periods in the Cooper-Helmstetter model.

Kinetics of Plasmid Amplification

Total DNA including amplified plasmid and chromosomal DNA was determined using flow cytometry at different times after Cm was added. Assay of total DNA is useful in this case since the *E. coli* chromosome is relatively small and the plasmid DNA can be amplified by more than one genome

equivalent so that the total DNA content is significantly increased. Furthermore, it was observed for HB101 cells that increase in DNA content contributed by chromosomal replication is negligible after 3-4 hours exposure to Cm . Beyond this time, all increase is solely due to plasmid amplification. Hereafter, the time basis used is time elapsed after Cm addition. Figure 3 highlights the time-course of DNA distributions for HB101 containing pDM248 (copy number before amplification = 122). Single-cell DNA distributions at different times for other strains are depicted in Figure 4.

Within 2-3 hours in all cases, the unimodal DNA distribution at steady-state has developed into two sharp modes representing cells containing 2 and 4 genome equivalents plus amplified plasmid DNA, respectively. Further incubation results in broadening and shifting of the modes towards greater fluorescence intensity. This effect is more evident in high copy number strains. The propagation of the first mode is plotted against time in Figure 5. Here, channel numbers of the first mode for plasmid-containing strains are normalized by the two-chromosome channel number determined from a control experimental with the plasmid-free HB101 strain. The cells accumulated in the first mode have 2 genome equivalents plus amplified plasmid DNA. As the fraction of cells in the first mode constitutes the majority of the distribution, the time trajectory of the first mode is indicative of the change of total DNA content.

The rate of plasmid replication in the presence of Cm, determined from the slope of total DNA increase with time after 4 hours, is proportional to the initial copy number (Figure 6). This is reasonable since, prior to amplification, rates of replication of higher copy number plasmids must be greater. At a stably maintained plasmid content, the average replication

rate is equal to average number of plasmids per cell/average time between cell divisions. The rates of plasmid replication given in Figure 6 are slightly lower than the average rate which obtains at steady-state growth prior to amplification. These preamplification rates of the strains considered are plotted as a dotted line in Figure 6.

It was difficult to determine the initial rate of plasmid amplification from measurements of total DNA content with flow cytometry because the increase in plasmid DNA content for an early period was masked by the chromosomal DNA synthesis. Clewell [6] has investigated amplification of ColE1 plasmids in different growth media using the experimental method described earlier. He has observed exponential increase in plasmid DNA content and transient stimulation of replication rate for the first 4 hours upon Cm addition. Investigation of CloDF13 plasmid synthesis in chromosome-free minicells has revealed an enhanced rate of replication after Cm addition [10]. Crosa *et al.* [8] have explored amplification of plasmid RSF1030 in M9 medium enriched with glucose and Casamino Acids using a procedure similar to that of Clewell, claiming a linear increase in plasmid content during the initial period following Cm addition.

The final plasmid content for the host-vector systems investigated here, determined after 18 hours incubation with Cm is proportional to the initial copy number (Table 1). However, the maximum degree of plasmid amplification, defined as the ratio of the final plasmid content to the preamplification content, is nearly identical for all strains studied. Clewell [6] has shown that the final plasmid content depends on growth medium used.

Interestingly, the rate of shift of the second mode, corresponding to

cells at a later stage of the cell cycle (four active chromosomal replication forks) at the time of Cm treatment (0.71 genome equivalents per hour), is higher by about 70% than that of the two chromosome peak shift for an HB101:pDM248 strain. As shown in Figure 2, cells in the second mode at larger DNA fluorescence are larger in volume (indicated by light-scattering intensity) than cells in the first mode, showing the former subpopulation harbors more proteins . Although *concentrations* of cellular components (proteins , plasmids, and so on) may be the same in the two cell types, amounts are not. Another interesting feature is decrease in size of Cm-treated cells with incubation time. The mean single-cell light-scattering intensity relative to that obtained at balanced growth is diagrammed in Figure 7 as a function of incubation time for plasmid-free HB101 and pDM247-containing HB101 populations. This change in cell volume may result from decay of cellular proteins, loss of membrane integrity, or other inactivation of normal processes.

Kinetic Model for Plasmid Amplification by Chloramphenicol (Cm)

A kinetic model has been formulated to describe these experimental observations of plasmid replication in the Cm-treated *E. coli* cells. This unstructured model consists of plasmid synthesis and deactivation of the replication system during incubation. The following material balance on plasmids and plasmid synthesis kinetics are postulated :

$$\frac{dn}{dt} = K_1 \, n \, (1 - c \, n) \qquad (1)$$

$$K_1 = K_{10} \, e^{-k_2 t} \quad . \qquad (2)$$

The initial condition is

$$n = n_0 \text{ and } K_1 = K_{10} \text{ at } t = 0 \quad . \tag{3}$$

Solving equations (1) and (2) subject to initial condition (3) gives :

$$\frac{n}{n_0} = \frac{\beta}{1 + c\, n_0 (\beta - 1)} \tag{4}$$

where :

$$\beta = \exp\left(\frac{K_{10}}{k_2}\left(1 - e^{-k_2 t}\right)\right)$$

n : plasmid content

t : time after Cm addition to culture

K_1 : replication system activity

k_2 : deactivation constant

c : constant .

The presumed kinetics for replication of plasmid DNA employs a logistic equation to represent replication inhibition at high plasmid content. Plasmid-mediated influences which reduce the host cells' biosynthetic activities have been reported previously in experiments relating the cloned-gene product level with plasmid copy number [12]. It can be reasonably presumed that the replication process is limited by biosynthetic precursors, replication enzymes and initiation factors, and metabolic energy in Cm-treated cells. Clewell [6] has also indicated that a decrease in replication rate at long incubation might be due to depletion of the limiting components necessary for DNA synthesis . In this model, the activity of the plasmid replication system is assumed to decay exponentially with time.

The degree of plasmid amplification for the HB101:pDM248 strain is shown as a function of time in Figure 8. The solid line in Figure 8 is based on Eq.(4) with kinetic constants evaluated by the least-square method. The amplified plasmid DNA content was estimated by subtracting the

chromosomal DNA from the total DNA content of Cm-treated cells. The total chromosomal DNA content in the Cm-treated cells was determined by multiplying the number fractions of the 2- and 4-chromosome subpopulations by the corresponding chromosome number. The values of K_{10} , k_2 and c determined for the HB101:pDM248 strain are 0.33 hr^{-1} , 0.053 hr^{-1} and 2.9×10^{-4} (number of plasmids)$^{-1}$, respectively. The values of constants estimated for other strains used are nearly the same in magnitude.

The maximum extent of amplification obtained at long incubation is, according to Eq.(4),

$$\frac{n}{n_o} = \frac{e^{\frac{K_{10}}{k_2}}}{1 + c\, n_0 \left(e^{\frac{K_{10}}{k_2}} - 1\right)} \qquad (5)$$

Eq.(5) indicates that the final plasmid content is proportional to the initial copy number, which is approximately consistent with experimental observations as listed in Table 1.

DISCUSSION

This work was performed to study the effect of chloramphenicol on ColE1-like pMB1 plasmid replication using flow cytometry. The data presented above clearly demonstrate that both the rate of plasmid amplification and final content of amplified plasmid DNA are directly proportional to the initial copy number determined at steady- state growth. These findings imply that, if the distribution of amplified plasmid content at different time intervals after Cm treatment could be determined from the

entire DNA distribution, then it would be possible, at least in principle, to estimate the plasmid content distribution in cells at steady-state growth by extrapolating to time zero assuming that plasmid amplification follows Eq.(4). The technical problem involved will be instrument sensitivity and resolution.

An unstructured kinetic model was formulated and found to be in good agreement with the experimental observations. The kinetic constants involved in the model were estimated based on the experimental results. The values of parameters are qualitatively consistent with previous experimental data. The constant c in Eq.(1) is of the order of $3x10^{-4}$, indicating that the maximum plasmid number accommodated by the host-cell is about 3300 plasmid copies per cell. This coincides with the case of temperature-sensitive plasmids which can reach this order of magnitude in plasmid content at a nonpermissive temperature [3]. The decay constant k_2 for replication system activity is around 0.05 hr^{-1} in LB medium. The value of k_2 obtained here is slightly higher than the average protein degradation rate (approximately 2% per hour) which has been determined for exponentially growing cells [19]. It has been reported that addition of Cm does not alter the rate of cellular protein degradation significantly, as opposed to the case where cells are starved for amino acids and other nutrients [20].

The application of flow cytometry can be extended to study physiological alterations in the recombinant population. Such information on the distribution of cell states will allow convenient and quantitative determination of parameters or kinetic forms at a single-cell level in connection with mathematical analysis of cell growth and plasmid propagation. In particular, experimental determination of the population composition based on the

number of active chromosomal replication forks will make possible estimation of the basic cell-cycle parameters of plasmid-containing *E. coli* populations. Further research on these aspects is in progress.

Acknowledgement: This research was supported by the National Science Foundation.

REFERENCES

1. Bazaral, M. and D.R. Helinski, *J. Mol. Biol.* , **36** , 185 (1968)

2. Clewell, D.B. and D.R. Helinski, *PNAS, USA.*, **62** , 1159 (1969)

3. Uhlin, B.E. and K. Nordstrom, *Mol. Gen. Genet.*, **165** , 167 (1978)

4. Uhlin, B.E., S. Molin, P. Gustafsson, and K. Nordstrom, *Gene* , **6** , 91 (1979)

5. Moser, D.R., C.D. Moser, E. Sinn and J.L. Campbell, *Mol. Gen. Genet.*, **192** , 95 (1983)

6. Clewell,D.B., *J. Bacteriol.* , **110** , 667 (1972)

7. Hershfield, V., H.W. Boyer, C. Yanofsky , M.A. Lovett and D.R. Helinski, *PNAS, USA* **71** , 3455 (1974).

8. Crosa, J.H., L.K. Luttropp , and S. Falkow, *PNAS, USA* **72** , 654 (1975)

9. Kahn, M., and D.R. Helinski, *PNAS, USA* , **75** ,2200 (1978)

10. Veltkamp, E., W. Barendsen and H.J. Nijkamp , *J. Bacteriol.*, **118** , 165 (1974)

11. Steen, H.B., E. Boye, K. Skarstad, B. Bloom, T. Godal and S. Mustafan, *Cytometry* , **2.** , 249 (1982)

12. Seo, J.H., and J.E. Bailey, *Biotech. Bioeng.* , in press (1985)

13. Moser, D., and J.L. Campbell, *J. Bacteriol.* , **154** , 809 (1983)

14. Dennis, K., F. Srienc and J.E. Bailey, *Biotech. Bioeng.* , **25,** 2485 (1983)

15. Boye, E., H.B. Steen and K. Skarstad, *J. Gen. Microbiol.* , **129** , 973 (1983)

16. Pato, M.L., *J. Bacteriol.*, **123** , 272 (1975)

17. Cooper, S., and C.E. Helmstetter, *J. Mol. Biol.* , **31** , 519 (1968)

18. Steen, H.B., *J. Bacteriol.* , **145** , 1091 (1981)

19. Pine, M.J., *Ann. Rev. Microbiol.*, **26** , 103 (1972)

20. Goldberg, A.L., and A.C. St.John, *Ann. Rev. Biochem.* , **45** , 747 (1976)

TABLE 1

Comparison of the mean chromosomal DNA content per cell exponentially grown in Luria broth medium at 37°C and final plasmid content determined 18 hours after Cm treatment

Strain	Plasmid[1] Copy no.	Gen. time[1] (min.)	(Genome)[2] theor.	(Genome)[3] exp.	Final plasmid[4] content per cell
HB101 only	—	32.8	2.40	2.44	—
	—	48.4[5]	1.80	1.76	—
pDM247	12	34.0	2.32	1.93	177
pDM246	24	34.1	2.32	2.09	341
RSF1050	60	35.6	2.23	1.96	1094
pDM248	122	37.7	2.13	1.83	1670

1. See Ref. 12 (copy number = number of plasmids per chromosome equivalent).

2. Cooper-Helmstetter equation : chromosomal DNA

$$\overline{DNA} = \frac{T}{C \cdot \ln 2} \left(2^{(C+D)/T} - 2^{D/T}\right)$$

were C = 40 min., D = 20 min., and T = generation time in min.

3. Chromosomal DNA only (these values were estimated by subtracting the plasmid DNA content from the average total DNA content).

4. Determined for recombinant *E. coli* populations 18 hours after Cm addition.

5. Grown in M9 medium enriched with 0.4% Casamino acids at 37°C.

FIGURE CAPTIONS

Figure 1 Dual parameter (single-cell stained DNA fluorescence - single-cell light scattering) distribution determined by flow cytometry for an *E. coli* HB101 population growing exponentially in LB medium at 37°C . The single-cell stained DNA fluorescence distribution is shown in the back panel.

Figure 2 Dual parameter (mithramycin (DNA) fluorescence - light scattering) flow cytometry data for an *E. coli* HB101 population treated with chloramphenicol for 4 hours. Integration of these data gives the one-parameter single-cell stained DNA distribution shown in the rear panel.

Figure 3 Single-cell DNA distributions at different times after Cm addition for HB101:pDM248 strain. DNA distributions at time 0 (1;——), time 1.8 (2;---), time 5.5 (3;·····), time 8.5 hours (4;-·-·-·-) after Cm addition are plotted together in the back panel

Figure 4 Total cellular DNA content distributions at different times after Cm addition :

(A) HB101 only at time 0 (1;——), and time 3.7 hours (2;---)

(B) HB101:pDM247 at time 0 (1;——), time 2.6 (2;---), and time 8.5 hours (3;·····)

(C) HB101:pDM246 at time 0 (1;——), time 2.7 (2;---), and time 8.6 hours (3;·····)

(D) HB101:RSF1050 at time 0 (1;——), time 1.8 (2;---), and time 6.2 (3;·····), and time 8.2 hours (4;-·-·-·-).

Figure 5 Shift in channel number of first mode of the DNA content distri-

bution with incubation time in Cm. Channel number has been normalized by the two-genome channel number.

Figure 6 Average rate of plasmid DNA replication after Cm addition as a function of initial copy number. The dashed line shows average replication rates in exponential growth prior to Cm addition.

Figure 7 Dependence of mean single-cell light-scattering intensity ($\overline{m}$) on incubation time in Cm for HB101 host cells only (●) and for recombinant strain HB101:pDM247 (▲). The single-cell light-scattering intensity for each population is normalized by that obtained at balanced growth (m_0).

Figure 8 Change in the degree of plasmid amplification with time after Cm addition. The solid line is based on Eq.(4) with constants as listed in the text.

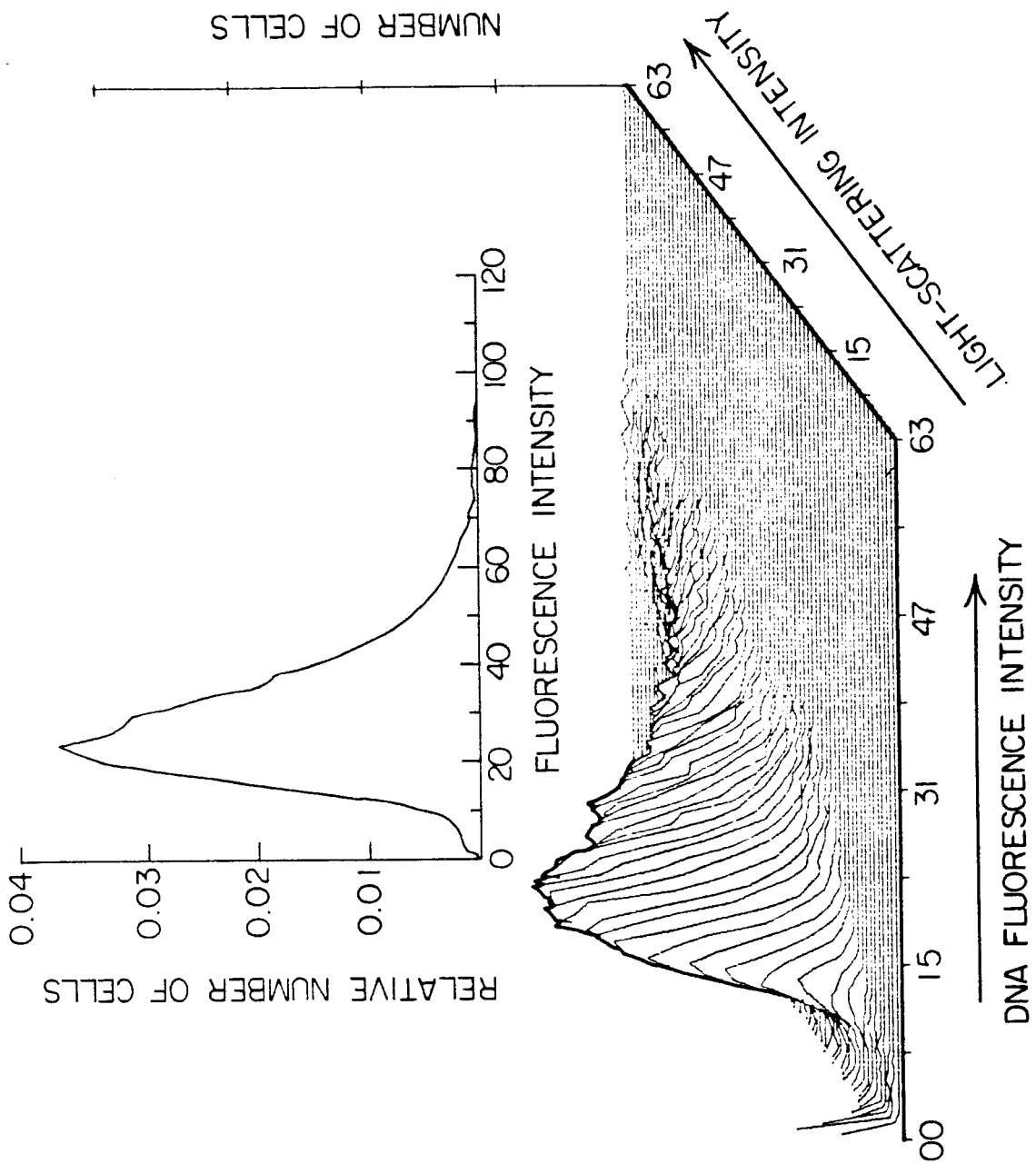
NUMBER OF CELLS
LIGHT-SCATTERING INTENSITY
63
47
31
15
00
63
47
31
15
DNA FLUORESCENCE INTENSITY
FLUORESCENCE INTENSITY
0
20
40
60
80
100
120
RELATIVE NUMBER OF CELLS
0.04
0.03
0.02
0.01

Figure 1

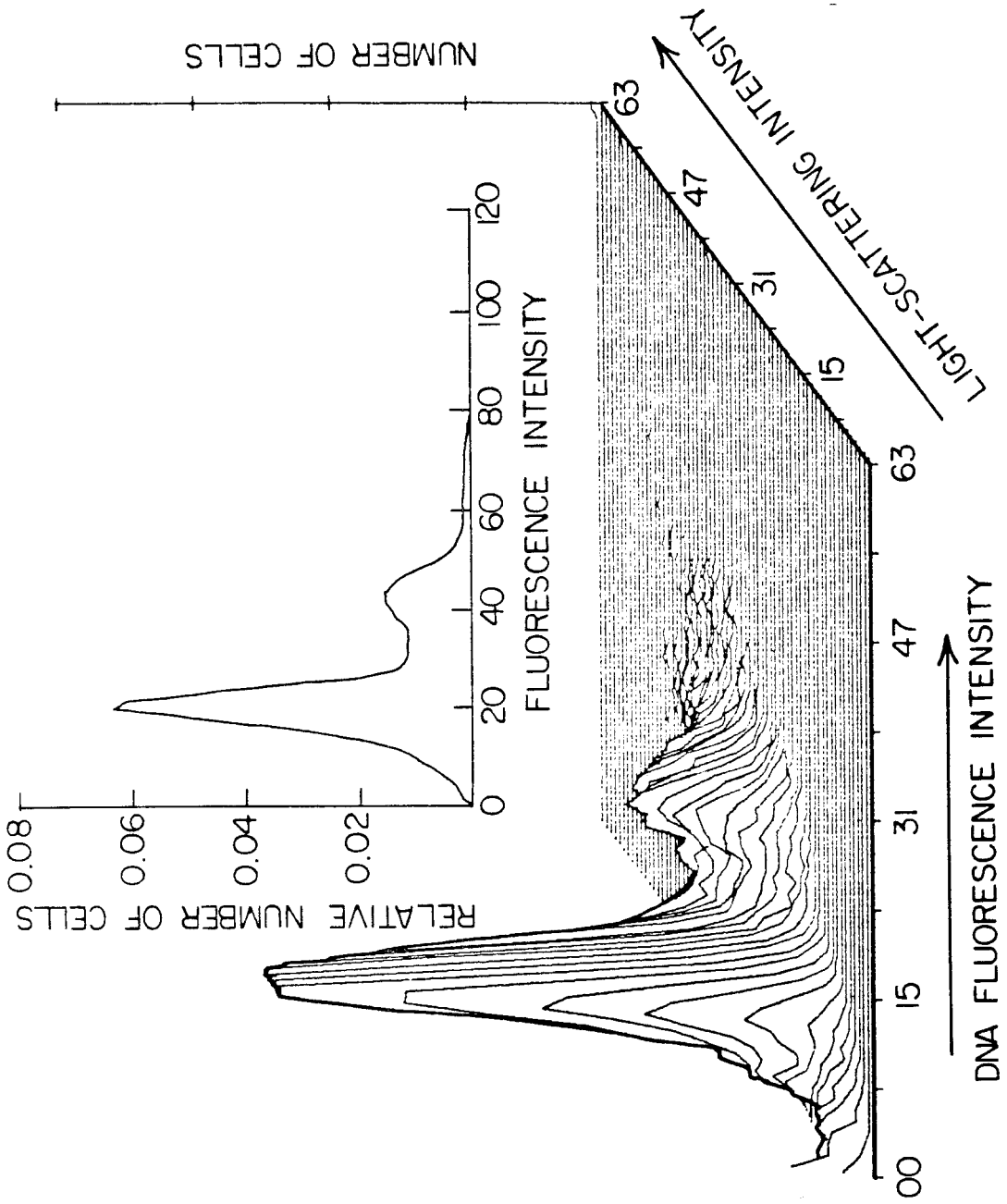
NUMBER OF CELLS
RELATIVE NUMBER OF CELLS
0.08
0.06
0.04
0.02
0
20
40
60
80
100
120
FLUORESCENCE INTENSITY
LIGHT-SCATTERING INTENSITY
63
47
31
15
00
DNA FLUORESCENCE INTENSITY

Figure 2

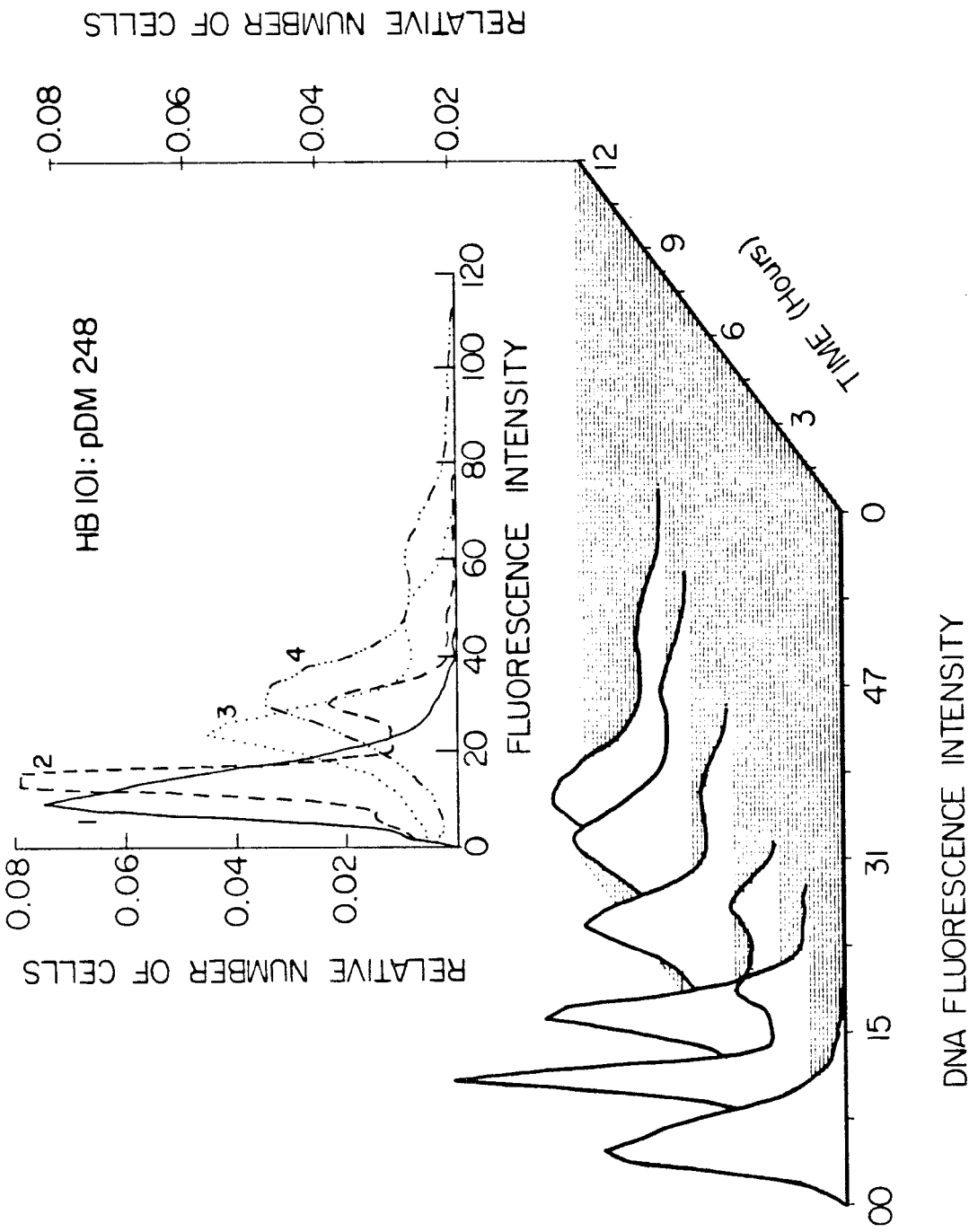
RELATIVE NUMBER OF CELLS
0.08
0.06
0.04
0.02
HB 101: pDM 248
1
2
3
4
0
20
40
60
80
100
120
FLUORESCENCE INTENSITY
RELATIVE NUMBER OF CELLS
0.08
0.06
0.04
0.02
TIME (Hours)
12
9
6
3
0
00
15
31
47
DNA FLUORESCENCE INTENSITY

Figure 3

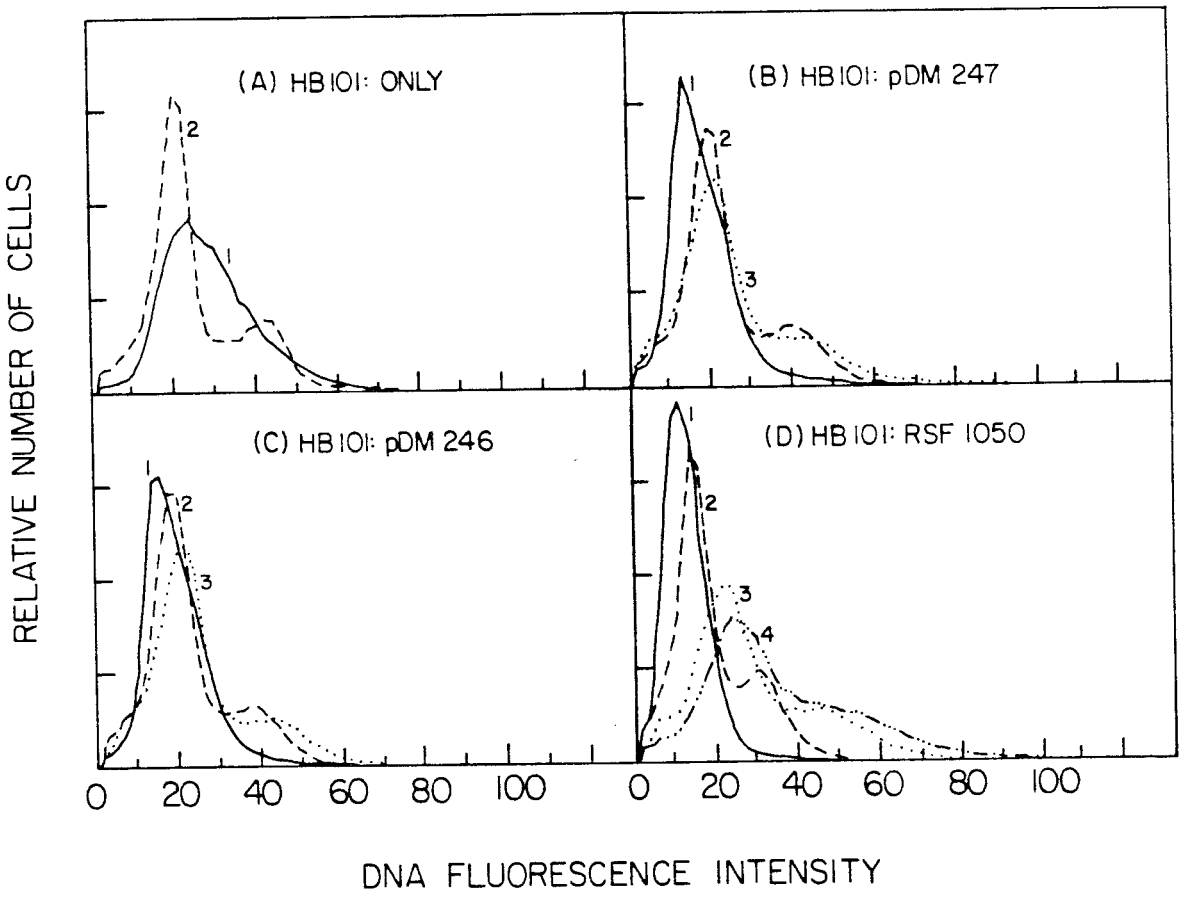
(A) HB101: ONLY
(B) HB101: pDM 247
(C) HB101: pDM 246
(D) HB101: RSF 1050
RELATIVE NUMBER OF CELLS
0 20 40 60 80 100
0 20 40 60 80 100
DNA FLUORESCENCE INTENSITY

Figure 4.

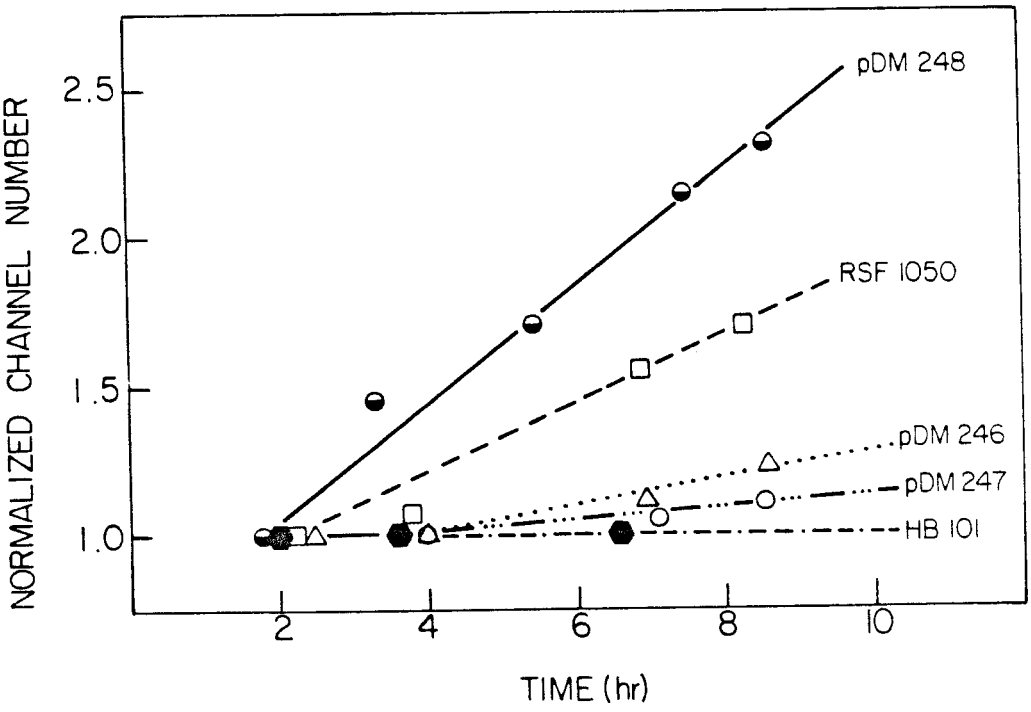
NORMALIZED CHANNEL NUMBER
2.5
2.0
1.5
1.0
2
4
6
8
10
TIME (hr)
pDM 248
RSF 1050
pDM 246
pDM 247
HB 101

Figure 5.

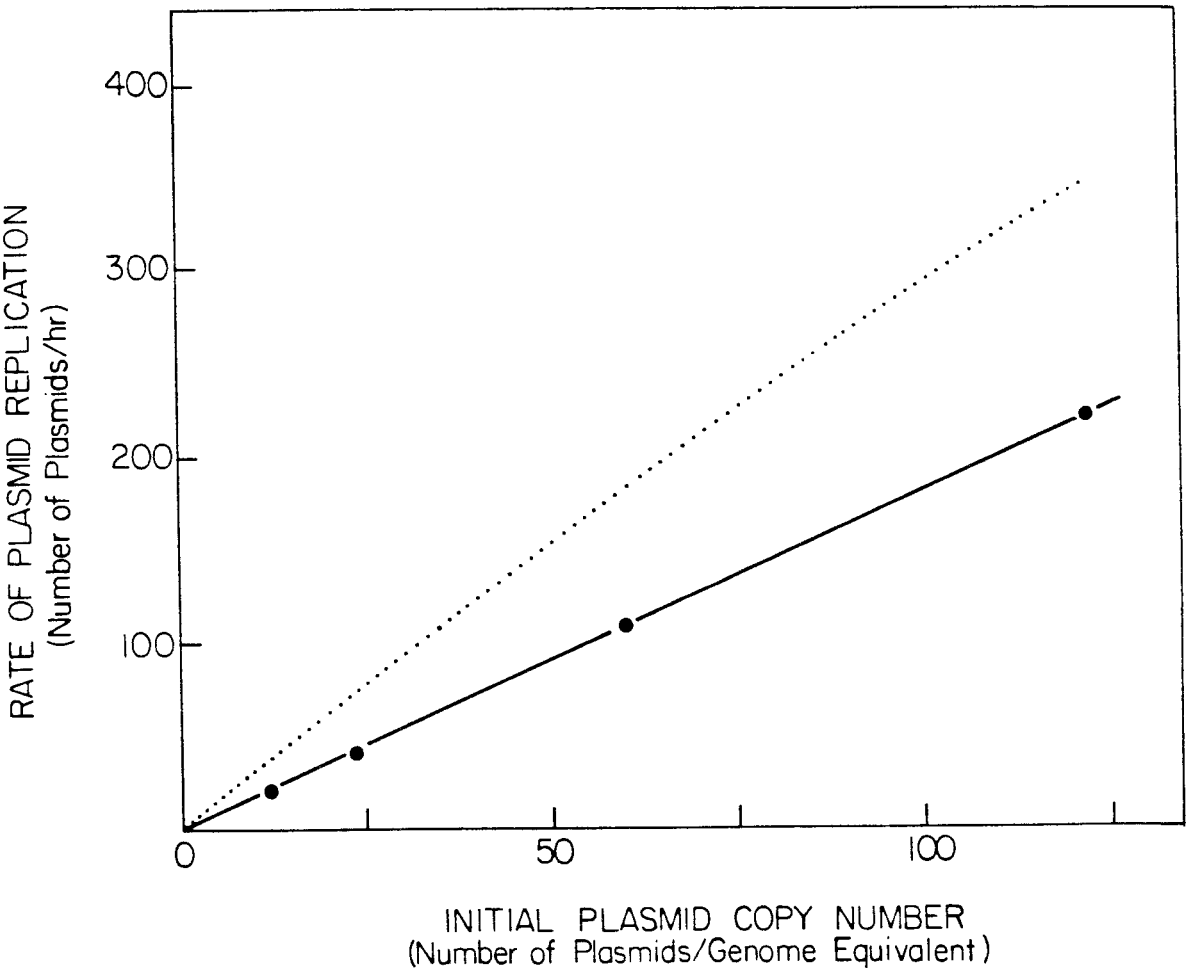
400
300
200
100
0
50
100
RATE OF PLASMID REPLICATION
(Number of Plasmids/hr)
INITIAL PLASMID COPY NUMBER
(Number of Plasmids/Genome Equivalent)

Figure 6.

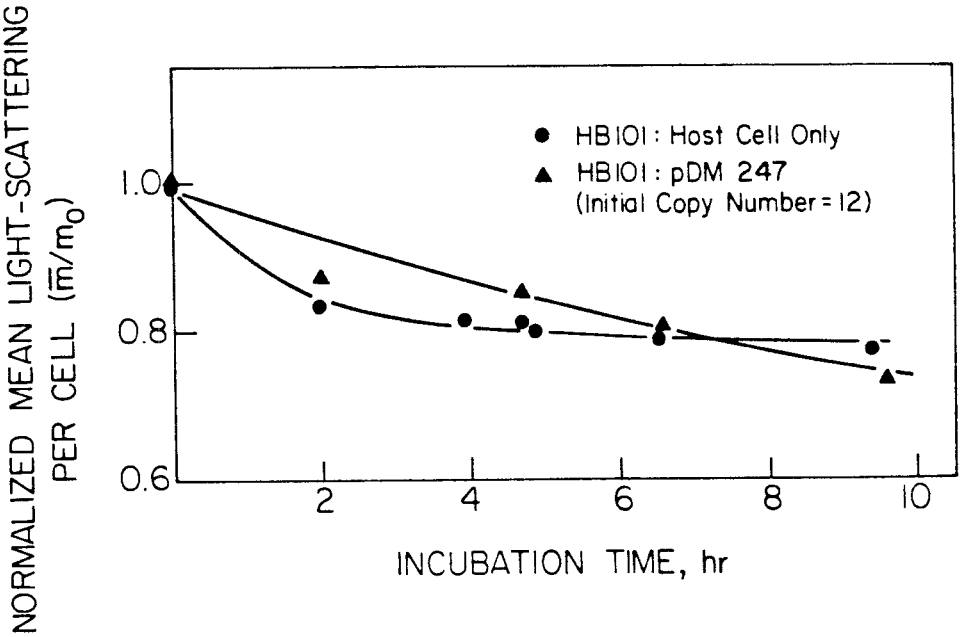
NORMALIZED MEAN LIGHT-SCATTERING PER CELL ($\bar{m}/m_0$)
1.0
0.8
0.6
2
4
6
8
10
INCUBATION TIME, hr
HB101 : Host Cell Only
HB101 : pDM 247
(Initial Copy Number = 12)

Figure 7.

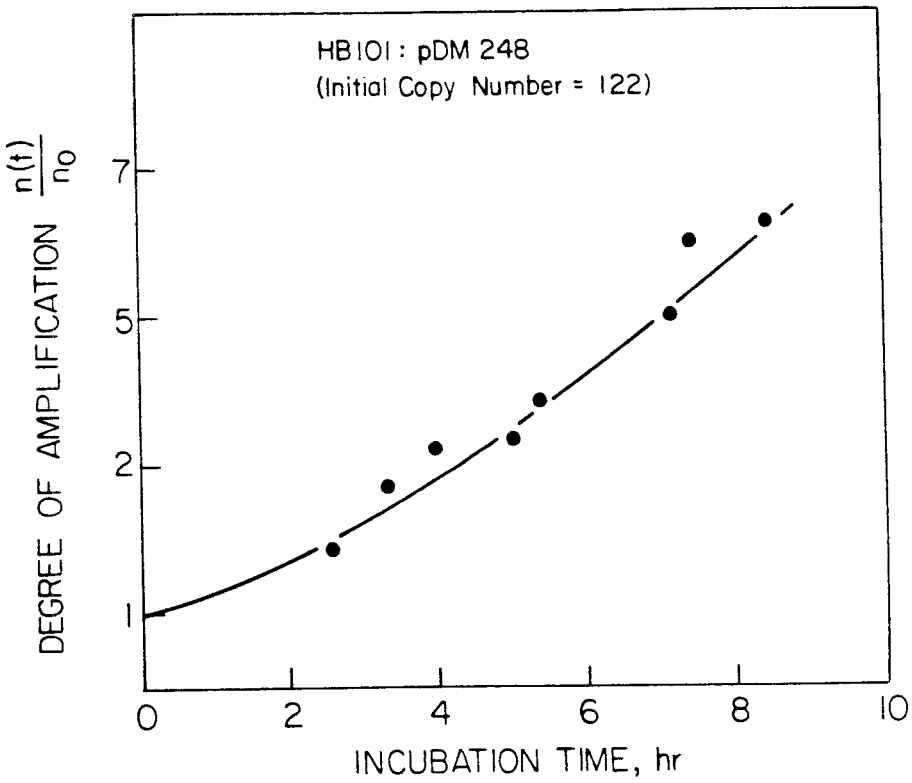
HB101 : pDM 248
(Initial Copy Number = 122)
DEGREE OF AMPLIFICATION $\frac{n(t)}{n_0}$
1
2
5
7
0
2
4
6
8
10
INCUBATION TIME, hr

Figure 8

CHAPTER 4: CELL CYCLE ANALYSIS OF PLASMID-CONTAINING *Escherichia coli* HB101 POPULATIONS WITH FLOW CYTOMETRY

INTRODUCTION

Plasmid-directed alterations in physiological properties of host-cells have been studied for some strains of *Escherichia coli* containing plasmids. Among the important properties which have been examined are specific growth rates, mean cell sizes, and cell cycle parameters. In general, plasmid-containing cells have lower specific growth rates than plasmid-free cells [1,2,3], suggesting that there is a competition between chromosomal and plasmid DNA for the cell's limited biosynthetic apparatus. The reduction in growth rates is enhanced as plasmid content per cell increases [3]. To study plasmid-host cell interactions in more detail, Helmstetter and his colleagues have determined cell-cycle parameters in *E. coli* B/r cells harboring the F' *lac* plasmid [4] and F' plasmids of various sizes [5]. The cell cycle parameters examined are the following two characteristic intervals: the time required for a replication fork to traverse the chromosome (C-time) and the interval between the end of a round of DNA replication and subsequent cell division (D-time) [6]. Helmstetter *et al.* have found no difference in C and D times between plasmid-containing and plasmid-free strains, claiming that there is an absence of competition between these two cell types for the DNA replication system.

Another approach to investigate the interactions in recombinant organisms is to measure mean cell sizes. Weinberger and Helmstetter obtained the size distributions of *E. coli* populations using a Coulter counter and reported a decrease in the cell size of the plasmid-containing strain compared to cell size of the plasmid-free strain [5]. *E. coli* cells with the F' *lac* plasmid have the same volume distribution as the strain without the plasmid when measured with the Coulter counter [7]. However, *E. coli* cells

carrying R factors have shown an increased mean cell size (defined as total cellular protein per cell), indicating that the presence of plasmids generates competition for rate-limiting components of the DNA replication or other systems connected with cell division cycle kinetics [8]. The discrepancy between these results may be due to the difference in plasmid-host cell systems or to the different experimental techniques employed to determine mean cell sizes.

Most research efforts on cell cycle analysis have been limited to the *E. coli* B/r strains and F plasmids. In the present work, we estimated the cell cycle parameters in *E. coli* HB101 harboring a series of pMB1-type plasmids at different copy number levels ranging from 12 to 122. Cell size distributions, here determined as the light-scattering intensity distribution, were measured for each recombinant strain.

Many experimental methods have been reported to determine the C and D periods in *E. coli* including the membrane elution technique, sedimentation, and gene-frequency method. Experimental errors and technical feasibility of each method have been extensively discussed elsewhere [9]. In this paper, two methods were used to determine the duration of the C and D times from experimental data obtained using flow cytometry : direct comparison of single-cell DNA distributions and determination of replication fork content using chloramphenicol (Cm) treatment. The first method compares the single-cell chromosomal DNA content distributions experimentally determined at balanced-growth with the theoretical distributions calculated using a single-cell model of DNA synthesis [10]. The second method uses chloramphenicol as an inhibitor of protein synthesis. The addition of Cm to an exponentially growing culture stops protein synthesis and thus initiation of

chromosome replication, but allows active replication forks to complete replication [11]. Consequently, the Cm-treated cells eventually attain an integer number of full chromosomes. Analysis of the Cm-treated population with flow cytometry permits determination of the population composition based on the number of active chromosomal replication forks. The subpopulation data can be further processed to estimate the cell-cycle parameters in *E. coli* HB101 cells.

MATERIALS AND METHODS

Bacterial Strains and Growth Conditions

Host *E. coli* strain HB101 ($Pro^-Leu^-Thi^-RecA^-$) was transformed with the plasmids pDM247, pDM246, RSF1050, and pDM248 [3,12]. The construction of these plasmids has been described previously [12]. The copy numbers of plasmids (number of plasmid copies per chromosome equivalent) in *E. coli* HB101 grown in Luria broth medium at 37°C are given in Table 1 [12,13]. All plasmids contain the origin of the pMB1 plasmid and the β-lactamase gene. The plasmids are nearly identical except the type and number of gene copies for RNA I, the plasmid-specified inhibitor of replication , giving variation of the plasmid copy number [12]. Luria broth (LB) medium buffered at pH 7 with phosphate was used as growth medium : (per liter of deionized water) 10 g of bactotryptone (Difco), 5 g of yeast extract (Difco), 5 g of NaCl, 3 g of K_2HPO_4 , and 1 g of KH_2PO_4 . Glucose (2 g/L) was used as a carbon source. Cultures were grown at 37°C in a shaker (New Brunswick, Edison, NJ) after preincubation in LB medium supplemented with ampicillin (Na-salt, Sigma)

for plasmid-containing strains. The measurements of growth rates were done on a Klett-Summerson spectrometer with a green filter. When grown to the mid-exponential phase, cells were taken for fixation and then 200 mg/L chloramphenicol (Sigma) was added to stop protein synthesis. The pH and temperature of the medium remained constant during incubation. Based upon replica-plate counts and specific growth rate measurements in selective and nonselective media, all plasmids used show highly stable behavior [3].

Fixation and DNA Staining

Samples taken before and after Cm addition were immediately fixed with 10 volumes of ice-cold 70 % ethanol and stored in a refrigerator overnight. DNA staining procedures followed the method described by Steen *et al.* [14]. The fixed cells were washed twice in 0.1 M Tris buffer (pH 7.4) , sedimented by centrifugation and resuspended in 0.1 M Tris buffer (pH 7.4) - 25 mM $MgCl_2$ - 100 mM NaCl containing 100 mg/L mithramycin (Sigma), the DNA-specific fluorescent dye. The stained cells were immediately used for flow cytometry analysis.

Flow Cytometry Analysis

Analysis of DNA-associated fluorescence and light-scattering intensities from individual cells were done on a flow cytometer (Model 50 H, Ortho Instruments, Westwood, MA) with an argon-ion laser tuned at 456 nm and 0.1 W. Dual-parameter frequency functions were obtained by measuring fluorescent intensities and light-scattering characteristics generated by 10^5 cells of a flow rate of approximately 2000 cells/sec. Data acquisition and analyses

were done on a Cytomic 12 computer (Kratel GbmH, Stuttgart, FRG) equipped with a plotter (Model CX-4800, Itoh Elect. Corp.) and a printer (Okidata).

THEORY

Single-Cell Distribution of Chromosomal DNA at Balanced-Growth

A single-cell model of the pattern of chromosomal DNA synthesis for *E. coli* has been formulated based on the Cooper-Helmstetter and Donachie hypotheses [10]. The frequency function for single-cell chromosomal DNA content has been obtained by a transformation of the age distribution for the population in balanced growth (at constant specific growth rate) which was derived by Powell [15] :

$$f^*(\xi) = (\ln 2) \cdot 2^{1-\xi} \quad ,\xi \in (0.1) \quad ; \tag{1}$$

here ξ is relative cell age, defined as time since birth divided by generation time. The chromosomal DNA content γ at cell age ξ is given by Eq.(2) for the population in steady-state growth [10]:

$$\gamma(\xi) = 1 + \frac{1}{C}\left\{\sum_{i\in P} 2^{i-1} \cdot (L - T(i-\xi)) - \sum_{j\in R} 2^{j-1} \cdot (D - T(j-\xi))\right\} \tag{2}$$

where

$$P(\xi) = \{1, \ldots, p\}, \quad 0 \le \xi \le a \tag{3.A}$$

$$\{1, \ldots, p+1\}, \quad a < \xi < 1 \tag{3.B}$$

$$R(\xi) = \{1, \ldots, r\}, \quad 0 \le \xi \le b \tag{4.A}$$

$$\{1, \ldots, r+1\}, \quad b < \xi < 1 \tag{4.B}$$

and

$$p = u\left[\frac{L}{T}\right] \tag{5.A}$$

$$a = p + 1 - \frac{L}{T} \tag{5.B}$$

$$r = u\left[\frac{D}{T}\right] \tag{5.C}$$

$$b = r + 1 - \frac{D}{T} \tag{5.D}$$

$$L = C + D \tag{6}$$

T : generation time

$u(\cdot)$: integer function .

Then, the frequency function in terms of chromosome content, f_D , can be calculated by coordinate transformation as follows :

$$f_D(\gamma) = \left| f^*(\gamma^{-1}) \frac{d\xi}{d\gamma} \right|_{\xi=\gamma^{-1}} \tag{7}$$

where γ^{-1} is the inverse function of γ .

In general, the chromosomal DNA frequency function, f_D , cannot be expressed in an explicit form since γ in Eq. (2) has discontinuities at $\xi = a$ and $\xi = b$. However, evaluation of the frequency function for chromosomal DNA is easily done using a computer. The function γ is determined using Eq. (2) at each ξ for a given set of C, D, and T periods. Then the inverse function

γ is determined, and, finally, Eq. (7) is employed to evaluate $f_D(\gamma)$.

The average chromosomal DNA content per cell is computed based on Eq. (8).

$$\bar{\gamma} = \int_0^1 \gamma(\xi) f^*(\xi) d\xi \tag{8}$$

Integration of Eq.(8) yields the average chromosome content, which is called the Cooper-Helmstetter equation [6]. It is interesting to note that alternative derivations give the identical equation.

$$\bar{\gamma} = \frac{T}{C \cdot \ln 2} \left(2^{(C+D)/T} - 2^{D/T} \right) \tag{9}$$

The number of active chromosome replication forks, g_f , in an exponentially growing cell can be described as follows:

$$g_f = 2^P \left\{ \sum_{i \in P} 2^{i-1} [u(L - T \cdot (i - \xi))] - \sum_{j \in R} 2^{j-1} [u(D - T(j - \xi))] \right\} \tag{10}$$

where u[*] is the integer function. For the present study in which LB medium is used as growth medium, p is equal to 1 and r equal to 0. Here, only the case where no cells are in the D-period (in other words a < b) will be considered. The other case is described in the Appendix.

The fraction of cells which contain two active chromosome replication forks, F_2 , is estimated using the age distribution from Eq. (1) in the integral.

$$F_2 = \int_0^a f^*(\xi) d\xi = 2 - 2^{1-a} \ . \tag{11}$$

In a similar way, the fraction of cells with four active chromosome replication forks is estimated by Eq.(12).

$$F_4 = \int_a^1 f^*(\xi)d\xi = 2^{1-a} - 1 \qquad (12.A)$$

or

$$F_4 = 1 - F_2 \ . \qquad (12.B)$$

Experimentally the fraction of cells with 2 and 4 replication forks can be determined from the flow cytometry data on the Cm-treated population. These subpopulation data are used to estimate values of cell age a and/or b and thus the sum of C and D when the generation time, T, is known. Individual estimates of C and D are then possible by considering in addition the average chromosomal DNA content per cell prior to Cm treatment.

RESULTS

Single-Cell DNA Distribution

The entire DNA content of individual cells was determined after staining the DNA with mithramycin, a DNA-specific fluorescence dye. In order to obtain a calibration factor of the fluorescence coordinate with regard to the cellular DNA content, an exponentially growing culture of (plasmid-free) *E. coli* HB101 was exposed to Cm. As described previously, the Cm-treated cells ultimately have an integer number of full chromosomes by finishing the round of chromosome replication in progress at the time of Cm addition. Figure 1 shows the dual parameter (mithramycin fluorescence - light scattering) frequency function for the Cm-treated *E. coli* HB101 cells. The dual-parameter flow cytometry data were integrated over the entire range of light-scattering coordinates to give the single parameter DNA fluorescence

histogram, which is illustrated in the back panel. The two modes in Figure 1 at smaller and larger fluorescence intensity correspond to cells containing 2 and 4 genome equivalents, respectively. This type of measurement was done for each experimental run to obtain a calibration factor of channels/genome equivalent. Steen *et al.* have also used Cm-treated *E. coli* cells as a fluorescence standard [14,16].

Contribution of plasmid DNA to total cellular DNA must be taken into account for plasmid-containing strains. Since copy number (CN) is the number of plasmid DNA molecules per chromosome, the chromosomal DNA content γ is equal to the total DNA content divided by $(1+ CN\varphi_{plasmid}/\varphi_{chromosome})$ where the chromosomal molecular weight $\varphi_{chromosome}$ is taken to be 2.5×10^9D [6]. Molecular weights $\varphi_{plasmid}$ for each of the plasmids considered are given elsewhere [3]. Using experimentally determined CN values for each strain, this factor was used to rescale single-cell total DNA content to single-cell chromosomal DNA content. This scaling procedure involves an assumption. The CN values used for these scalings are based upon population-average chromosomal DNA and plasmid DNA values. Application of a scale factor based on average population properties to single-cells, as is done here, presumes that plasmid DNA : chromosomal DNA ratios do not change significantly during the cell cycle. Since chromosomal DNA synthesis is expected to be continuous at the specific growth rates studied [6], and since plasmid replication in *E. coli* appears to be continuous throughout the cell cycle [4,7,17], this assumption should not introduce substantial error in this analysis.

The coefficient of variation (CV), as a measure of instrumental resolution, was determined from the modes obtained with the cells exposed to Cm.

The coefficient of variation is the ratio of the standard deviation to the mean of the mode. The CV for these measurements on the flow cytometry used in these experiments was found to be about 0.25 for both the two-chromosome and four-chromosome peaks. Approximately constant CV values for these two peaks indicate that the standard deviation of instrumental resolution increases proportional to DNA content.

Estimation of C and D Times

The length of the C and D periods in plasmid-free and plasmid-containing *E. coli* HB101 strains was determined in two different ways: (1) direct comparison of the single-cell DNA content frequency function and (2) comparison of theoretical and experimental F_2 and $\bar{\gamma}$ values.

(1) Direct Comparison Method

Using the calibration factor determined by separate control experiments as just described, the single-cell DNA content frequency function in channel number can be converted to the distribution in chromosome equivalents which will be denoted by $f_E(\gamma)$. The single-cell chromosomal DNA frequency functions determined by flow cytometry differ substantially between plasmid-containing and plasmid-free cells as Figure 2 illustrates. The existence of such clear distinctions in these data indicates that significant differences in cell cycle operation are caused by plasmids. Next we consider methods for determination of quantitative cell cycle parameters based on these data. The theoretical single-cell DNA distribution is calculated from Eq. (7) for the presumed C and D periods and the observed generation time of the corresponding strain. Before comparison with experi-

mentally determined DNA frequency functions, the theoretical frequency function must be modified to include the influence of measurement noise. Assuming a Gaussian signal distribution at each chromosomal content, the following equation relates the ideal chromosome content frequency function $f_D(\gamma)$ and the corresponding noise-affected model frequency function $f_N(\gamma)$ [18].

$$f_N(\gamma) = \frac{1}{\sqrt{2\pi}} \int_0^\infty \frac{f_D(x)}{\delta(x)} \cdot \exp\left[-\frac{1}{2}\left[\frac{x-\gamma}{\delta(x)}\right]^2 \right] \cdot dx \qquad (13)$$

where x is the chromosomal DNA content in genome equivalents, and $\sigma(x)$ is the standard deviation. Here, x is a dummy variable representing the chromosomal DNA content. Generalizing the experimental observation for the peak widths, the standard deviation, $\sigma(x)$ is taken to be linearly proportional to the DNA content and given by x times CV. This approach is similar to methods previously suggested for analysis of the flow cytometry data for mammalian cells [19].

Comparison of the model chromosomal DNA frequency function, $f_N(\gamma)$, with the single-cell DNA content frequency function, $f_E(\gamma)$, experimentally determined using flow cytometry, allows estimation of C and D times for known generation time, T. A nonlinear least-squares algorithm was used to estimate the C and D periods which minimize the sum-of-square deviation between f_N and f_E [20]. Figure 2 illustrates computer fitting of the single-cell DNA content frequency function for the plasmid-free HB101 strain. Flow cytometry data and optimized model frequency functions for the recombinant strains are plotted in Figure 3.

Table 2 summarizes the C and D periods determined for HB101 cells and

for cells harboring various copy numbers of pMB1 plasmids, all grown in LB medium at 37°C. The values of C and D times of the plasmid-free parental strain are the same in magnitude as those known for many *E. coli* strains [6,21,22]. However, the presence of plasmids decreases both C and D periods by approximately 20% with respect to the parental strain. However, no significant differences in the cell cycle parameters are found among the plasmid-harboring strains. Weinberger and Helmstetter also found the same or slightly reduced C and D times in the *E. coli* B/r cells containing F plasmid [5].

(2) Chloramphenicol Treatment Method

Flow cytometry measurements of the Cm-treated cells make possible differentiation of the population in terms of the number of chromosomes, which in turn is equal to the number of active replication forks at the time of Cm treatment. As noted earlier, the fraction of each subpopulation based on replication fork content is a function of the C , D and generation (T) times. Before comparing model and experiment to estimate cell cycle parameters, the effect of Cm on plasmid replication must be examined.

The plasmids used for this study are amplifiable in the presence of Cm. This is clearly evident in flow cytometry measurements of DNA frequency functions for plasmid-containing *E. coli* populations at different times after Cm addition to exponentially growing culture. Figure 4 illustrates such data for strain HB101:pDM248 at times 1.8, 5.5, 8.5 hours following treatment with chloramphenicol. All these frequency functions evidence clear bimodal character, but first- and second-mode positions increase with time. Separate experiments with plasmid-free HB101 populations show that chromosomal replication under these conditions is completed approximately 4

hours after Cm treatment [23]. Thus, mode shifts after this time are attributable solely to plasmid replication. However, the population fractions associated with the two modes (relative peak areas) do *not* change during incubation in Cm. Accordingly, even with concurrent plasmid amplification, the flow cytometry data may be used to determine the population fractions F_2 and F_4 . From these results, the values of cell age a (see Eqs. (11) or (12)) and thus the sum of C and D periods may be estimated using .

$$a = 2 - \frac{(C+D)}{T} \quad . \tag{14}$$

The mean chromosomal DNA content per cell was obtained using flow cytometry by applying the calibration factor and plasmid content correction factors discussed above. The average chromosomal DNA content per cell so determined for the strains investigated is listed in Table 2. Since the sum of C + D is known from Eq.(14), Eq.(9) may now be applied to estimate the individual C and D parameters, with results as summarized in Table 2. The C and D times determined by this method are almost identical to those obtained from the direct comparison approach. Figure 5 highlights the C, D, and generation times determined for HB101 cells as a function of plasmid copy number.

Cell Light-Scattering Distribution : Estimation of Relative Initiation Mass

The single-cell light scattering intensity, which is a measure of cell size, is known to depend on the total cellular protein content which in turn is directly correlated with total cell mass [24]. The single-parameter light scattering frequency functions for three of the strains investigated are shown in Figure 6. The plasmid-free population has a larger and broader distribution than the plasmid-containing populations. However, the plasmid-containing populations have very similar light scattering intensity frequency functions although plasmid copy number differs in these strains. The average light scattering intensities of the strains studied are also listed in Table 3. The results obtained are consistent with previous observations of *E. coli* B/r carrying F plamids which show that plasmid-free cells are larger than the plasmid-harboring cells [5].

The cell mass at (the first) initiation of DNA synthesis, M_i , the average cell mass M, and the C, D, and T cell cycle intervals are related by the equation [10,25]

$$M = M_i 2^{\frac{C+D}{T}} . \qquad (15)$$

Given the correspondence between single-cell light scattering intensity and single-cell mass, it is reasonable to assume these properties are proportional over a narrow range of mass and light-scattering values. Then, using Eq.(15), it follows that the relative initiation mass M_{i2}/M_{i1} is given by

$$\frac{M_{i2}}{M_{i1}} = \frac{\bar{I}_2}{\bar{I}_1} \cdot 2^{\left[\frac{C_1+D_1}{T_1} - \frac{C_2+D_2}{T_2}\right]} . \qquad (16)$$

This equation has been used to determine the initiation mass for plasmid-

containing strains relative to the initiation mass for plasmid-free HB101 cells. The results, listed in Table 3, indicate that plasmid presence reduces initiation mass by approximately 18 %. Estimated initiation masses for plasmid-containing strains do not differ significantly. Copy number does not have a major influence on this cell cycle parameter.

DISCUSSION

We have determined experimentally the C and D periods in both plasmid-free and plasmid-containing *E. coli* HB101 populations using flow cytometry and cell populaton theory. The presence of pMB1 plasmids results in an increased generation time and decreased C and D periods, mean cell size, and initiation mass. These results are in a qualitative agreement with previous findings with *E. coli* B/r containing F plasmids [5]. Although plasmid copy number has a significant influence on generation time, C and D times, mean-cell size, and initiation mass are relatively independent of copy number for the recombinant *E. coli* strains investigated. In view of these findings, it is interesting to consider some of the molecular level interactions that have been identified for plasmid and chromosome replication in *E. coli*.

It is generally recognized that plasmids with replication origins similar to that of ColE1 plasmids require DNA polymerase I, while the chromosome requires DNA polymerase III [26]. The role of DNA polymerase I in the replication of the chromosome includes primer degradation and gap filling between DNA fragments. Consequently, it is anticipated that plasmid replication does not directly compete for DNA polymerase against chromosomal replication.

The fact that plasmid-containing cells have shorter C and D times than plasmid -free cells is somewhat unexpected. It is reasonably presumed that DNA chain elongation rate is controlled by the rate of DNA synthesis in the *lagging* strand based on consideration of the number of DNA polymerase molecules and their maximum catalytic rates (10 molecules of DNA polymerase III per cell and 250 nucleotides added per second per molecule of DNA polymerase III [27]). More time is usually needed in the lagging strand to synthesize the primer necessary for DNA polymerase III to add nucleotides than in the leading strand, since each Okazaki fragment in the lagging strand requires the primer. The intrinsic rate of the primase (the primer-making enzyme) is known to be much slower than the rate of DNA polymerase [27]. The ColE1-like plasmids, including the pMB1 plasmids used here, require for replication initiation a primer RNA catalyzed by the DNA-dependent RNA polymerase. Also, expression of plasmid genes requires RNA polymerase. At present it is unclear whether the primase is identical to RNA polymerase, or whether RNA polymerase has primase activity. This may be one locus of host-plasmid interaction which could influence the recombinant cell C interval.

Accumulating results concerning mechanisms of ColE1-like plasmid replication reveal that only one plasmid molecule is selected at random for replication from the pool of plasmid molecules in the cell [28]. This random selection process implies that the plasmid-containing cell has no more than one *active* origin of plasmid DNA during the cell cycle, independent of plasmid copy number. The absence of significant differences in the C time and mean cell size among plasmid-containing cells appears consistent with the random selection model, and indicates that the governing interactions involve only the plasmid selected for replication, not the entire pool of plasmids in the cell.

Decrease in both C and D times as a result of plasmid presence is consistent with the hypothesis that the duration of the D time is triggered at the time of termination of a round of chromosome replication [29]. The D period is considered to be the time for completion of septum formation, and/or the interval between completion of the septum and cell separation. In this connection, the shorter D period may be due to the smaller cell size for plasmid containing cells which appears to be primarily a consequence of reduced initiation mass.

Acknowledgement: This research was supported by the National Science Foundation.

REFERENCES

1. Collin,J. and R.H. Pritchard, *J. Mol. Biol.* **78**, 143 (1973)
2. Inselburg, J., *J. Bacteriol.* **133**, 433 (1978)
3. Seo, J.H. and J.E. Bailey, *Biotech. Bioeng.*: in press (1985)
4. Steinberg, D.A. and C.E. Helmstetter, *Plasmid* **6**, 342 (1981)
5. Weinberger,M. and C.E. Helmstetter, *J. Bacteriol.* **137**, 1151 (1979)
6. Cooper, S. and C.E. Helmstetter, *J. Mol. Biol.***31**, 519 (1968)
7. Andresdottir, V. and M. Masters, *Mol. Gen. Genet.* **163**, 205 (1978).
8. Engberg, B., K. Hjalmarsson, and K. Nordstrom, *J. Bacteriol.* **124**, 633 (1975)
9. Churchward, G. and H. Bremer, *J. Bacteriol.* **130**, 1206 (1977)
10. Nishimura, Y. and J.E. Bailey, *Mathe. Biosci.* **51**, 305 (1980)
11. Clewell, D.B., *J. Bacteriol.* **110**, 667 (1972)
12. Moser, D.R., and J.L. Campbell, *J. Bacteriol.* **154**, 809 (1983)
13. Dennis, K., F. Srienc, and J.E. Bailey, *Biotech. Bioeng.*: in press (1985)
14. Steen, H.B., E. Boye, K. Skarstad, B. Bloom, T. Godal, and S. Mustafan, *Cytometry* **2**, 249 (1982)
15. Powell, E.O., *J. Gen. Microbiol.* **15**, 492 (1956)
16. Skarstad, K., H.B. Steen, and E. Boye, *J. Bacteriol.* **154**, 656 (1983)
17. Gustafsson, P., K. Nordstrom, and J.W. Perram, *Plasmid* **1**, 187 (1978)
18. Bailey, J.E., D.W. Agar, and M.A. Hjortso, in *Computer Applications in Fermentation Technology, London*: Soc. Chem. Indus. (1982)
19. Gray, J.W., P.N. Dean, and M.L. Mendelsohn, in *Flow Cytometry and Sorting* (Ed. by M.R. Melamed, P.F. Mullaney, and M.L. Mendelsohn), John Wiley & Sons (1979)
20. Marquardt, D.W., *Soc. for Industr. Appl. Math. J.* **11**, 431 (1963)
21. Chandler, M., R.E. Bird, L.Caro, *J. Mol. Biol.* **94**, 127 (1975)
22. Helmstetter, C.E., and O. Pierucci, *J. Mol. Biol.* **102**, 477 (1976)
23. Seo, J.H., F. Srienc, J.E. Bailey, *Biotech. Prog.*: in press (1985)
24. Boye, E., H.B. Steen, and K. Skarstad, *J. Gen. Microbiol.* **129**, 973 (1983)
25. Donachie, W.D., *Nature* **219**, 1077 (1968)
26. Scott, J.R., *Microbiol. Rev.* **48**, 1 (1984)
27. Ingraham, J.L., O. Maaloe, and F.C. Neidhardt, in *Growth of the Bacterial Cell*, Sinauer Assoc., Inc. Sunderland, M.A. (1983)
28. Matsubara, K., *Plasmid* **5**, 32 (1981)
29. Meacock and R.H. Pritchard, *J. Bacteriol.* **122**, 931 (1975)

APPENDIX

Consideration of a Population Containing D-phase during the Cell Cycle

Upon addition of Cm, a cell which is experiencing the D-phase will eventually divide to produce two cells but with one-half chromosome content. In fact, Kubitschek (*Mol. Gen. Genet.* **135**, 123 (1974)) has estimated the duration of the D period by measuring the kinetics of residual cell division after exposure of an exponentially growing culture to Cm. The fraction of cells with 2 genome equivalents long after Cm-addition is theoretically provided by Eq.(A).

$$F_2 = \int_a^b f^*(\xi)d\xi = 2 - 2^{1-b} \qquad (A)$$

In a similar way, the fraction of cells with 4 genome equivalents is given by Eq.(B).

$$F_4 = \int_a^b f^*(\xi)d\xi = 2^{1-a} - 1 \qquad (B)$$

The fraction of cells in the D-phase, F_D , will divide to have one genome equivalent.

$$F_D = \int_a^b f^*(\xi)d\xi = 2^{1-b} - 2^{1-a} \qquad (C)$$

or

$$F_1 = 2F_D \qquad (D)$$

Flow cytometric measurements give F_1 instead of F_D. We should make corrections to obtain the true estimates of the subpopulation data as follows

$$(F_2)_{true} = \frac{(F_2)_{exp}}{1 - \frac{(F_1)_{exp}}{2}} \qquad (E)$$

$$(F_4)_{true} = \frac{(F_4)_{exp}}{1 - \frac{(F_1)_{exp}}{2}} \qquad (F)$$

where the subscript exp means the fraction of cells experimentally determined from the flow cytometry data.

Table I

Plasmids used, copy numbers, generation times, and average chromosome content for recombinant *E. coli* HB101 stains grown in LB medium at 37° C

Strain	Copy number[1]	Generation time T[1] (min)	Chromosome[2] (genome equiv.)
HB101 only		32.8	2.44
HB101:pDM247	12	34.0	1.93
HB101:pDM246	24	34.1	2.09
HB101:RSF1050	60	35.6	1.96
HB101:pDM248	122	37.7	1.83

1. See Ref. 3. (Copy number = number of plasmids per chromosome equivalent).
2. Chromosomal DNA only.

Table II

Estimated C and D periods for recombinant HB101 strains

Growth Conditions: Luria broth medium at 37°C at pH 7.0

Strain	Cm-treatment			Direct comparison		
	C (min)	D (min).	L (min)	C (min)	D (min)	L (min)
HB101 only	36.8	19.9	56.7	37.3	20.5	57.8
HB101:pDM247	30.3	15.4	45.7	31.0	15.5	46.5
HB101:pDM246	30.9	16.7	47.6	31.8	15.0	46.8
HB101:RSF1050	33.3	16.2	49.5	33.8	13.7	47.6
HB101.pDM248	32.1	15.0	47.1	33.5	14.6	48.1

Table III

Mean light-scattering intensities and estimated relative initiation masses for recombinant *E. coli* strains growth conditions

Strain	Relative mean light-scattering intensity[1]	relative initiation mass[1]
HB101 only	1.0	1.0
HB101:pDM247	0.65	0.85
HB101:pDM246	0.62	0.80
HB101:RSF1050	0.61	0.79
HB101:pDM248	0.61	0.85

1. Normalized by the value for the plasmid-free HB101 strain.

FIGURE CAPTIONS

Figure 1 Calibration of the fluorescence coordinate. Dual parameter (mithramycin (DNA) fluorescence - light scattering) flow cytometry data for an *E. coli* HB101 population treated with chloramphenicol for 4 hours. Integration of these data gives the one-parameter single-cell stained DNA distribution shown in the rear panel.

Figure 2 Experimental flow cytometry single-cell DNA frequency function data for *E. coli* HB101 and for the plasmid-containing strain HB101:pDM247. The dashed line is the model fit to the HB101 data based upon optimization of C and D cell-cycle paarameters.

Figure 3 Computer fit (----) by the least-squares method of experimental flow cytometry single-cell DNA frequency function data (——) for recombinant *E. coli* populations. (A) HB101:pDM247 (copy number 12) (B) HB101:pDM246 (copy number 24) (C) HB101:RSF1050 (copy number 60) (D) HB101:pDM248 (copy number 122).

Figure 4 Change in the single-cell DNA content distribution with incubation time in Cm-containing medium for HB101:pDM248 strain. Flow cytometry analyses conducted at times 0 (1;——), 1.8 (2;·····), 5.5 (3;-·-·-·—), 8.5 hours (4;-----) after Cm addition.

Figure 5 C, D, and generation times in *E. coli* HB101 cells as a function of plasmid copy number (Symbols: , C period; , D period; , generation time; , C + D times) determined by the direct comparison method (closed symbols) and by the Cm treatment

method (open symbols).

Figure 6 Single-cell light scattering intensity distributions in balanced growth. (A) HB101 only (——), (B) HB101:pDM247 (– – –), (C) HB101:pDM248 (·····).

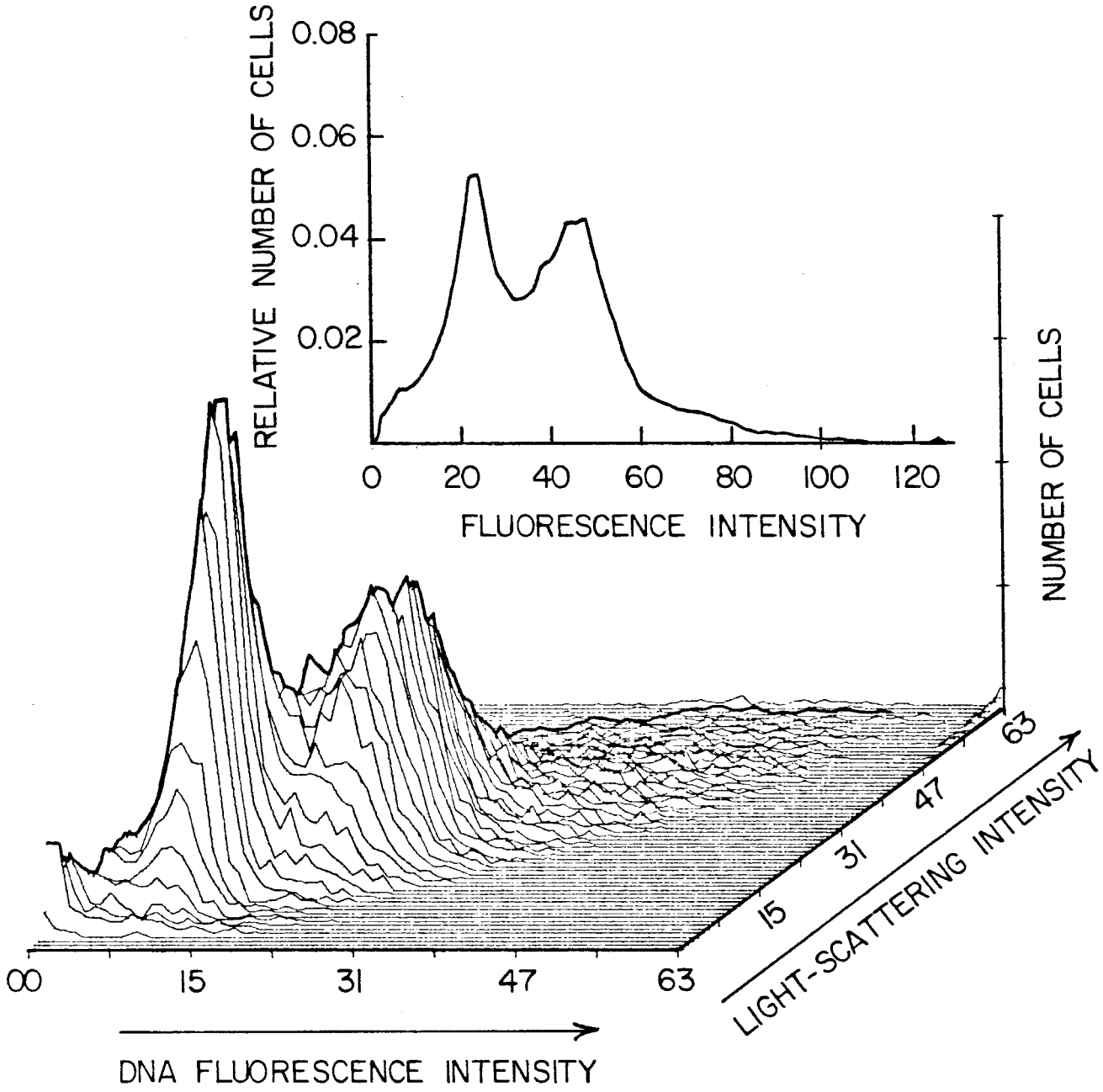
RELATIVE NUMBER OF CELLS
0.08
0.06
0.04
0.02
0
20
40
60
80
100
120
FLUORESCENCE INTENSITY
NUMBER OF CELLS
00
15
31
47
63
DNA FLUORESCENCE INTENSITY
15
31
47
63
LIGHT-SCATTERING INTENSITY

Figure 1

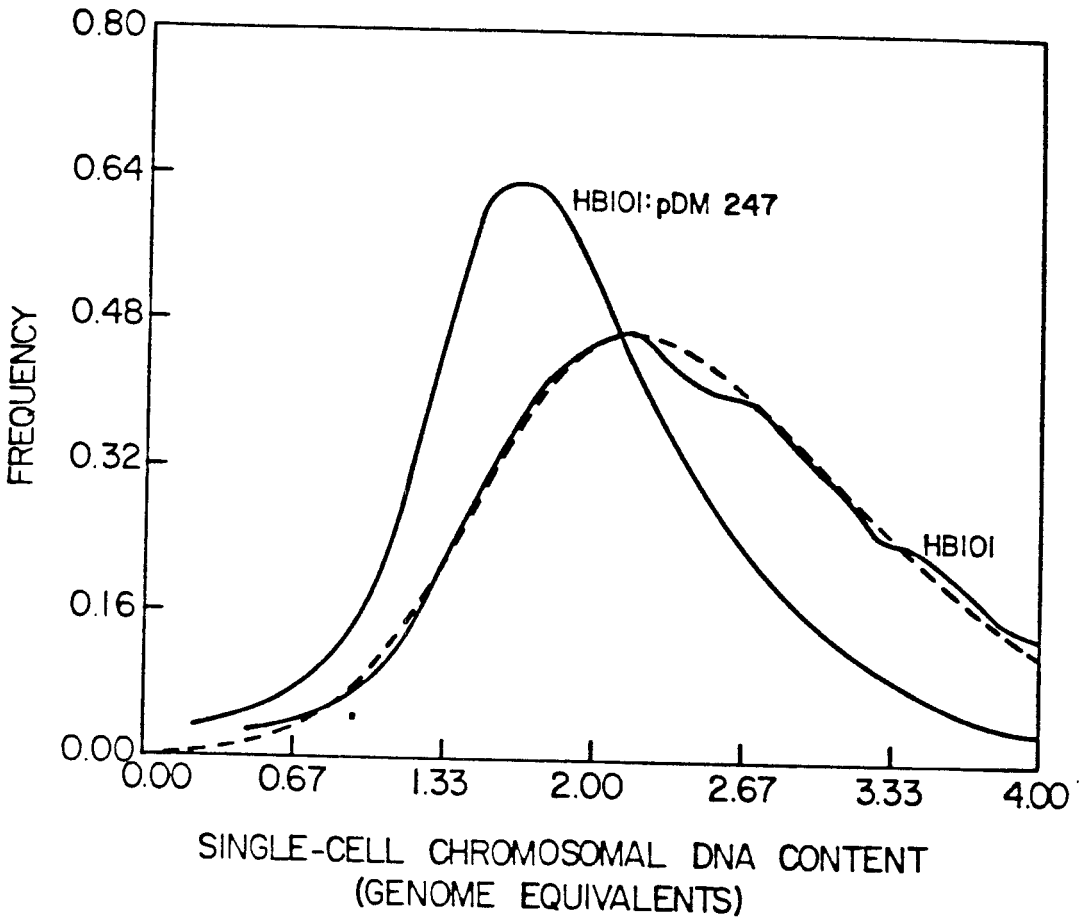
0.80
0.64
0.48
0.32
0.16
0.00
FREQUENCY
HB101:pDM 247
HB101
0.00
0.67
1.33
2.00
2.67
3.33
4.00
SINGLE-CELL CHROMOSOMAL DNA CONTENT
(GENOME EQUIVALENTS)

Figure 2

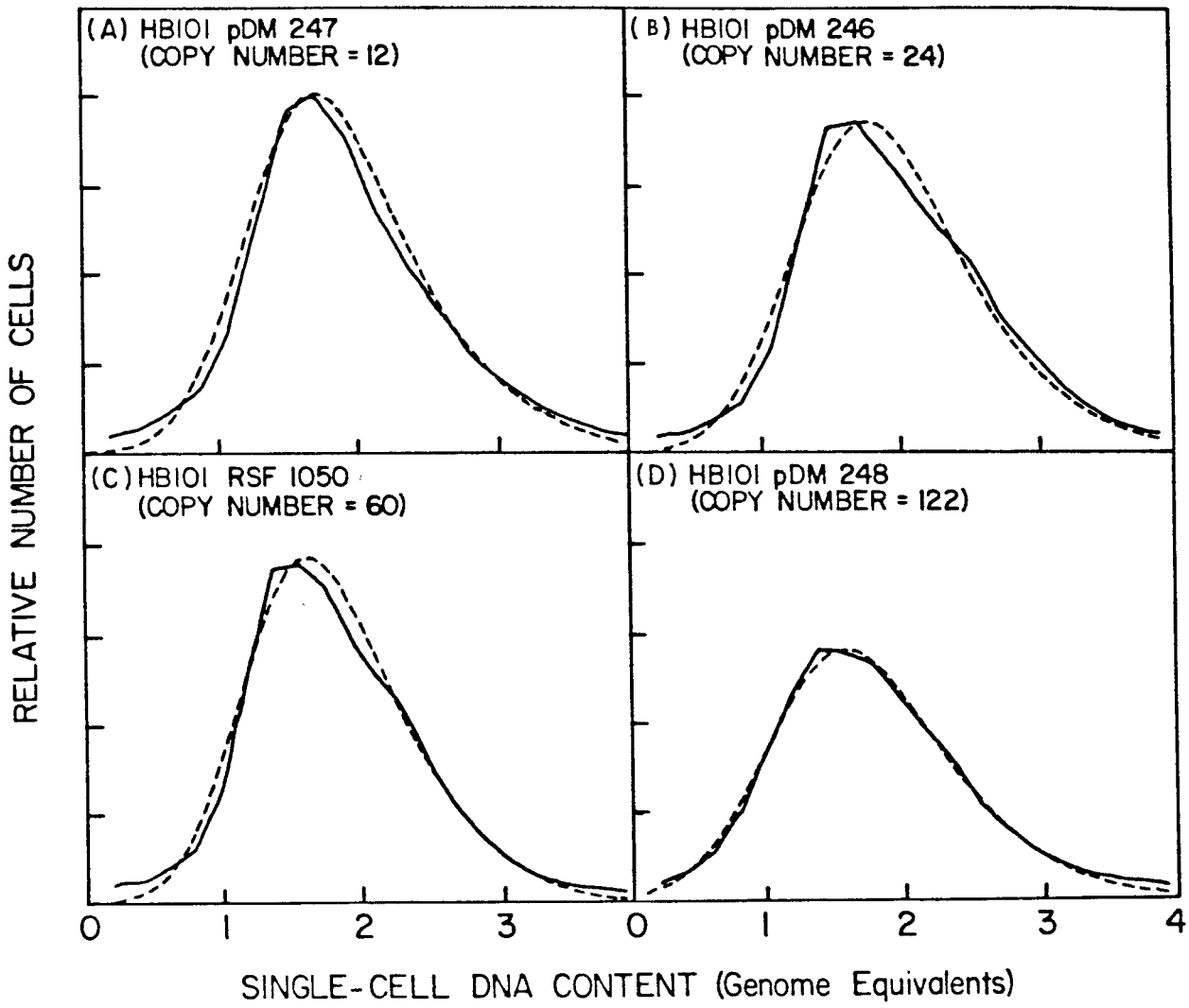
(A) HBIOI pDM 247
(COPY NUMBER = 12)
(B) HBIOI pDM 246
(COPY NUMBER = 24)
(C) HBIOI RSF 1050
(COPY NUMBER = 60)
(D) HBIOI pDM 248
(COPY NUMBER = 122)
RELATIVE NUMBER OF CELLS
0
1
2
3
0
1
2
3
4
SINGLE-CELL DNA CONTENT (Genome Equivalents)

Figure 3

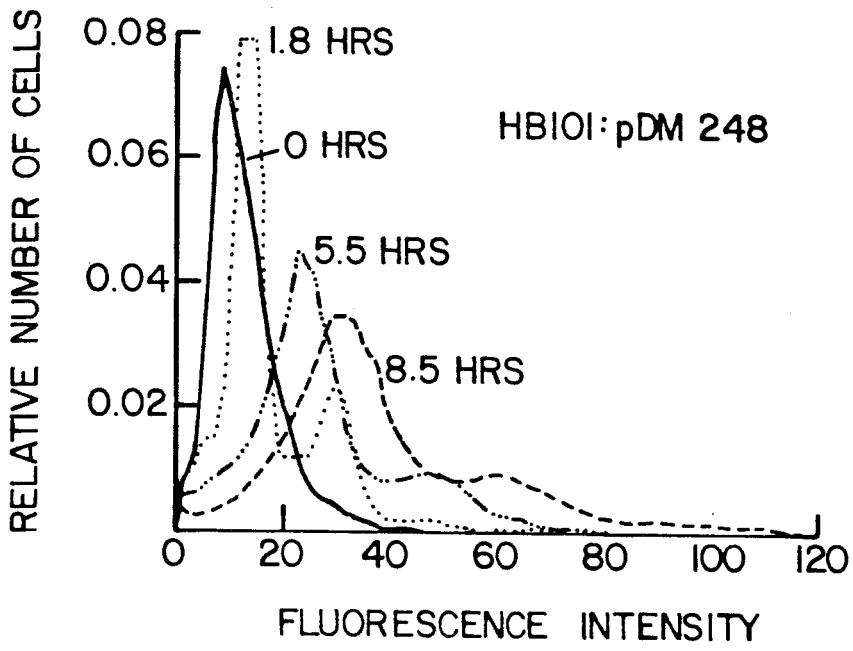
RELATIVE NUMBER OF CELLS
0.08
0.06
0.04
0.02
1.8 HRS
0 HRS
5.5 HRS
8.5 HRS
HB101: pDM 248
0
20
40
60
80
100
120
FLUORESCENCE INTENSITY

Figure 4

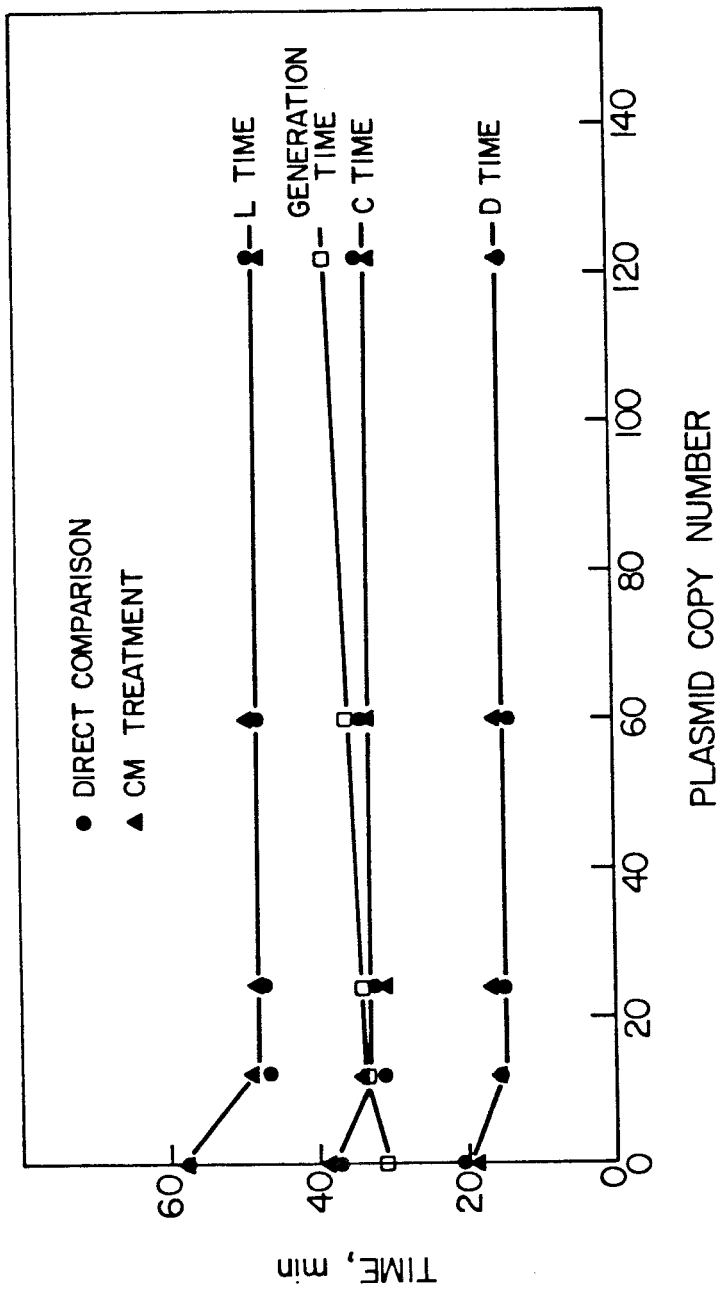
● DIRECT COMPARISON
▲ CM TREATMENT
L TIME
GENERATION TIME
C TIME
D TIME
TIME, min
60
40
20
0
0
20
40
60
80
100
120
140
PLASMID COPY NUMBER

Figure 5

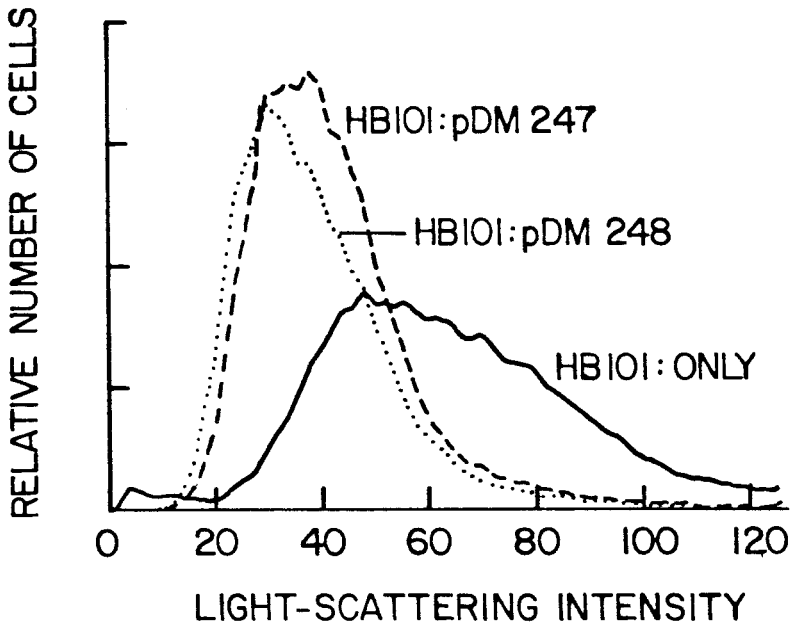
RELATIVE NUMBER OF CELLS
HB101:pDM 247
HB101:pDM 248
HB101:ONLY
0
20
40
60
80
100
120
LIGHT-SCATTERING INTENSITY

Figure 6

CHAPTER 5: A SEGREGATED MODEL FOR PLASMID CONTENT AND PRODUCT SYNTHESIS IN UNSTABLE BINARY FISSION RECOMBINANT ORGANISMS

(The text of Chapter 5 consists of an article which appeared in *Biotechnol. Bioeng.* **27**, 156 (1985).)

SUMMARY

Plasmid propagation in populations of unstable, binary fission recombinant organisms has been studied using a segregated, population balance, mathematical model. Segregated models have the advantage of direct incorporation of basic information on mechanisms and kinetics of plasmid replication and segregation at the single-cell level. The distribution of cellular plasmid content and specific rates of plasmid-gene expression have been obtained for several single-cell models of plasmid replication, partition, and gene expression. Plasmid replication kinetics during cell growth significantly influences the plasmid content distribution. In the case of transient growth of plasmid-containing and plasmid-free cells in partially selective medium, the degree of selection required for stable maintenance of plasmid-containing cells has been determined. Guidelines are presented for applicability of simpler, nonsegregated models and for evaluation of the parameters in these models based on single-cell mechanisms and associated parameters.

INTRODUCTION

Production of valuable proteins using recombinant DNA technology is generally achieved by introduction into a suitable host of a plasmid DNA which carries the genetic instructions for the protein of interest. In some respects the productivity of such recombinant cells and the efficiency of reactor and raw material utilization is directly related to the plasmid content of the recombinant cell population. Many previous studies demonstrate that plasmids may be unstable in the sense that the fraction of the cell population containing plasmids declines from unity initially to smaller values as growth proceeds.[1-4] It is known that plasmid stability may be influenced by both genetic and environmental factors. For example, inclusion of the par sequence in Escherichia coli plasmids has been shown to provide stabilization of plasmid retention in the population.[5] Chemostat experiments under different conditions show different plasmid loss rates.[6-8]

Most previous experiments on plasmid stability are designed to determine the relative numbers of plasmid-containing and plasmid-free cells. Similarly, several previous mathematical models of unstable recombinant cell populations, in formulating the model in terms of a non-segregated, mixed-culture description, consider and calculate only the numbers of plasmid-containing and plasmid-free cells. No further information is provided concerning the distribution of states in the growing population of cells. Knowledge of the population fraction which do not contain plasmids is clearly an important parameter, both in scientific investigations of mechanisms of plasmid and genetic stability and in technological applications in which retention of plasmids in the recombinant cells is a major objective.

Further information important in the same applications may be obtained by considering the distribution of cell states, in particular the distribution of cellular plasmid content and product synthesis activities, in individual cells in the population. Individual cells containing different numbers of plasmids are expected to have different probabilities of plasmid loss at division. Furthermore, synthesis of a plasmid-encoded gene product in an individual cell is expected to depend upon the number of cloned-gene copies contained in the host cell. Indeed, the experimental methodology proposed by Uhlin and Nördstrom for estimating the average plasmid copy number is based upon presumed proportionality between this quantity and the measured population-average activity of a marker enzyme, β-lactamase, expressed from a plasmid gene.[9] Extrapolating this concept to the single-cell level, it is apparent that one should be concerned not only with whether or not cells contain plasmids but also with how many plasmids on the average the cells contain, and perhaps with the distribution of plasmids within the population.

The objective of this work is formulation and solution of mathematical models for the distribution of cellular plasmid content and population product synthesis activity in unstable recombinant organisms that segregate their volume and mass by binary fission upon division. Examples of this type of organism include the bacteria E. coli and Bacillus subtilis of current great interest as genetic engineering hosts. Many other bacteria also exhibit this same binary fission division pattern. Also, Saccharomyces cerevisiae grown at maximal growth rates,[10] the fission yeast Schizosaccharomyces pombe, and many plant and animal cell lines are examples of binary fission eucaryotes.[11] In these models alternative hypotheses concerning regulation of plasmid replication and regulation of plasmid segregation, based upon possibilities suggested by the current

literature, will be considered. Besides the motivations already mentioned, a central advantage of segregated models is the opportunity of direct utilization of fundamental information from biological science studies of basic mechanisms and kinetics.

The following equation for the rate of synthesis of the product protein (also called the cloned-gene product) per unit volume of bioreactor provides a useful framework for the presentation to follow:

$$Q_p = N_p \int_0^\infty W(n,s) r_e(n) dn \quad . \tag{1}$$

N_p is the number of cells per unit volume of reactor containing plasmids, n denotes single cell plasmid content, and s denotes symbolically the condition of the cell environment. In this work, environmental effects will not be considered. It is presumed in writing Eq. (1) that the single-cell rate of product synthesis r_e depends only upon the number of plasmids n contained by the cell. This is obviously an approximation; a generic disadvantage of population balance approaches is the restriction of the number of variables used to describe cellular processes in order to avoid excessively complicated and unwieldy mathematics. However, although this representation is simplified, it is more detailed than product formation kinetics expressions frequently applied in biotechnology.

Furthermore, this model is based at the single-cell level which allows information concerning the distribution of states W(n,s) to be taken into account. In particular W(n,s)dn is the fraction of cells in the population containing a number of plasmid molecules between n and n+dn. The initial objective of the following analysis is determination of the plasmid content distribution in steady-state balanced growth. Following this analysis, the overall product synthesis rate is evaluated based upon Eq. (1). Finally,

the steady-state distribution of states is used as an initial condition in an analysis of transient growth of an unstable recombinant population in nonselective medium. Conditions for stable maintenance of the plasmid-containing population are also derived. In the concluding discussion, connections between these results and earlier models are discussed, and implications for future experimental directions are suggested.

SINGLE-CELL PLASMID CONTENT DISTRIBUTION IN STEADY-STATE BALANCED GROWTH

Derivation of the distribution of states W(n) is obtained by first determining the age distribution of the cells and subsequently converting that age distribution to a plasmid distribution based upon regulation of plasmid replication and segregation at the single-cell level. It is presumed throughout this part of the analysis that the culture is grown in selective medium in which plasmid-free cells do not grow. Only plasmid-containing cells are considered at this point.

Steady-State Age Distribution

Let a denote cell age since birth (newborn cells have age 0 and dividing cells have age P, the generation time). In the case of steady-state exponential growth, the population balance based upon cell age takes the following form

$$\frac{dW(a)}{da} = -\nu W(a) \quad , \tag{2}$$

where W(a) is the cell age distribution and ν is the overall specific growth rate of plasmid-containing cells. The solution of Eq. (2) must satisfy the normalization condition

$$\int_0^P W(a)da = 1 \quad . \tag{3}$$

A cell balance relating dividing and newborn cells gives

$$W(0) = (2 - \theta)W(P) \quad . \tag{4}$$

where θ is the probability of birth of a plasmid-free cell upon division of a plasmid-containing cell. The solution of Eq. (2) subject to conditions (3) and (4) is

$$W(a) = \left(\frac{2-\theta}{1-\theta}\right)\nu\, e^{-\nu a} \quad . \tag{5}$$

Substituting Eq. (5) into the cell balance of Eq. (4) yields the following relationship between the specific growth rate of plasmid-containing cells ν, the generation time P of the cells, and the parameter θ which characterizes plasmid instability.

$$\nu = \frac{\ell n(2-\theta)}{P} \tag{6}$$

As indicated by Eq. (6), the overall growth rate decreases with increasing θ for a given generation time P which represents the single-cell growth rate. (The single-cell growth rate should not be confused with the overall growth rate.[12] The overall growth rate corresponds to the quantity measured by population-average experiments such as optical density monitoring or the growth rate which is equal to the dilution rate in a steady-state chemostat.) Consequently, the shape of the age distribution broadens as plasmid instability increases as shown in Fig. 1.

For the special case of maximal growth rates, the results obtained here are also applicable to budding yeast S. cerevisiae which contain unstable plasmids. Cell division of S. cerevisiae is asymmetric at all but maximal growth rates, generating two offspring which differ in size and

maturation time. However, division is symmetric at the highest growth rates.[10] In this case, the present results are identical to those derived earlier for unstable plasmid-containing yeast.[13] With $\Theta = 0$, the age distribution of cells becomes that derived earlier by Powell.[14]

Plasmid Number Distribution at Birth

The first step in obtaining the plasmid content distribution in steady-state growth is determination of the distribution of plasmid numbers in individual cells at birth (age zero). Here, several different control mechanisms for plasmid replication are assumed and the plasmid number distribution at birth is derived for each.

It is useful to subdivide the plasmid-containing cells into subpopulations according to the number of plasmids at birth. The age distribution of cells which have x plasmids at birth is written as

$$W_x(a) = C_x e^{-\nu a} \quad . \tag{7}$$

The age distribution W(a) may be obtained by summing the $W_x(a)$ functions over all x values allowed by the model under consideration. Determination of C_x for various patterns of plasmid partition and control of plasmid replication is considered next.

Model I

In this model it is assumed that plasmids are distributed to daughter cells randomly at cell division and that all cells contain N plasmids at division. Similar models have been proposed previously in studies of *E. coli* plasmid biology.[15] In such a model, it is presumed that the plasmid has a control mechanism which can recognize the plasmid content of the cell and which stops replication when a particular plasmid level is reached, independent of the number of plasmids at birth.[16]

Based on these assumptions, C_x may be evaluated using Eq. (5) to evaluate W(P) and making use of Eq. (6) to simplify the expression for C_x. The result is the following equation

$$C_x = \frac{\nu}{(1-\theta)} \left[f(x;N) + f(N-x;N) \right] \quad , \tag{8}$$

and θ may be written explicitly

$$\theta = f(0;N) + f(N;N) \quad . \tag{9}$$

In Eqs. (8) and (9), $f(\cdot;\cdot)$ is the binomial distribution

$$f(x;N) = \frac{N!}{x!(N-x)!} \cdot \gamma^x \cdot (1-\gamma)^{N-x} \quad . \tag{10}$$

$f(x;N)$ is the probability that a daughter cell obtained by division of a cell with N plasmids will contain x plasmids. γ is the probability that a plasmid in the dividing cell remains in one of the particular daughters upon division. For organisms dividing by binary fission in which the two daughter cells are identical in all respects, the value of γ would be reasonably placed at 0.5. However, in some cases there may be some differentiation between the two cells which influences plasmid segregation, as in the case of symmetric volumetric division of a budding yeast into a mother and daughter cell. Alternatively, γ may be viewed as an empirical parameter which characterizes any mechanisms which tend to bias plasmid segregation towards one of the daughter cells.

Model II

The assumptions underlying this model are similar to those of Model I except that here some plasmids, 2M in number, are presumed to partition

evenly between the daughter cells. The remaining plasmids are segregated at random. Regular segregation of at least some of the plasmids in a dividing cell is suggested by the observation that replicating molecules of chromosomal and plasmid DNA are bound to replicon-specific sites on the plasma membrane of E. coli. Accordingly, regular segregation of those replicating molecules is expected as the membrane elongates during cell growth.[17] It has also been claimed that partitioning of plasmids may take place by association with the host cell chromosome which would also imply regular partitioning for at least some of the plasmid population within an individual cell.[5]

By setting 2M equal to N, the number of plasmids in the dividing cell, this model becomes one of completely regular segregation. Several experiments have demonstrated stable inheritance of some plasmids, including some with low copy number, in nonselective medium.[5,18,19] An E. coli genetic locus designated par which is implicated in stable plasmid maintenance has been identified and characterized in several plasmid systems including P1 and ColE1-like pSC-101 plasmids.[18,20] Model II is a reasonable hypothesis for partitioning behavior of high copy number plasmids containing the par sequence.

Since all cells receive at least M plasmids at birth in this model, θ is equal to zero. C_x then becomes

$$C_x = \nu[f(x-M:N-2M) + f(N-x-M:N-2M)] \qquad (11)$$

for $x \geq M$, $2M < N$.

Model III

This model assumes that all plasmids in the dividing cell are distributed randomly to the daughter cells and that K plasmids are

synthesized during each cell cycle unless the plasmid number reaches some maximum value N_m.

This model is based upon experimental observations for some plasmids, including the E. coli R1 plasmid, which indicate the number of plasmids synthesized during the cell cycle is regulated and not the number of plasmids in the dividing cell.[21] Also, detailed computer simulations of λdv plasmid replication using a molecular mechanism model also suggest that the assumption of a given number of synthesis events per cell cycle is a more accurate approximation of the replication control system's behavior than is presumption of a constant plasmid number at cell division.[22]

Few previous investigators have suggested an upper limit on plasmid content in connection with this mechanism. The maximum copy number N_m is introduced here primarily as a mathematical device which serves to close the set of equations.[13] If this maximum copy number is chosen sufficiently large with respect to the number of plasmids replicating during the cell cycle (K), computed cellular plasmid content distributions are independent of N_m.

This model is more complicated since here the plasmid distribution in a given cell cycle affects the distribution in a subsequent cell cycle. No such effects occur for Model I or Model II. For Model III, C_x values are given by

$1 \le x \le K + 1$:

$$C_x = \frac{1}{2-\theta}\left\{\left[f(x;N_m) + f(N_m - x;N_m)\right]\sum_{i=N_m-K}^{N_m} C_i + \sum_{i=K+1}^{N_m-1}\left[f(x;i) + f(i-x,i)\right]C_{i-K}\right\} \quad (12)$$

$K + 2 \leq x \leq N_m$:

$$C_x = \frac{1}{2-\theta}\left\{\left[f(x;N_m) + f(N_m - x;N_m)\right]\sum_{i=N_m-K}^{N_m} C_i + \sum_{i=x}^{N_m-1}\left[f(x;i) + f(i-x,i)\right]C_{i-K}\right\} \quad (13)$$

θ is determined by numerical solution of the following equation

$$\theta = \frac{1}{\sum_{i=1}^{N_m} C_i}\left\{\left[f(N_m;N_m) + f(0;N_m)\right]\sum_{i=N_m-K}^{N_m} C_i + \sum_{i=K+1}^{N_m-1}\left[f(i;i) + f(0;i)\right]C_{i-K}\right\} \quad (14)$$

Eqs. (12) through (14) are solved simultaneously numerically using Model I C_x values as initial guesses in the iteration scheme.

Fig. 2 shows the plasmid number distribution at birth (C_x) for Models I and III for reasonable values of N and K. The two models are not much different if γ is 0.5.

Single Cell Plasmid Content Distribution

The age distribution and distribution of plasmid content at birth obtained previously can be applied to obtain the distribution of single-cell plasmid content in the population after specification of plasmid replication kinetics. The model considered here is based primarily upon observations of plasmid replication in E. coli. Modification of the model for other replication kinetics should be relatively straightforward.

In E. coli replication of many plasmids occurs by random selection with single plasmid copies being replicated in sequence independent of

chromosome replication.[23-25] The event of plasmid replication does not appear to be connected with any particular point in the host cell cycle.[24,26-28] Furthermore, the rate of the replication process, once initiated, is relatively independent of cellular condition or growth environment.[22] Based on the above arguments, it is reasonable to employ zero-order kinetics for plasmid synthesis so that the relationship between the initial plasmid content x of the cell and the number of plasmids of a cell at age a is given by

$$n = x + k_n a \tag{15}$$

where k_n is the plasmid synthesis rate constant. If the number of plasmids at some particular age reaches an upper limit presumed by the model, plasmid synthesis terminates at that point and the number of plasmids remains constant until cell division. Since Models I and III represent the most different types of plasmid replication regulation, the plasmid content distribution has been found for both of these models. Detailed calculations and methods are shown here for Model I, and derivations for Model III are given in the Appendix.

In Model I, the upper limit on cellular plasmid content is N, the number of plasmids in a dividing cell. Schematic diagrams of the relationship between initial plasmid content and plasmid content at age a implied by Model I and Model III are given in Fig. 3. Here $S_1(x)$, given by

$$S_1(x) = \frac{(N-x)}{(N-1)} \cdot P \quad , \tag{16}$$

is the cell age at which cells containing initially x plasmids reach their maximum plasmid content N. The plasmid content n is given then as a function of cell age by

$$n = x + \frac{(N-x)}{S_1(x)} \cdot a \quad ; \quad a \leq S_1(x) \tag{17}$$

$$n = N \quad ; \quad a > S_1(x) \quad .$$

Examination of Fig. 3 shows clearly that two subpopulations may be identified with respect to the state of plasmid replication. The first subpopulation of cells are not replicating plasmids at their cell cycle position. All such cells contain N plasmids and contribute a delta function weighted by the fraction of the subpopulation F_N. F_N is given by

$$F_N = \int_0^P C_N \, e^{-\nu a} da + \sum_{x=1}^{N-1} \int_{S_1(x)}^P C_x \cdot e^{-\nu a} da \tag{18}$$

which upon integration yields

$$F_N = \frac{\theta}{2-\theta} + \sum_{x=1}^{N-1} \frac{C_x}{\nu} \left[e^{-\nu S_1(x)} - \frac{1}{2-\theta} \right] \quad , \tag{19}$$

where C_x and θ are determined by Eqs. (8) and (9), respectively. The plasmid content distribution $W_x(n)$ of the second subpopulation of cells, which are those synthesizing plasmids, can be obtained by transformation of the age distribution according to Nishimura and Bailey[29]

$$W_x(n) = W_x(a) \left| \frac{da}{dn} \right| \tag{20}$$

from which

$$W_x(n) = C_x \left(\frac{S_1(x)}{N-x} \right) \exp \left[- \frac{\nu \cdot (n-x) \cdot S_1(x)}{(N-x)} \right] \quad . \tag{21}$$

The complete plasmid content distribution W(n) is the sum of contributions from the two subpopulations described above

$$W(n) = F_N \delta(x - N) + \sum_{x=1}^{N-1} W_x(n) \cdot H_n \quad . \tag{22}$$

where

$$H_n = H(n - x) - H(n - N) \tag{23}$$

and where $H(\cdot)$ is the Heaviside unit step function.

Plasmid content distributions W(n) calculated for Model I and Model III (solution in Appendix) are shown in Fig. 4. Here, comparable parameters have been chosen for the two models (N = 20 for Model I and K = 10 for Model III). For the case shown in Fig. 4, F_{20} is 0.393 for Model I. It is clear from this result that, although the plasmid content at birth is relatively similar for the two models, the plasmid content distributions are more different. Cellular plasmid content is distributed over a much broader range for Model III. In Model I, unlike Model III, a significant fraction of cells have the same plasmid content. In this particular case, for example, 39.3% of the cells of Model I contain 20 plasmids. These differences arise because patterns of plasmid synthesis are different in the two cases. Plasmid replication kinetics during cell growth have an important influence on the plasmid content distribution.

Analyses of plasmid propagation with replication controls corresponding to current Models I and III have been presented previously by Nordström *et al.*[15] In that work, which presumes $\gamma = 0.5$ throughout, equations which can be solved to give an unnormalized form of the C_x values were presented. The present study, which is based on a different

mathematical approach, adds to this earlier work by explicit solution for C_x values, by consideration of the effects of replication kinetics, by analytical determination of the complete plasmid number distribution, by development of an explicit equation for the important parameter Θ, and by introduction of the γ parameter and of Model II.

Product Synthesis Rate

The form of the single-cell rate of gene expression r_e is based upon several experimental and previous modeling investigations. As noted previously, it has been shown that at sufficiently low copy number, the rate of gene expression is proportional to the number of plasmids in the cell.[9] On the other hand, it is known that cells containing plasmids grow more slowly than those without plasmids.[30] Recent experiments in this laboratory with a series of copy number mutants show decreasing growth rate with increasing plasmid content. Also, it has been observed that cells harboring runaway plasmids become nonviable as the plasmid numbers per cell approach 1000 in order of magnitude.[31] A detailed mathematical model of cloned lac promoter-operator function in E. coli suggests a parabolic relationship will reasonably approximate the relationship between cloned gene transcription level and the number of plasmids per cell.[32] Based upon all of these observations, the following kinetic model is adopted for single-cell gene expression rate:

$$r_e = k_p n(1 - cn) \tag{24}$$

where k_p and c are constants.

Dividing both sides of Eq. 1 by N_p yields the specific rate of product synthesis, q_p:

$$q_p = \int_0^\infty W(n) \cdot r_e(n) dn \quad . \tag{25}$$

Substituting Eq. (24) into (25), the dimensionless specific product synthesis rate has been evaluated as a function of a characteristic dimensionless plasmid number for Models I and III with results shown in Fig. 5. The dimensionless specific product synthesis rate is defined as $q_p\ c/k_p$, and the dimensionless plasmid number is defined as cN and 2cK for Model I and Model III, respectively. It is noteworthy that there is an optimum plasmid number to maximize the specific product formation rate. While this form of relationship is not unexpected in view of the form of Eq. (24), it is interesting that altering the plasmid replication kinetic model shifts the optimum plasmid number.

This segregated product formation model may be used to assess the feasibility of determining single-cell gene expression kinetics based upon population-average or nonsegregated data. Suppose that the specific product formation rate defined in Eq. (25) is measured directly experimentally as is the average plasmid content per cell $\bar{N}$, which in terms of the present nomenclature, may be written as

$$\bar{N} = \int_0^\infty nW(n) dn \quad . \tag{26}$$

Is the functional relationship between q_p, which is a population average rate of synthesis, and $\bar{N}$ a reasonable approximation to the single-cell product synthesis rate function r_e? If the single-cell rate of gene expression r_e is a strictly concave function of n as it is in Eq. (24) ($d^2 r_e d/n^2 < 0$ is necessary and sufficient for strict concavity), the following inequality holds:[33]

$$q_p = \int_0^\infty r_e(n)W(n)dn \leq r_e\left(\int_0^\infty nW(n)dn\right) = r_e(\bar{N}) \quad . \tag{27}$$

This shows that the overall specific product synthesis rate measured is less than or equal to the single cell rate of gene expression evaluated at the average plasmid content. Consequently, efforts to estimate the single cell gene expression rate from population-average data will underestimate the true single cell rate so long as the single-cell gene expression rate function r_e has the concave properties mentioned.

Model calculations employing the kinetics in Eq. (24) have been explored to determine the extent of deviation between q_p and $r_e(\bar{N})$. Results are shown in Fig. 6 for Model I and Model III and for two different values of the parameter γ which characterizes the bias for nonuniform plasmid segregation upon division. These results show that the deviation between the two different rates is substantial when the plasmid number N or 2K approaches the inhibitory level c^{-1} or if γ deviates significantly from 0.5. It is interesting to note that for $\gamma = 0.9$, the functional relationship between dimensionless plasmid number and the production rate ratio is much different for Models I and III.

SIMULTANEOUS TRANSIENT GROWTH OF PLASMID-CONTAINING AND PLASMID-FREE CELLS

A simultaneous mixed-culture population balance model is used to calculate the time course of growth of plasmid-containing and plasmid-free cells in a medium supporting growth of both. As initial condition, it is presumed that a cell population consists of plasmid-containing cells with steady-state age distribution as given in the previous section. This model serves to describe a number of situations including growth of the two cell types in nonselective medium and growth in medium which does bias the

growth rate ratio of the two populations but in which both cell types are able to multiply. The overall growth rate of plasmid-containing cells will be denoted by ν. P and P^- denote the generation times of plasmid-containing and plasmid-free cells, respectively. The state of the cell population now depends upon two variables, cell age a and time t since shift to the medium in which both cell types grow.

The transient population balance equations for the two populations are given by[34]

$$\frac{\partial U}{\partial a} + \frac{\partial U}{\partial t} = 0 \qquad 0 < a < P \tag{28}$$

and

$$\frac{\partial U^-}{\partial a} + \frac{\partial U^-}{\partial t} = 0 \qquad 0 < a < P^- \quad , \tag{29}$$

where U and U^- are the transient age distributions of the plasmid-containing cells and the plasmid-free cells, respectively. The initial conditions are

$$U(a,0) = \frac{2-\theta}{1-\theta}\, \nu e^{-\nu \cdot a} \tag{30}$$

and

$$U^-(a,0) = 0 \quad . \tag{31}$$

Boundary conditions connecting cell division and cell birth are given by

$$U(0,t) = (2-\theta)U(P,t) \tag{32}$$

and

$$U^-(0,t) = \theta U(P,t) + 2U^-(P^-,t) \quad . \tag{33}$$

Eq. (33) couples the solution for the plasmid-free population to that for the plasmid-containing population. The first term on the right-hand side of Eq. (33) represents plasmid-free segregants produced by division of

plasmid-containing cells, and the second term on the right-hand side of Eq. (33) denotes binary fission reproduction of the plasmid-free cells.

The above equations are most conveniently solved by the method of characteristics and by noting that solutions in certain domains of the time-age coordinate plane have a common form. The solution domain for each cell type is diagrammed in Fig. 7. Characteristics for this problem are straight lines with a slope of +1 since da/dt is unity. The transient age distribution of plasmid-containing cells is independent of the domain considered and is given by

$$U(a,t) = \left(\frac{2-\theta}{1-\theta}\right) \nu \cdot e^{\nu(t-a)} \quad ; \quad t \geq 0 \quad . \tag{34}$$

Since the solution of the transient age distribution of the plasmid-containing cells is independent of the domain, the contribution of the the plasmid-containing cells to the plasmid-free cells by segregation becomes constant. This makes it easy to solve for the transient age distribution of the plasmid-free cells. The solution of Eq. (29) subject to Eq. (33) is obtained for each domain using Eq. (31) as an initial condition. The solution for the plasmid-free population in domain E_i, denoted $U_i^-(a,t)$, is given by

$$\begin{aligned} U_1^-(a,t) &= 0 \\ U_i^-(a,t) &= \frac{\theta}{1-\theta} \nu \sum_{k=0}^{i-2} \beta^k e^{\nu(t-a)}; \; i \geq 2 \quad ; \quad t \geq 0 \quad , \end{aligned} \tag{35}$$

where

$$\beta = \frac{2}{(2-\theta)^{1/\alpha}} \quad , \qquad \alpha = P/P^- \quad . \tag{36}$$

Eq. (35) can be verified by induction.

The total number of each cell type as a function of time is obtained by integrating the corresponding age distribution over all cell ages. Letting $N_p(t)$ and $N_p^-(t)$ denote the total number of cells with and without plasmids at time t, respectively, the fraction of the population containing plasmids is given by

$$\Phi_p(t) = \frac{N_p(t)}{N_p(t) + N_p^-(t)} \quad . \tag{37}$$

Evaluating this equation at integer multiples of plasmid-containing cell generation time ($t = mP$), Φ_p may be written in the form

$$\Phi_p(m) = \frac{1}{1 + \frac{\theta}{(1-\theta)} \cdot \frac{(1-\eta)}{(2-\eta)} \left[1 - \left(\frac{2^\alpha}{2-\theta}\right)^m\right]} \tag{38}$$

where

$$\eta = (2-\theta)^{1/\alpha}$$

The fraction of plasmid-harboring cells Φ_p is essentially a function of two parameters, the single cell growth rate ratio α and the probability of plasmid loss θ. α may be controlled by adjustment of the growth environment, and θ is characterized by plasmid genetic functions. Table I lists the θ values for several different cases of dividing cell plasmid content or plasmids synthesized per generation for Models I and III, respectively. These θ values correspond to $\gamma = 0.5$. Fig. 8 illustrates the change in the fraction of the population containing plasmids as a function of the number of generations m of the plasmid-containing cells for the different cases enumerated in Table I and with single cell growth rate ratio α equal to unity. Even though the growth rates of the two cell types on the single-cell level are identical, the fraction of the plasmid-containing population decreases to zero with the number of generations. This is due to plasmid instability, which causes the plasmid-containing

population to have a lower overall specific growth rate than the plasmid-free population by a factor of $\ell n(2-\theta)/\ell n 2$.

For stable maintenance of the plasmid-containing cells, which corresponds to the mathematical condition

$$\lim_{m \to \infty} \Phi_p(m) \neq 0 \quad , \tag{39}$$

it may be shown from Eq. (38) that α must satisfy the following condition:

$$\alpha < \frac{\ell n(2-\theta)}{\ell n 2} \quad . \tag{40}$$

This equation connects the degree of plasmid instability with the required adjustment of the growth medium so that plasmid-containing cells can compete adequately with plasmid-free cells. When α satisfies the inequality given in Eq. (40), the fraction of the population containing plasmids approaches asymptotically the value given by

$$\Phi_p = \frac{1}{1 + \frac{\theta}{1-\theta}\left(\frac{1-\eta}{2-\eta}\right)} \quad . \tag{41}$$

Again, the population-balance approach to the problem provides explicit connection between regulation of plasmid-replication, as indicated by the model type, the characteristic plasmid copy number, and overall operating parameters of the system which are of practical importance.

Although it is impossible to obtain this sort of inner relationship with nonsegregated models, it is interesting to note that earlier treatments of simultaneous growth of plasmid-containing and plasmid-free cells based on nonsegregated, mixed-population models have obtained some results identical to those given above. Eq. (38) here is identical to the equation for the fraction of plasmid-containing cells derived by Anderson

and Lustbader[35] after noting that their parameter h, the probability that a particular daughter cell contains a plasmid, is related to the present parameter θ by the equation

$$h = \frac{1}{2}\left(2-\theta\right) \quad . \tag{42}$$

Also, the analysis by Imanaka and Aiba[36] gives a result identical to Eq. (38) after noting that the plasmid loss per division of host cell parameter (denoted p in the original paper and denoted p_{IA} here to avoid ambiguity) is related to θ by

$$p_{IA} = 1 - \frac{\ell n(2-\theta)}{\ell n\, 2} \quad . \tag{43}$$

Stewart and Levin[37] studied a conjugative plasmid system. Plasmids used as cloning vehicles do not usually contain conjugative properties for containment safety reasons. When the term for conjugation in Stewart and Levin's work is deleted, the equations become exactly the same as those formulated by Imanaka and Aiba. Previous investigators[35,37] have also derived a criterion for stable maintenance of plasmid-containing cells, which is identical to Eq. (40) after taking into account the notational differences. These equivalencies between certain of the present results and those of other investigators are interesting in view of substantial differences in the basic modeling framework in each case.

CONCLUSIONS

Mathematical descriptions of plasmid propagation in growing cell cultures have been obtained based upon a segregated, population balance approach. In such segregated models, different hypotheses concerning regulation of plasmid replication, plasmid replication kinetics, and intrinsic product synthesis kinetics at the single-cell level may be

readily incorporated. The plasmid content distribution and specific rates of plasmid gene expression have been obtained for several different single-cell models of plasmid replication, segregation, and gene expression. In a study of the transient case, it has been shown how single-cell replication regulation properties influence parallel growth of plasmid-containing and plasmid-free cells and the degree of selection required for stable maintenance of plasmid-containing cells.

In contrast to a previous investigation of budding yeast in which division is frequently asymmetric, analysis of simultaneous plasmid-free and plasmid-containing transient growth by the segregated, population-balance approach gives major results concerning overall population properties, which are identical to those obtained by a nonsegregated model. Nonsegregated and segregated models give reasonably consistent product synthesis rate expressions (see Fig. 6) so long as the plasmid number per cell does not approach too closely the inhibitory level or there is not a substantial bias in plasmid segregation upon division. Consequently, the present analysis provides guidelines as to when a simpler, nonsegregated model may appropriately be used. This work also provides guidance on the relationship between parameters in those models and parameters of single-cell plasmid replication and segregation processes.

Acknowledgement: This work was supported by the National Science Foundation.

NOMENCLATURE

a	cell age (hr)
c	constant in Eq. (24)
C_x	fraction of plasmid-containing cells which have x plasmids at birth
D_j	solution domain for plasmid-containing cells
E_i	solution domain for plasmid-free cells
F_N, F_{N_m}	population fraction which contains the maximum plasmid content (N for Model I and N_m for Model III)
$f(\cdot;\cdot)$	the binomial distribution
h	probability that a particular daughter cell contains a plasmid
$H(\cdot)$	Heaviside unit step function
K	number of plasmids replicated during each cell cycle for Model III
k_n	plasmid synthesis rate constant
k_p	product synthesis rate constant
M	number of plasmids distributed uniformly to daughter cells upon division for Model II
m	number of generations of the plasmid-containing cells
N	number of plasmids at cell division for Model I
$\bar{N}$	average plasmid content
n	plasmid content parameter
N_m	maximum number of plasmids for Model III
N_p	number of plasmid-containing cells per unit volume of bioreactor
P	generation time of plasmid-containing cell (hr)
p_{IA}	plasmid loss probability used by Imanaka and Aiba[36]
Q_p	product synthesis rate per unit volume of bioreactor
q_p	specific product synthesis rate
r_e	single-cell rate of product synthesis
s	cell environment parameter

S_1, S_3 cell age to reach maximum plasmid content

t time after shift to nonselective medium (hr)

U transient age distribution of plasmid-containing cells

W distribution of cell states

W(a) age distribution of plasmid-containing cells at steady-state

W(n) plasmid content distribution

W(n,s) plasmid content distribution at cell environment s

$W_x(a)$ age distribution of the cells which contain x plasmids at birth

$W_x(n)$ plasmid content distribution of the cells which contain x plasmids at birth

Superscript

- plasmid-free cells

Greek Letters

α ratio of the single-cell growth rate of the plasmid-free cell to that of the plasmid-containing cell

β, η constants in Eq. (35) and Eq. (38), respectively

θ probability of plasmid loss

γ probability that a plasmid remains in a particular daughter cell upon division

ν overall specific growth rate of the plasmid-containing cells (hr^{-1})

ϕ_p fraction of plasmid-containing cells

REFERENCES

1. J. Inselburg, J. Bacteriol., **147**, 962 (1981).

2. R. B. Helling, T. Kinney, and J. Adams, J. Gen. Microbiol., **123**, 129 (1981).

3. J. T. M. Wouters, F. Driehuis, P. Polaczek, H. van Oppenraay, and J. van Andel, Antonie van Leeuwenhoek, **46**, 353 (1980).

4. A. J. Alldrich and J. T. Smith, Antonie van Leeuwenhoek, **49**, 133 (1983).

5. P. A. Meacock and S. N. Cohen, Cell, **20**, 529 (1980).

6. D. Godwin and J. H. Slater, J. Gen. Microbiol., **111**, 201 (1979).

7. I. M. Jones, S. B. Primrose, A. Robinson and D. C. Ellwood, Molec. Gen. Genet., **180**, 579 (1980).

8. D. Noack, M. Roth, R. Geuther, G. Muller, K. Undisz, C. Hoffmeier, and S. Gasper, Molec. Gen. Genet., **184**, 121 (1981).

9. B. Uhlin and K. Nordstrom, Plasmid, **1**, 1 (1977).

10. L. H. Hartwell and M. Unger, J. Cell Biol., **75**, 422 (1977).

11. J. M. Mitchison, The Biology of The Cell Cycle, Cambridge University Press, Cambridge, Great Britain, 1971.

12. M. Hjortso and J. E. Bailey, Math. Biosci., **63**, 121 (1983).

13. M. Hjortso and J. E. Bailey, Biotechnol. Bioeng., **26**, 528 (1984).

14. E. O. Powell, J. Gen. Microbiol., **15**, 492 (1956).

15. K. Nordstrom, S. Molin and H. Aagaard-Hawsen, Plasmid, **4**, 215 (1980).

16. B. Polisky, D. Gelfand, and H. M. Shepard, Plasmids and Transposons, C. Stutard and K. Rozee, Eds. (Academic Press, 1980).

17. F. Jacob, S. Brenner and F. Cuzin, Cold Spring Harbor Symp. Quart. Biol., **28**, 329 (1963).

18. N. Sternberg and S. Austin, Plasmid, **5**, 20 (1981).

19. T. Miki, A. M. Easton, and R. H. Rownd, J. Bacteriol., **141**, 87 (1980).

20. C. A. Miller, W. T. Tucker, P. A. Meacock, P. Gustafsson, and S. N. Cohen, Gene, **24**, 309 (1983).

21. P. Gustafsson and K. Nordstrom, J. Bacteriol., **141**, 106 (1980).

22. S. B. Lee and J. E. Bailey, Plasmid, **11**, 151 (1984).

23. J. Collins and R. H. Pritchard, J. Mol. Biol., 78, 143 (1973).

24. R. H. Pritchard, M. G. Chandler and J. Collins, Molec. Gen. Genet., 138, 143 (1975).

25. K. Matsubara, Plasmid, 5, 32 (1981).

26. J. Zeuthen, E. Morozow and M. L. Pato, J. Bacteriol., 112, 1425 (1972).

27. P. Gustafsson, K. Nordstrom and J. W. Perram, Plasmid, 1, 187 (1978).

28. D. A. Seinberg and C. E. Helmstetter, Plasmid, 6, 342 (1981).

29. Y. Nishimura and J. E. Bailey, Math. Biosci., 51, 305 (1980).

30. J. Inselburg, J. Bacteriol., 133, 433 (1978).

31. B. E. Uhlin, S. Molin, P. Gustafsson and K. Nordstrom, Gene, 6, 91 (1979).

32. S. B. Lee and J. E. Bailey, Biottechnol. Bioeng., 26, 1383 (1984).

33. G. H. Hardy, J. E. Littlewood and G. Polya, Inequalities (Cambridge University Press, 1934).

34. D. Ramkrishna, p. 1 in Advances in Biochemical Engineering (T. K. Ghose, A. Fiechter, N. Blakebrough, eds.), Springer-Verlag, Berlin, 1979.

35. T. F. Anderson and E. Lustbader, Proc. Natl. Acad. Sci., U.S.A., 72, 4085 (1975).

36. T. Imanaka and S. Aiba, Annals of N.Y. Acad. Sci., 369, 1 (1981).

37. F. M. Stewart and B. R. Levin, Genetics, 87, 209 (1977).

APPENDIX: PLASMID CONTENT DISTRIBUTION W(n) FOR MODEL III

As done for Model I, the plasmid content distribution can be obtained after specifying the kinetics of plasmid replication and the plasmid number distribution at birth. The latter distribution is given in Eqs. (12) through (14). Based on the assumptions for Model III, the plasmid content, n, and the cell age a are related as follows:

For $1 \leq x \leq N_M - K - 1$

$$n = x + \frac{K}{P} \cdot a \qquad \text{(A-1.a)}$$

For $N_M - K \leq x \leq N_M - 1$

$$n = x + \frac{(N_M - x)}{S_3(x)} \cdot a \qquad \text{(A-1.b)}$$

The fraction, F_{N_M}, of the subpopulation of cells that are not replicating plasmid at their cell cycle position is computed from

$$F_{N_M} = \int_0^P C_{N_M} e^{-\nu a} \cdot da + \sum_{x=N_M-K}^{N_M-1} \int_{S_3(x)}^P C_x e^{-\nu a} \cdot da \qquad \text{(A-2)}$$

or

$$F_{N_M} = \frac{C_{N_M}}{\nu} \cdot \left(\frac{1-\theta}{2-\theta}\right) + \sum_{x=N_M-K}^{N_M-1} \frac{C_x}{\nu} \cdot \left[e^{-\nu S_3(x)} - \frac{1}{2-\theta}\right] \qquad \text{(A-3)}$$

where C_x and θ are determined by Eqs. (12) through (14).

The plasmid content distribution $W_x(n)$ of the second subpopulation of

cells which are synthesizing plasmids is obtained by transformation of the age distribution:

$$W_x(n) = W_x(a)\left[\frac{da}{dn}\right] . \qquad \text{(A-4)}$$

For $1 \le x \le N_M - K - 1$

$$W_x(n) = C_x \frac{P}{K} \cdot e^{-\frac{\nu(n-x)\,P}{K}} \cdot H_1 \qquad \text{(A-5)}$$

where $H_1 \equiv [H(n-x) - H(n-x-K)]$ and $H(\cdot)$ is the Heaviside unit step function.

For $N_M - K \le x \le N_m - 1$

$$W_x(n) = C_x \frac{S_3(x)}{(N_M-x)} \cdot e^{-\frac{\nu(n-x)S_3(x)}{(N_M-x)}} \cdot H_2 \qquad \text{(A-6)}$$

where $H_2 \equiv [H(n-x) - H(n-N_M)]$ and

$$S_3(x) = (N_M - x)P/K . \qquad \text{(A-7)}$$

Finally, the complete plasmid content distribution, W(n), is obtained by summing both contributions to yield

$$W(n) = F_{N_M} \cdot \delta(x - N_M) + \sum_{x=1}^{N_M-1} W_x(n) \qquad \text{(A-8)}$$

where δ is the delta function.

TABLE I

Effect of Plasmid Copy Number on the Probability of Plasmid Loss for Model I and Model III ($\gamma = 0.5$)

Plasmid copy number (N or 2K)	Probability of plasmid loss (θ)	
	Model I	Model III
2	0.5	0.362
4	0.125	0.128
6	0.0313	0.0417
8	0.0078	0.0129
10	0.0020	0.0039

FIGURE CAPTIONS

FIGURE 1. Cell age distribution of population grown at steady state for different degrees of plasmid stability with single-cell generation time P = 0.5 hr. ($\theta = 0$ —— $\theta = 0.5$ ---- $\theta = 0.9$ ·-·-·).

FIGURE 2. Plasmid number distribution at birth for Model I (dashed curve N = 20) and Model III (solid curve; K =10, N_M = 75) for $\gamma = 0.5$ and $\nu = 1\ hr^{-1}$.

FIGURE 3. Schematic diagrams of plasmid replication patterns for Model I and Model III.

FIGURE 4. Plasmid content distribution W(n) for Model I (dashed curve) and Model III (solid curve) with $\gamma = 0.5$. (N = 20 in Model I and K = 10 in Model III).

FIGURE 5. The dimensionless specific product synthesis rate cq_p/k_p as a function of characteristic dimensionless plasmid number for Model I (dotted curve) and Model III (solid curve) (Abscissa = cN for Model I, 2cK for Model III; $\gamma = 0.5$, $c = 0.011$).

FIGURE 6. Comparison of nonsegregated and segregated product synthesis kinetic models. The ratio on the ordinate is the specific product synthesis rate based on the nonsegregated model divided by the specific product synthesis rate based on the segregated model. The characteristic dimensionless plasmid number is defined for both models as in Fig. 5.
(Model I, $\gamma = 0.5$ -●-●- Model I, $\gamma = 0.9$ -■-■-■- ,
Model III, $\gamma = 0.5$ —— Model III, $\gamma = 0.9$ ——).

FIGURE 7. Solution domains for plasmid-containing population (A) and plasmid-free population (B).

FIGURE 8. Change in the fraction of the plasmid-containing poulation as a function of the number of generations with $\gamma = 0.5$ and $\alpha = 1.0$. The plasmid loss probability θ corresponding to each curve is listed in Table I.
(Model I, N = 4; curve 1; Model I, N = 6: curve 2;
Model I, N = 8; curve 3; Model III, K = 2: curve 4;
Model III, K = 3; curve 5; Model III, K = 4: curve 6).

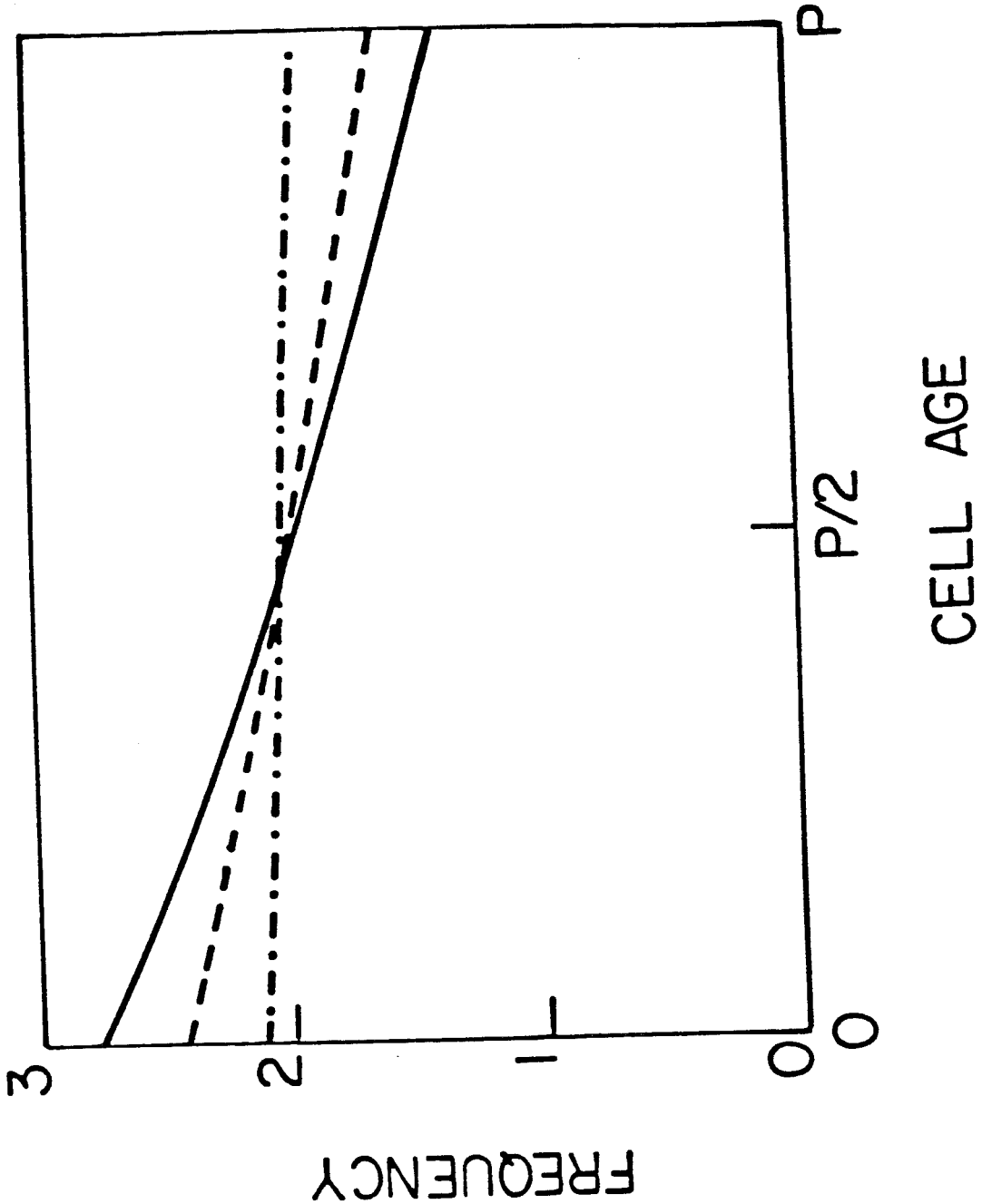

FIGURE 1

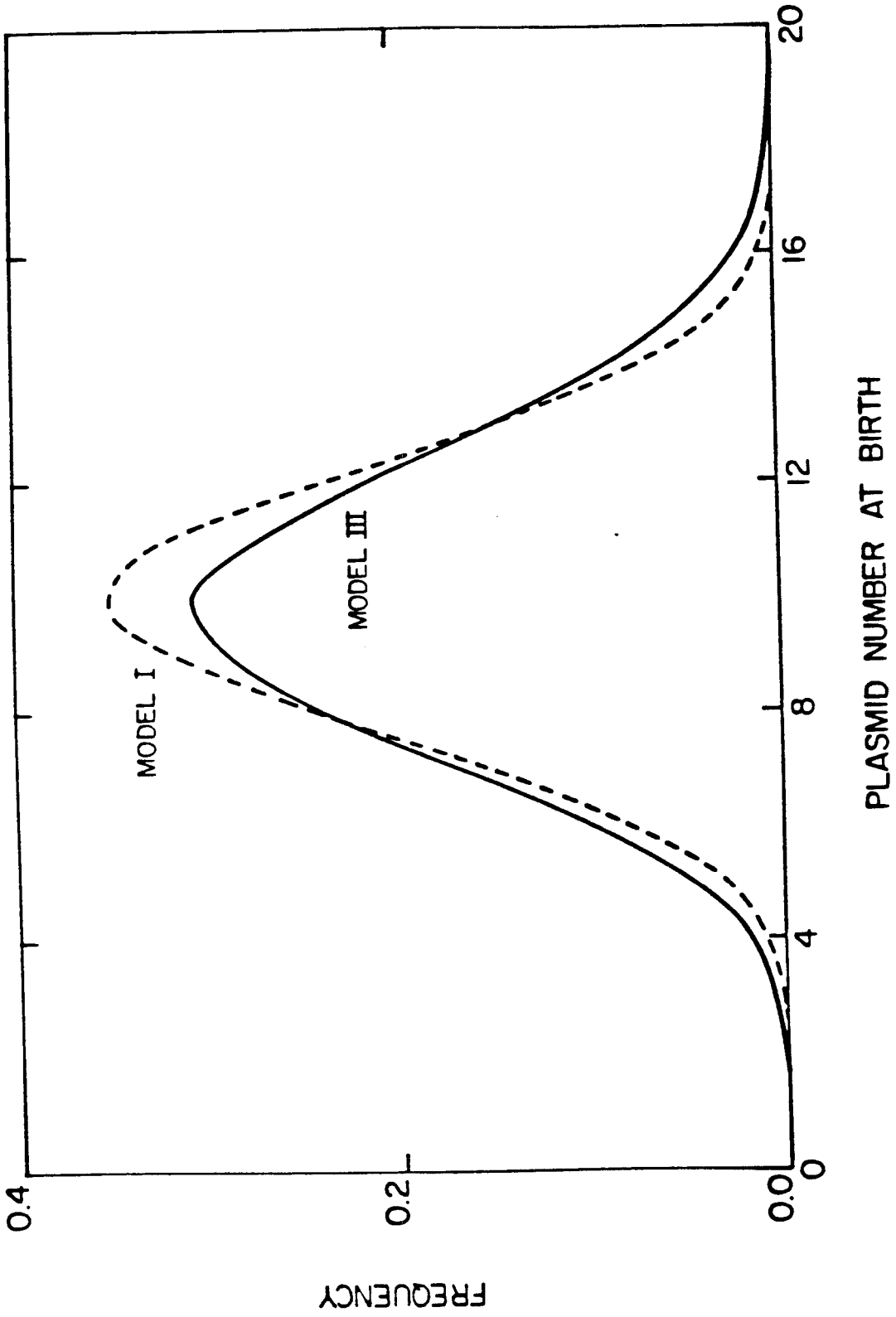
MODEL I
MODEL III
FREQUENCY
0.0
0.2
0.4
0
4
8
12
16
20
PLASMID NUMBER AT BIRTH

FIGURE 2

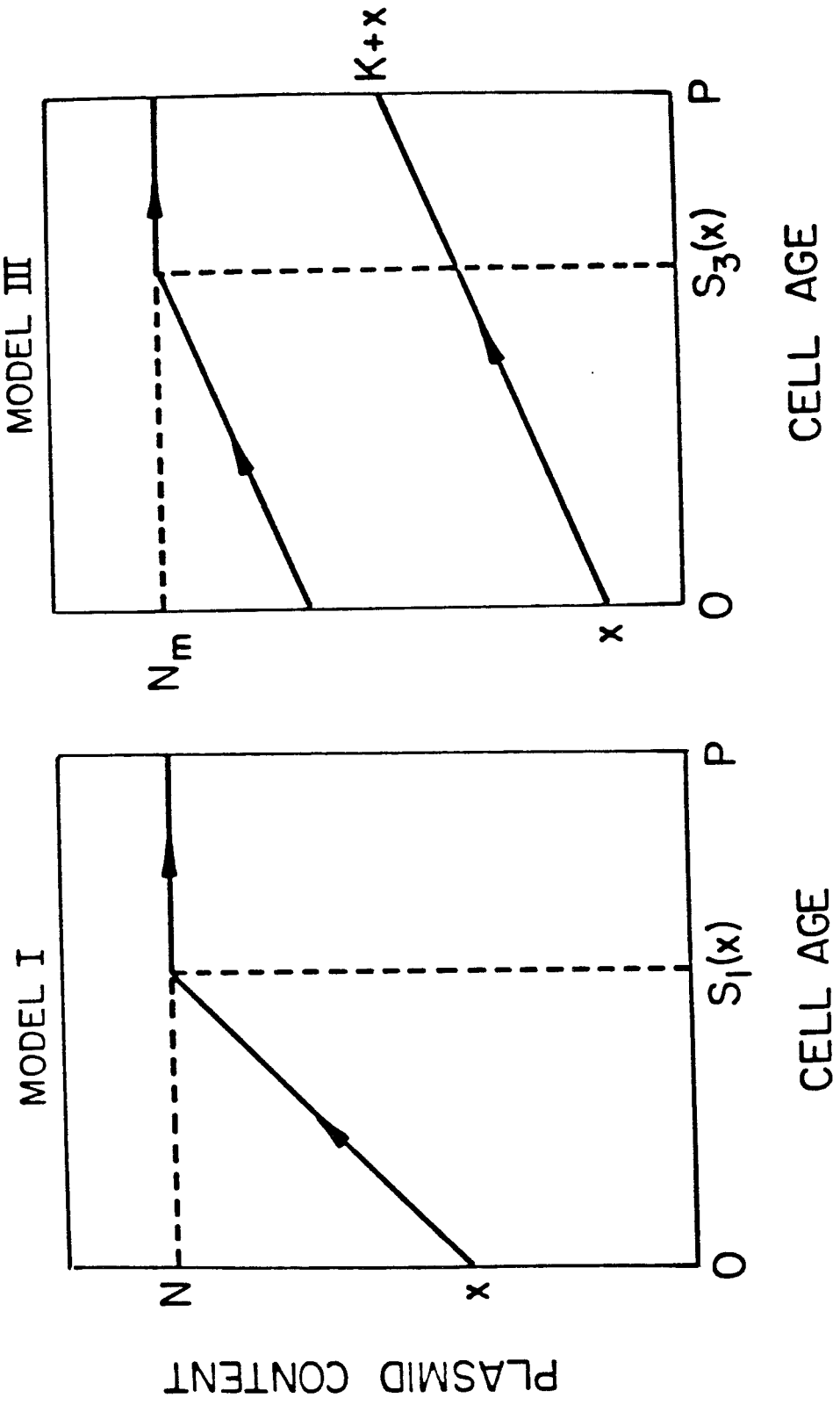
MODEL III
K+x
P
$S_3(x)$
O
N_m
x
CELL AGE
MODEL I
P
$S_1(x)$
O
N
x
CELL AGE
PLASMID CONTENT

FIGURE 3

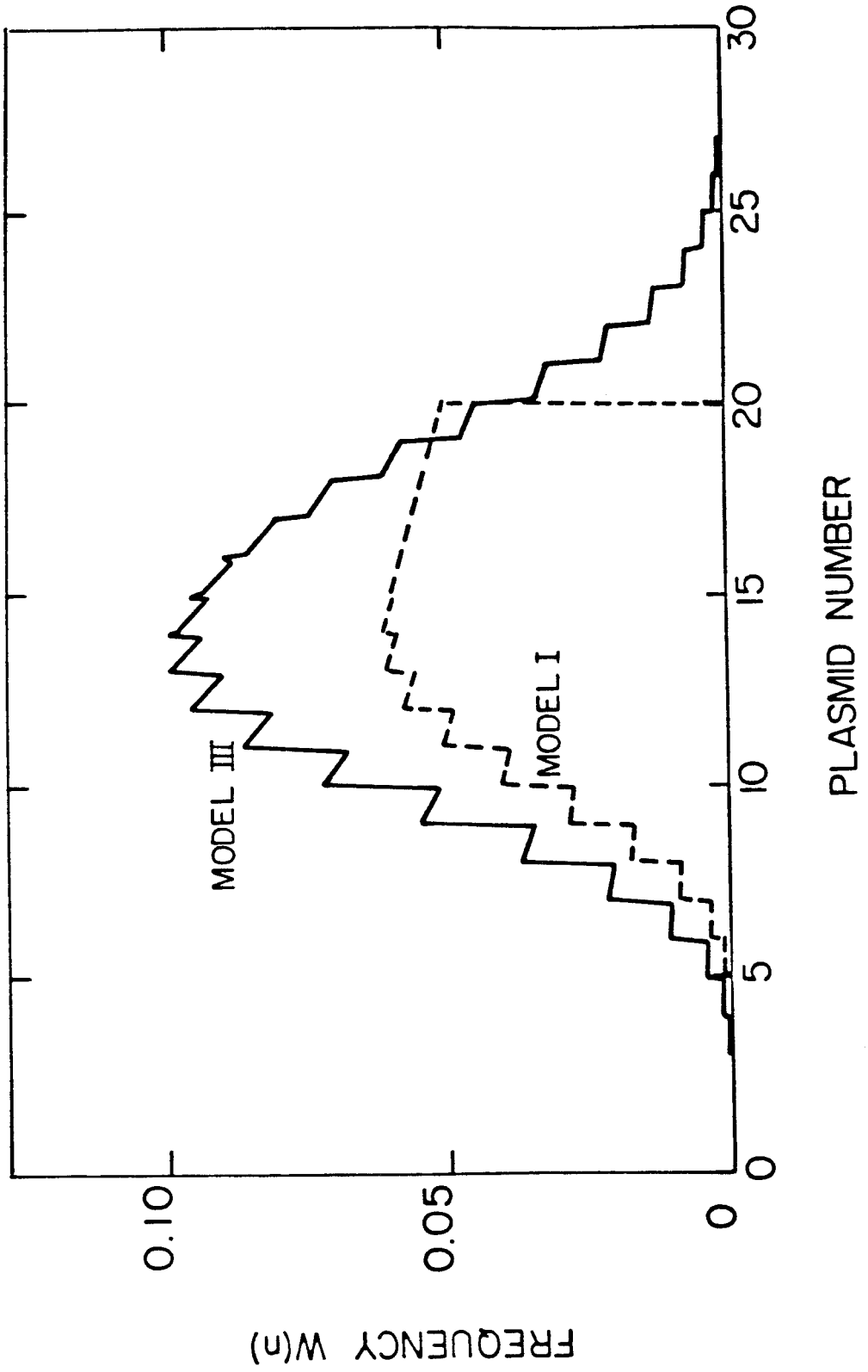
FREQUENCY W(n)
0.10
0.05
0
0
5
10
15
20
25
30
PLASMID NUMBER
MODEL III
MODEL I

FIGURE 4

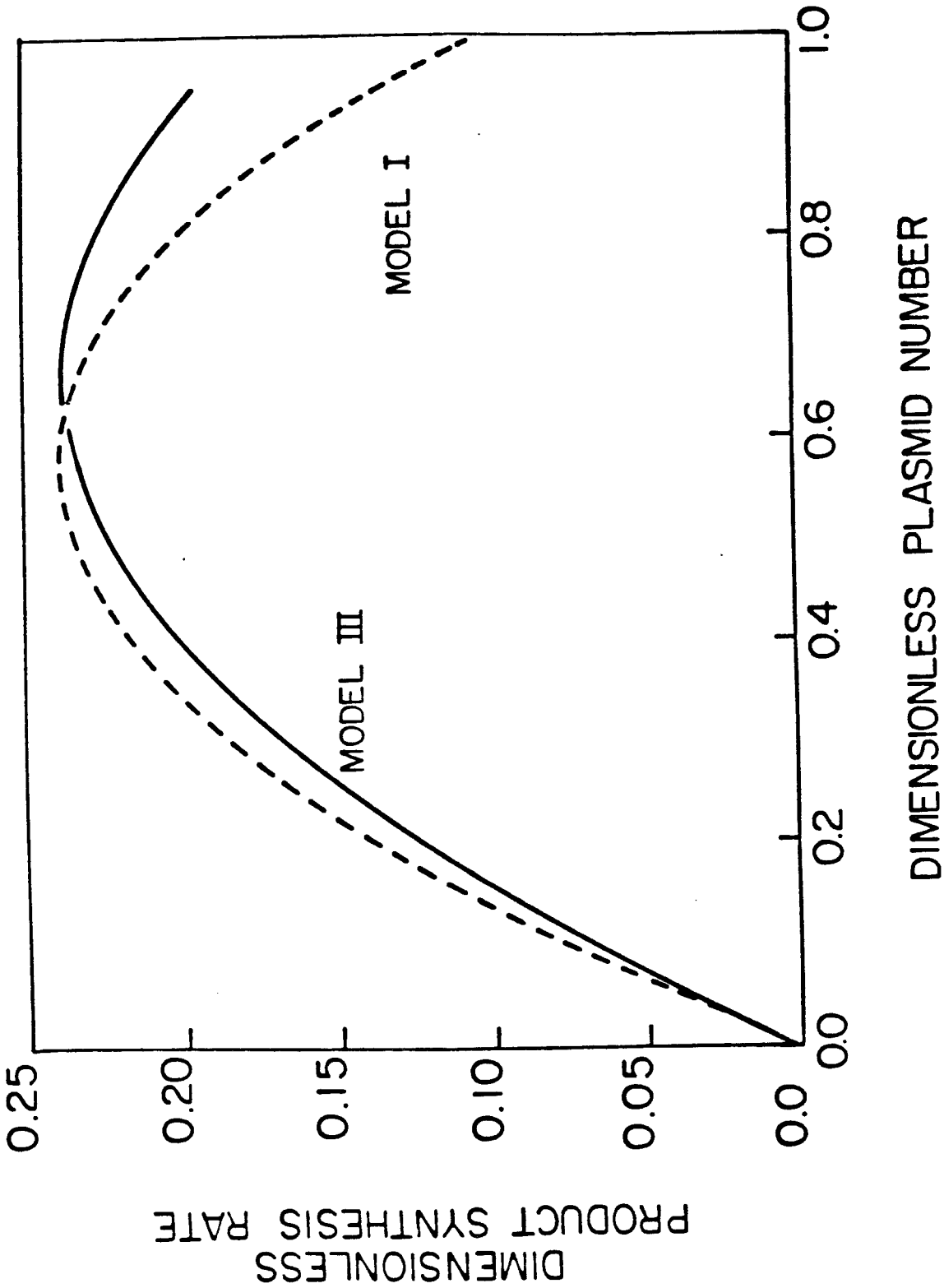
MODEL I
MODEL III
0.0
0.2
0.4
0.6
0.8
1.0
DIMENSIONLESS PLASMID NUMBER
0.25
0.20
0.15
0.10
0.05
0.0
DIMENSIONLESS
PRODUCT SYNTHESIS RATE

FIGURE 5

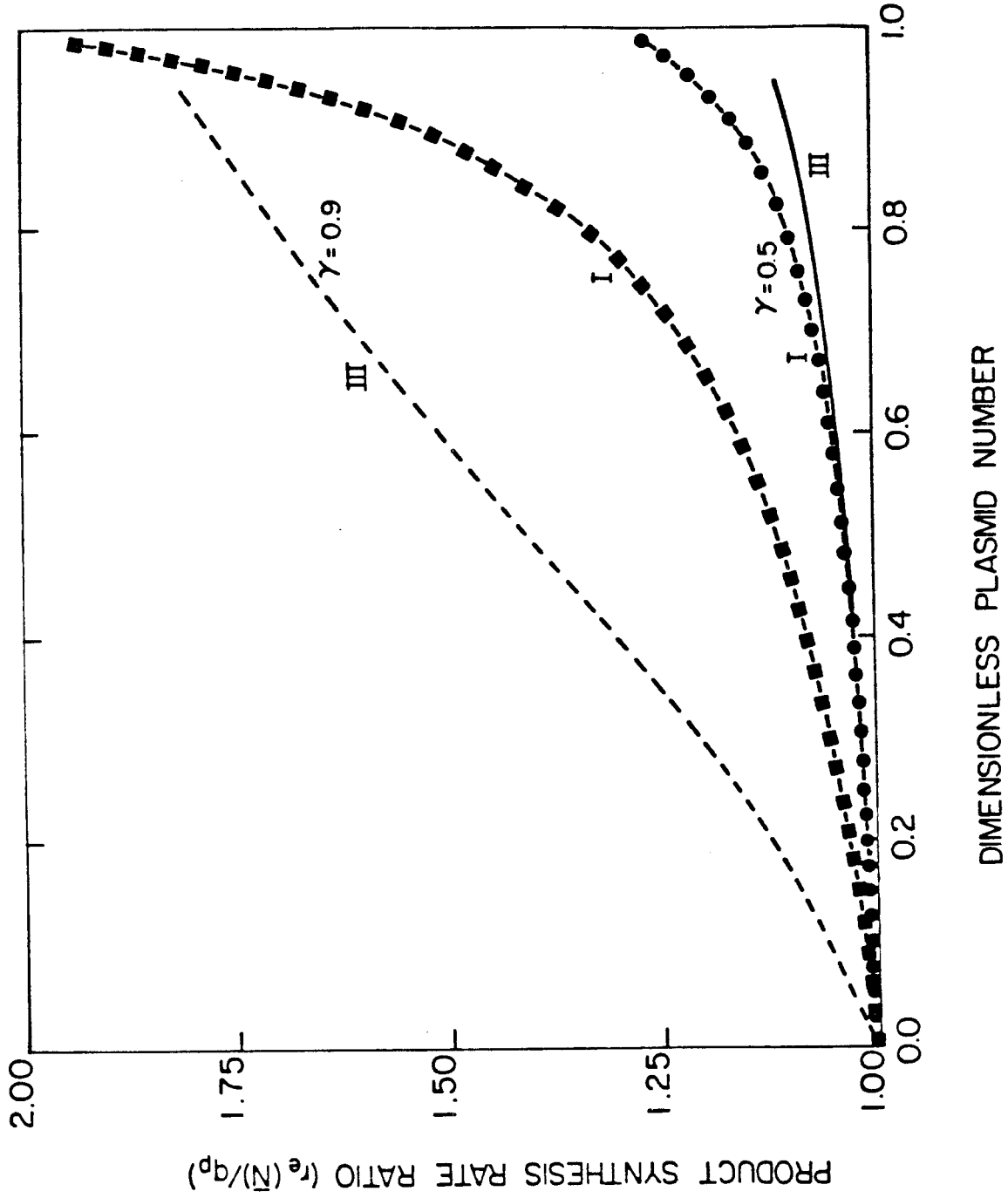
PRODUCT SYNTHESIS RATE RATIO ($r_e(\bar{N})/q_p$)
2.00
1.75
1.50
1.25
1.00
0.0
0.2
0.4
0.6
0.8
1.0
DIMENSIONLESS PLASMID NUMBER
γ=0.9
γ=0.5
I
III
I
III

FIGURE 6

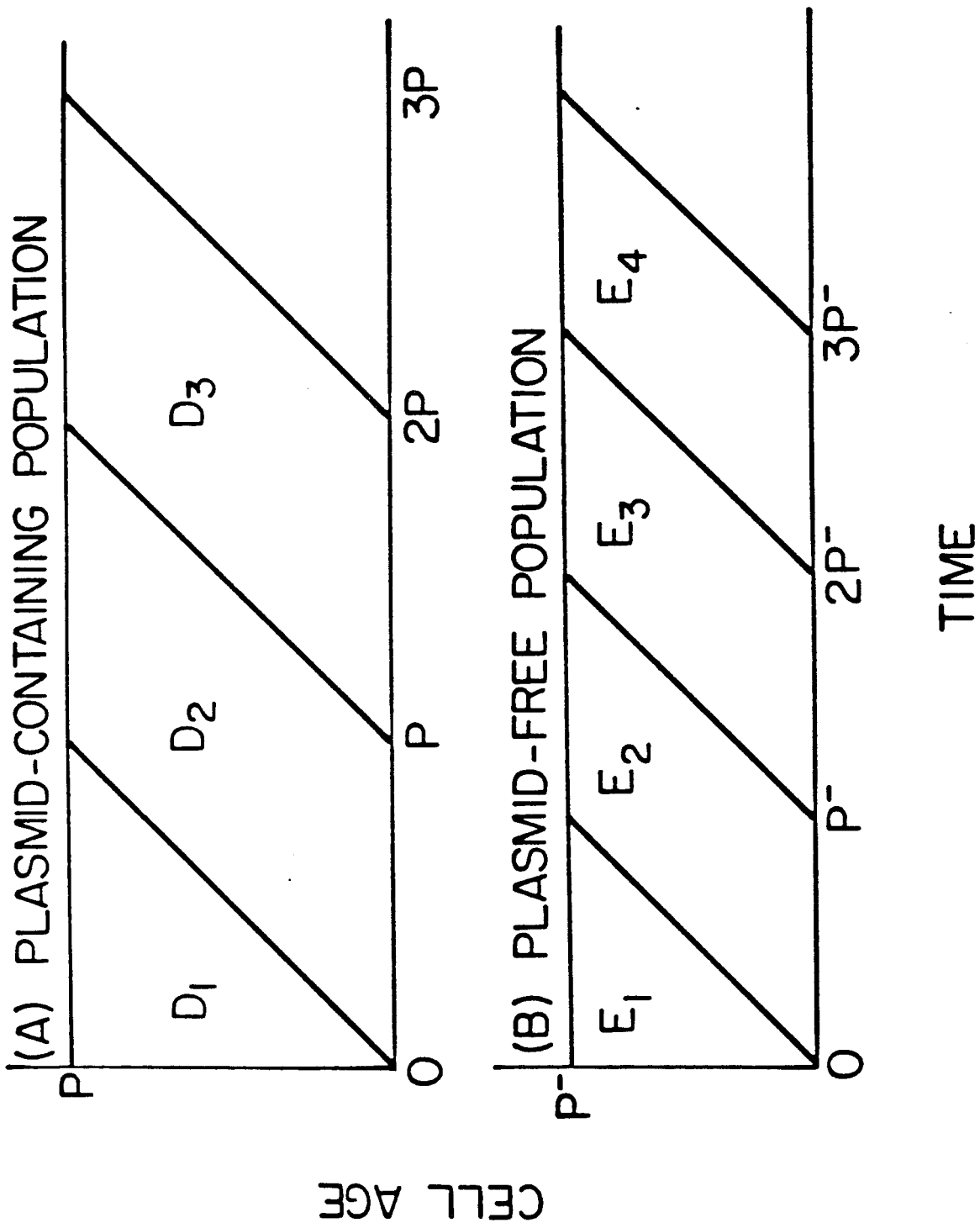
(A) PLASMID-CONTAINING POPULATION
P
O
P
2P
3P
D1
D2
D3
(B) PLASMID-FREE POPULATION
P-
O
P-
2P-
3P-
E1
E2
E3
E4
CELL AGE
TIME

FIGURE 7

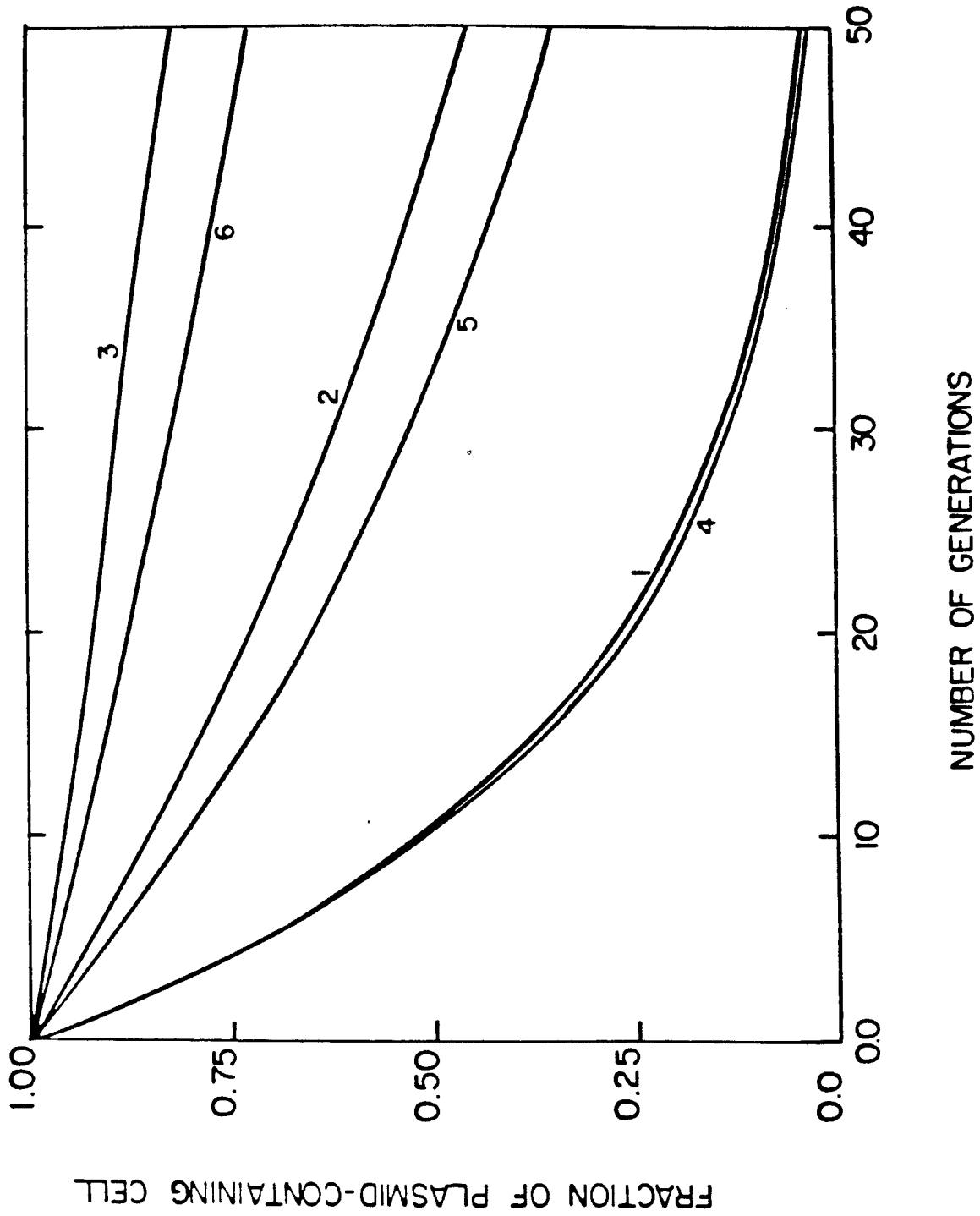
1.00
0.75
0.50
0.25
0.0
0.0
10
20
30
40
50
NUMBER OF GENERATIONS
FRACTION OF PLASMID-CONTAINING CELL
1
2
3
4
5
6

FIGURE 8

CONCLUDING DISCUSSION

Several major conclusions concerning interactions between plasmid and host cell functions can be drawn from this research. These conclusions may be summarized as follows:

- The presence of pMB1 plasmids reduces cell-cycle characteristic intervals (C and D times), mean-cell size, and initiation cell mass of host cells relative to plasmid-free cells.
- The cell-cycle parameters in plasmid-containing and plasmid-free *E. coli* HB101 strains were measured combining experimentally determined single-cell DNA content frequency functions with mathematical analysis of cell growth.
- Maximum specific growth rates and overall gene expression efficiency decrease for increasing plasmid content per cell.
- Plasmid copy number declines as specific growth rate increases.
- Both plasmid content and growth conditions are important in determining the productivity of recombinant cell populations.
- Continuous cultivation of plasmid-carrying cells showed the existence of an optimum dilution rate for maximum gene product concentration.
- Investigations of chloramphenicol-mediated plasmid amplification kinetics revealed that both rates of plasmid amplification and final contents of amplified plasmids are proportional to the average preamplification copy number.

- The probability of plasmid loss and condition for stable maintenance of plasmid-harboring populations were derived for an unstable binary fission recombinant organism using a segregated, population balance model.

APPENDIX

Copy Number Determination

I. Quantitative Method using an Internal Standard

The internal standard used for this copy number determination is pACYC184 [*J. Bacteriol.*, **134** , 1141 (1978)]. Its minimum copy number is 18 and molecular weight is 2.65 x 10^6D . It contains genes for tetracycline (Tet) and chloramphenicol (Cm) resistances.

Grow cells overnight at 37°C in 5ml Luria broth supplemented with 15 mg/L Tet for pACYC 184 and with 50 mg/L ampicillin (Amp) for sample plasmids.

Inoculate 200 ml media with 2 ml of preincubated culture. If more than one plasmid is going to be investigated, be sure to have 200 ml of pACYC 184 culture for each plasmid.

Place cells on ice for at least 10 minutes when cells grow to mid-exponential phase (OD_{590} = 0.5 or Klett reading with green filter = 190). If you want to determine directly plasmid content in culture samples, those samples will be mixed with pACYC184 culture as described soon.

Mix volumes of pACYC184 with plasmids to be analyzed according to their optical density so that the final mixture is 1:1. Make all sample flasks up to the same volume with fresh medium.

Transfer cells to centrifuge tubes and spin them down for 5-10 min, 8 K - 12 K rpm 0°C. Discard supernatant.

Resuspend cells in 1 ml 25 % sucrose dissolved in 0.05 M Tris buffer (pH 8).

Move the suspended cells to 5 ml ultracentrifuge tubes. Add 0.16 ml lysozyme solution (20 mg/ml in 0.25 M Tris pH 8). pH of lysozyme solution should be adjusted at 8. Sit on ice for 15 min.

Add 0.32 ml 0.25 M EDTA (pH 8) to chelate metal ions. Sit on ice for 15 min.

Add 1.28 ml 2 % Triton solution slowly while stirring with the end of pipet tip. Sit on ice for 15 min.

Centrifuge for 30 min at 50 K rpm or 1 hour at 30 K rpm to pellet out chromosomal DNA.

Carefully transfer supernatant to a 15 ml test tube to do Cesium Chloride gradient centrifugaton.

Add 4.46 gm CsCl to the centrifuge tube containing the plasmid DNA.

Add 0.24 ml Etidium Bromide (EtBr) solution (10mg/ml).

Add TEN buffer to make the weight 9.3 gm and mix.

Spin down the contents in a desk top centrifuge to separate protein layer (it will be a cake-like layer on top).

Pipet out the lower layer into heat-sealable tubes (volume capacity 5.4 ml). Be sure to fill, so there are not any trapped air bubbles.

Seal the tubes by heating and place in a

vertical rotor 50 K 20 hours

or angled rotor 50 K 48 hours at 17°C .

Remove tubes from centrifuge being careful not to agitate them or the gradient could be destroyed.

With a UV light, locate the plasmid band (it will be the lower of two bands).

Mark the area of the band with a felt pen.

Cover the area of the mark with scotch tape to add support for piercing.

With an 18-20 gauge needle, pierce a hole in the top of the tube for venting (leave the needle in the tube).

Using a 5 cc syringe and an 18-20 gauge needle, remove all the air from the syringe and pierce the tube just below the plasmid band.

-- be careful not to shove the needle through the other side.

-- *Once a needle has pierced the tube, do not remove it until the band has been collected.*

Draw out approximately 1 ml fluid. Try to avoid the leftover protein layer (dark pink viscous part) or it will clog the needle. If some of the fluid has been drawn and the needle clogs before finishing, *leave the needle in*; then insert another needle near the first one and draw the rest out.

Transfer the fluid to clear test tubes.

Remove the EtBr by extracting three times with n-butanol in a 1:1 volume ratio, discarding the top layer each time.

The plasmid DNA will be purified by ethanol precipitation in a cold room.

Add 2 ml sterile water to the sample to dilute their salt content. Final volume should be near 3 ml.

Transfer samples to a 15 ml corex tube and add 6 ml ethanol (100 %) and mix.

Place the tubes in dry ice for about 5 min (check periodically for a white ppt, which is CsCl and is not desired). Don't keep on ice too long.

Centrifuge at 12 K rpm for 20 min at 0°C .

Discard supernatant and gently rinse with 1 ml *cold* 95 % ethanol and discard.

Dry in vacuum for 10 min.

Resuspend in 0.25 ml 0.3 M Na-Acetate (pH 5.2) and add 3 volumes cold ethanol. Transfer to 1.5 ml Eppendorf tube.

Chill in dry ice for 5 min. Spin down in microfuge for 10 min in a cold room.

Discard supernatant. Rinse with 0.5 ml cold ethanol, centrifuge 5 min, discard supernatant.

Dry in vacuum for 10 min or until dry.

Resuspend pellet in 30 μl 10 mM Tris buffer.

Mix samples with loading solution (0.1 volume, 1 μl loading solution + 9 μl sample to make 10 μl).

Load on 1 % agarose gel to run for 500 Volt-hour. The plasmid DNA moves towards the positive electrode. pACYC 184 migrates faster than the sample DNA due to smaller molecular size.

Remove and soak in EtBr dissolved in electrophoresis buffer (1 μg /ml) for 30 min.

Place the gel on a transilluminator.

Take gel photographs.

Measure band densities in negatives of gel pictures with a scanning densitometer coupled to a digital integrator.

Solutions

Luria broth growth medium (per liter)

5 g yeast extract

10 g bactotryptone

5 g NaCl

3 g K_2HPO_4

1 g KH_2PO_4

2 g glucose

2 % Triton solution

20 % Triton 2.5 ml

0.25 M EDTA 6.25 ml

1.0 M Tris (pH 8) 1.25 ml

Water 15.0 ml

Loading solution

30 % Ficole

0.2 % Xylene cyanol

0.2 % Bromophenol blue

12.5 mM EDTA

II. Relative Method

Cultivation is the same as before.

Centrifuge cells 10 min 8K, 4°C . Drain pellet well of supernatant.

On ice:

Resuspend cells in 2 ml 50 mM Tris pH 8.0 + 10 % sucrose.

Transfer cell suspension to ultracentrifuge tube and 0.2 ml 10 mg/ml lysozyme dissolved in 25mM Tris pH 8.0 .

Sit on ice for 5 min.

Add 0.2 ml 0.25 M EDTA pH 8.0 and sit 5 min.

Add 2 ml 0.2 % Triton X-100 + 50 mM Tris pH 8.0 + 25mM EDTA . Add this slowly while stirring in well with end of pipet.

Place at room temp for 10-15 min.

Be sure tubes are balanced and then spin in ultracentrifuge for 1 hour at 35 K and 2–4°C.

Carefully pour off supernatants from chromosomal DNA and cells debris pellet.

Supernatant contains plasmid DNA but must be purified by several extraction processes (Approx. volume is 4.5 ml).

Add half-volume 20 % LiCl and mix.

Add 1.5 volume isopropanol and mix.

Freeze on dry ice, thaw, and spin 12 K, 4°C, and 10 min.

Remove supernatant *completely* . Otherwise, phase separation problems in extraction steps would occur.

Resuspend pellet in 0.35 ml 10 mM Tris (pH 7.5) and 1 mM EDTA.

[Extraction Steps]

Do two phenol extractions (equal volume of phenol equibrated to pH 8.0 with 0.2 M Tris pH 8.0 just before use).

Do two chloroform:isoamyl alcohol (99:1) extractions (equal volume). In each case take uper phase.

Add 0.5 volume 7.5 M NH_4 Acetate; then add 2.5 volume 100 % ethanol. Chill on dry ice for 10-20 min. Spin for 5 min at room temp. Rinse carefully with 1.5 ml cold 80 % ethanol.

Vacuum-dry pellet for 10-30 min.

Add 0.3 ml RNAse solution, resuspend, and incubate at 37°C for 1 hour. (RNAse solution must be boiled when preparing to destroy DNAse activity.)

Add 0.15 ml 7.5 M NH_4 Acetate and ethanol ppt by adding 0.9 ml 100 % EtOH.

Chill on dry ice for 10-15 min and spin down for 10 min at room temp.

Remove supernatant and rinse pellet with 1.2 ml 80 % EtOH. Vacuum-dry for 10-30 min. Resuspend pellet in 80 μl TE buffer.

Mix sample with 0.1 volume of loading solution.

Load volumes into teeth and run on 0.9 % gel for 500 V-hr.

Soak gel in EtBr solution (1 μg /ml in E buffer) for 30 min.

Soak gel in water for 30 min.

Take pictures and measure band densities in negatives of gel pictures.